NEDCON Intelligent Storage Solutions and University of Twente

Determining Load Capacity of Upright Profiles Subject to Pinching due to Diagonal Bolts

Bachelor Thesis Civil Engineering

Fabian Schuurman
July 2015

UNIVERSITY OF TWENTE.

NEDCON

Technical Research Report for the partial fulfilment of requirements for the Bachelor education programme Civil Engineering at the University of Twente in Enschede, the Netherlands.

Student: Fabian Schuurman (University of Twente Student number: s1356291)

fabian.schuurman@gmail.com

UNIVERSITY OF TWENTE.

Supporting Professors:

Dr. Ir. Irina Stipanovic Oslakovic

Ing. Gerrit H. Snellink

Company: NEDCON Intelligent Storage Solutions / NEDCON Magazijninrichtingen B.V.

Nijverheidsweg 26, 7005 BJ Doetinchem, the Netherlands

NEDCON

Supporting Colleagues at NEDCON

Ms. Sandra Junier (Project Coordinator Innovation Centre)

Ir. Jan-Willem Frederiks (Manager Design Principles)

Dhr. Han Woerts (Test Operator)

Maarten Casteelen (Structural Engineer)

Mark Assink (Structural Engineer)

Execution period for research:

Starting: 1st of April, 2015

Ending: 19th of June, 2015

Note: A list of used Abbreviations can be found on page 6 and also in Appendix A.

Acknowledgements

This Bachelor thesis marks the end of my graduation process and my time as a student at the University of Twente. I would like to say thanks to everyone who supported me and gave me the opportunity to carry out my Bachelor thesis at NEDCON.

First I would like to thank my supervisors from the University of Twente, Gerit Snellink and Irina Stipanovic for their guidance provided during the entire process. I am grateful for the critical feedback from meetings.

Then, I would like to thank my supporting colleagues at the NEDCON company, Jan-Willem Frederiks and Sandra Junier for daily useful advice and knowledge input for the project. I also would like to thank Maarten Casteelen, Jan Hermanek and Mark Assink for providing valuable technical details. Their sincere interest and caring attitude gave me a great drive to continue with alternative methods when previous trials seemed not to work out.

I would like to thank Han Woerts for his seemingly endless patience and hard work for the experiments carried out. I received much help from his practical insight and many spontaneous meetings with tips and tricks.

Finally, I would like to thank all employees of NEDCON for the pleasant conversations and the great time I had.

Ulft, June 2015

Fabian Schuurman

Executive Summary

During the past three months I carried out an internship for the final Bachelor thesis. I participated in a research project at the company NEDCON in the city of Doetinchem, the Netherlands. NEDCON produces and develops storage racking for large warehouses. Storage racks are build out of beams and frames. Frames consist of two uprights with diagonals in between. This research will focus on the uprights.

Production tolerances in the upright profiles are expressed in the opening of the upright which can be 3 to 4 mm larger than required, see also the red line in Figure 1. At the stage of assembly a diagonal spacer is inserted between the upright opening and a bolt should serve as a fastener. When an upright opening is substantial larger than the spacer, tightening the bolt will cause an initial imperfection in the upright due to the pinching. The objective of this research is to find out what the effect is towards the bearing capacity of the uprights profiles.

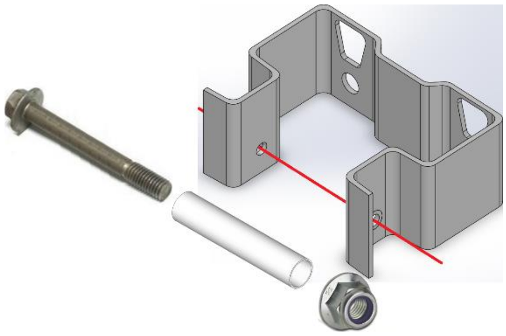

Figure 1. Expression of production tolerances and position of diagonal spacer.

In general, there are three groups of potential buckling modes most common in NEDCON's upright profiles. These groups are the global, distortional and local buckling modes. In global buckling, the cross sectional geometry will not deform while the profile is bending out or rotating globally. In distortional buckling, the cross section deforms over a large part of the upright's length. Distortional buckling can occur in symmetric and A-symmetric shapes. The other buckling mechanism is local buckling, where the profile deforms locally. It is assumed that the pinching effect will mostly affect the distortional and local buckling modes due to the deformation in the cross section.

A series of tests was carried out to catch the effect of pinching experimentally. Two types of profiles were selected from standard range dimensions, one lipped and the other non-lipped. The extra lip at the ends near the upright opening are expected to have significant influence on bearing capacity. The first type of test setup was the Stub column test. The idea of the Stub test is to find the compressive strength of a column which is sufficiently short to only trigger the local failure mechanism. This test pointed out that local buckling effects are not significantly affected by pinching effects. A complete frame test setup is used to assess the pinch effect on the distortional buckling mode. The distortional buckling tested showed potentially significant influence in buckling capacity after pinch.

There are two ways of modelling stability problems in open thin walled profiles. The first one is the Finite Strip Method and the second the Finite Element Method. The Finite Strip Method is fast in computational time, but lacks the ability of having any changes in geometry or boundary conditions along the length of the profile. The method is suitable for quick estimation of modal behaviour of profiles without spacers and can be useful for finding lengths of the upright with least resistance against buckling. The Finite Element Method should be employed to take into account various amounts of pinching. On first sight, both models seem to be rather good at estimating failure mode shapes. However, estimating actual failure load is difficult and results are inaccurate. The combination of models can be used to fin the 'worst case' scenario, in which the length applied in the construction leads to the weakest resistance in combination with substantial sensitivity to buckling effects.

This research resulted in a development of a new frame test setup. Numerical simulation can be used as a tool to find the 'worst case' scenario which can be tested to find the critical load after pinching.

Table of Contents

List of Abbreviations

Abbreviation:	Meaning / Explanation:
‘100-68-20’ or ‘68’ or ‘Non-lipped’	Short for Upright Profile PRF 100-68-2.0-4050 PR (S355); one of the used profiles. See Appendix D.4. for explanation of profile codes.
‘100-72-25’ or ‘72’ or ‘Lipped’	Short for Upright Profile PRF 100-72-2.5-4050 PR (S355); one of the used profiles. See Appendix D.4. for explanation of profile codes.
‘120-78’ or ‘78’ or ‘Non-lipped’	Short for Upright Profile PRF 120-78-2.5-5070 PR (S355); one of the used profiles. See Appendix D.4. for explanation of profile codes.
‘120-83’ or ‘83’ or ‘Lipped’	Short for Upright Profile PRF 120-83-2.5-5070 PR (S355); one of the used profiles. See Appendix D.4. for explanation of profile codes.
BIM	Building Information Modelling
BSc.	Bachelor of Science
CAD/CAM/CAE	Computer Aided Design / Computer Aided Modelling / Computer Aided Engineering
cFSM	Constrained Finite Strip Method; Method in which a number of strips are used to access the buckling modes and load factor of thin walled cross sections. See also section ‘03.2 ; Constrained Finite Strip Method’.
CiT	Civil Engineering
CU-FSM	Application Cornell University Finite Strip Method solver using cFSM, see above.
DOF (also nDOF)	Degrees of Freedom, used to indicate number of degrees of freedom in discretized Finite Elements
DTB	Distortional Buckling testing (As described in Annex A of EN 15512:2009). The DTB-test setup with spacer, as used in this research, is described in Figure 6 on page 17.
FBy	Flexural Buckling over Major (y-)Axis (See section 02.1)
FBz	Flexural Buckling over Major (z-)Axis (See section 02.1)
FE	Finite Elements
FEA	Finite Elements Analysis
FEM	Finite Elements Method; Not to be confused with its homonyme abbreviation for: Federation Europeenne De La Manutention, the committee for Eurocodes involving storage racks and similar structures.
FSM	Finite Strip Method
FTB	Flexural Torsional Buckling (See section 02.1)
ISO	Isometric View
OTW	Open Thin Walled; (~Profiles or ~Sections) Structural components are classified as ‘Thin Walled’ when one of the dimensions is small compared to the other two. (Podolskii, 1979) Profiles are considered ‘Open’-sections when no closed paths are present in it cross-section. A closed path will deliver additional torsional resistance.
UTS	Ultimate Tensile Strength

01.Introduction

A brief introduction to NEDCON and the issued research project is given in this chapter.

01.1. Background

NEDCON is a company that develops and sells storage scaffoldings for large organisations worldwide. NEDCON's establishment in the city of Doetinchem is currently focussing on research, development, planning and design. NEDCON is an independent corporation that has been part of the international Steel group Voestalpine since 2004. Production activities have been moved to Pardubice (Czech Republic). (NEDCON, 2015)

In general, most storage scaffoldings are made out of thin-walled, shaped steel profiles. These thin walled profiles are lightweight, inexpensive in manufacturing and still possess a relatively substantial bearing capacity. An example of a standardized storage rack is shown in Figure 2.

Figure 2. Representation of a standardized scaffolding. Constructions like these can reach over 25 meters in height, supporting dozens of pallets. The orange profiles are called 'beams' (Dutch: 'liggers') and the straight vertical profiles are called 'uprights' (Dutch: 'staanders').

Storage racks acquire their stability from frames. A frame consists of two uprights facing each at a few metres distance. One side of the uprights shows an opening in which diagonals are placed in both directions.

The strength of a company like NEDCON originates from continuous research on all components, loads, configurations and optimisation of structures. This research will focus on phenomena encountered in uprights, which is a result of production method, discussed in next section 01.1.1.

01.1.1. Upright Production Line

To create an image in mind of the manufacturing process, this section will show the production line of upright profiles in a nutshell.

Upright profiles are made by cold-forming and perforating plain sheet metal. Sheet metal plates (mostly Black Steel S355 JR, sometimes S420 or S460) always have a constant initial width. These sheets are firstly given all perforations by a punching machine then the strips are led into a series of roll-bending machines which bend the sheets in several steps to the final characteristic storage rack upright shape, see also Figure 3 After this process a series of painting and coating might be applied to improve several corrosive properties or only to change appearance.

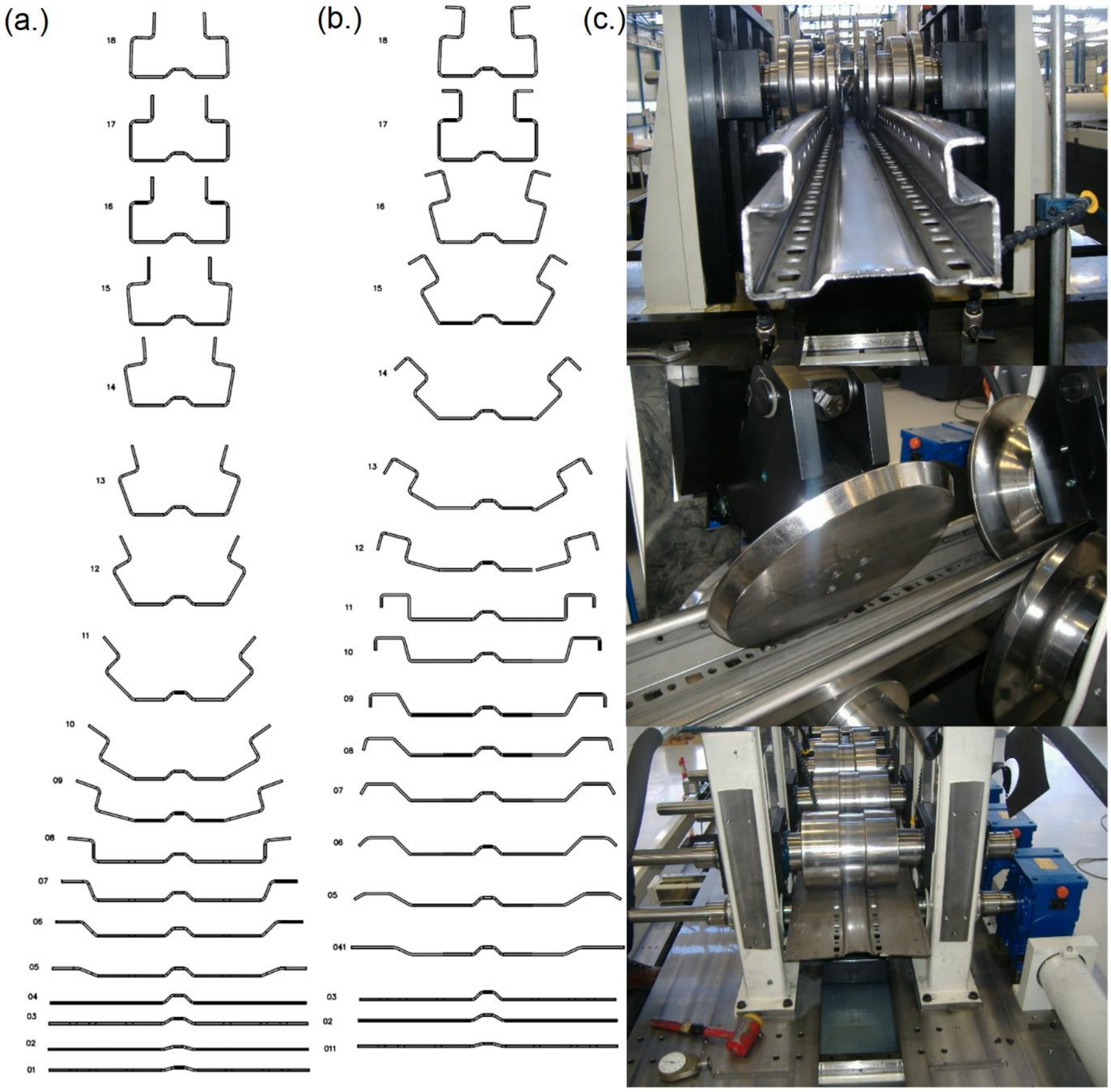

Figure 3. Upright Production Line. (a.) 'non-lipped'- (b.) and 'lipped' upright profiles. The effect of the additional lips will be studied in the next sections. In (c.) some stages of the production of a 'lipped' profile are shown. Source: (NEDCON, 2015).

To speed up the production process, literally the rotating speed of the rollers is increased, resulting in a less 'smooth' cold forming process. Besides production speed the machine costing is an important consideration. Lower quality bearings and roller steel grades might become less expensive but also increase magnitude of potential deviations in dimensions of the final upright. In fact engineering the right installation and finding optimal performance of the produced profiles is an optimization challenge.

01.2. Problem Description

Storage racks own their stability from frames. At the manufacturing of profiles out of plain sheet metal, some productions errors might be introduced according to classifications towards prescribed tolerances. A substantial production error is expressed in the distance between the end-sheets, like 'd_UprightOpening' as sketched in Figure 4. Tolerances and dimensions are stated in the design phase while taking into account pragmatic requirements of the diagonal's diameter chosen smaller upon fitting into the upright opening.

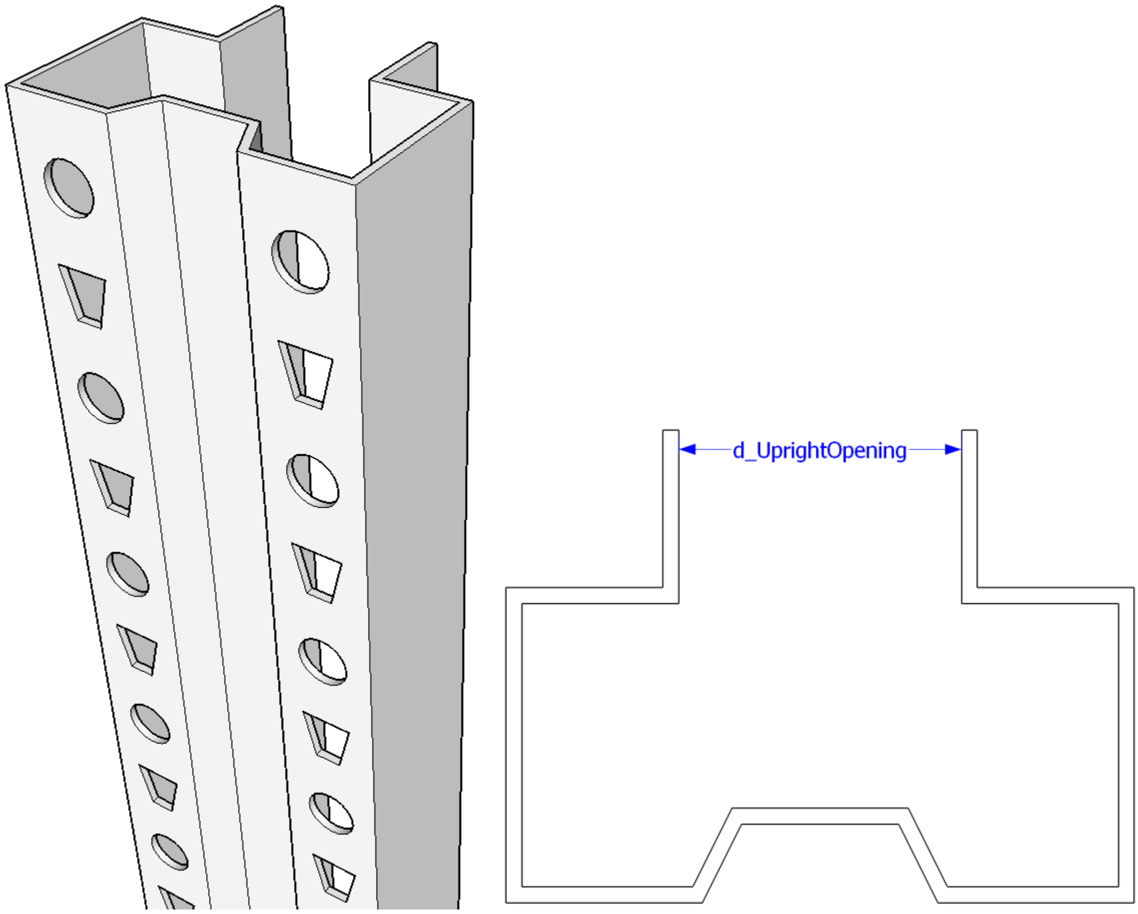

Figure 4. 3D Rendering and Cross Sectional view of a non-lipped upright profile. Source: Owned source, visualized by Open GL Graphics. Obviously, uptight profiles can be classified as Open Thin Walled Sections 'OTW-sections'.

At the moment when narrower diagonals are placed inside the frames during the construction phase, the bolts will pinch the upright together, introducing an initial imperfection. Small variations in gap size can influences the initiated buckling mode with different critical failure loads. The effect of this pinching effect on the bearing capacity has to be assessed.

During the month of March 2015, several tests of columns are being executed to find the relation in gap size and buckling strength. The test results need to be verified with theory and numerical Finite Element Method (FEM) models.

01.3. Objectives

An overview of the goals and objectives of the research project is given here.

In modern science of structural mechanics, three major approaches can be recognised. A visualization of these three approaches in Figure 5 also describes the continuous interaction between them. In every research, the multiple approaches are used to validate and supplement each other with valuable knowledge.

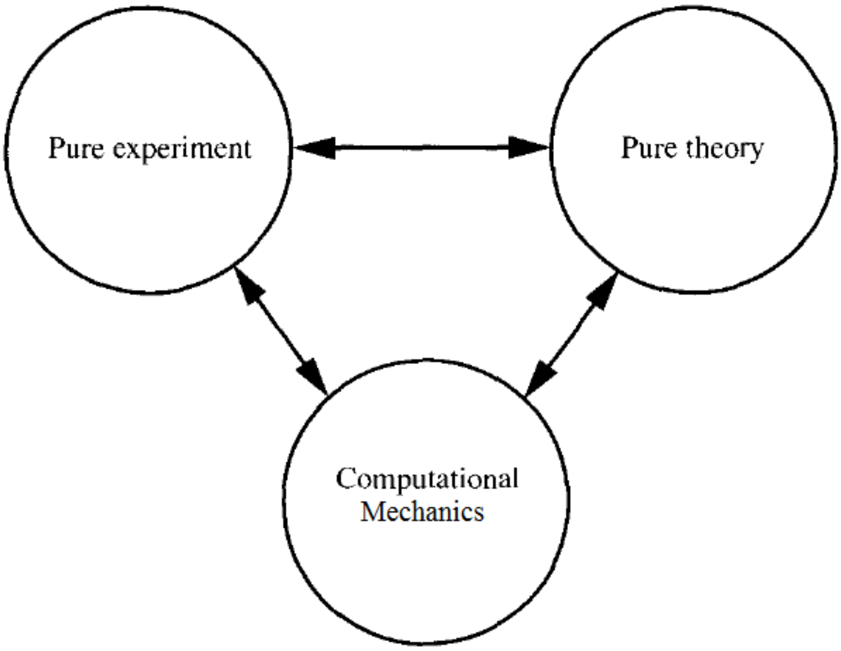

Figure 5. The three equal partners of modern structural mechanics. Source: (Anderson, 2011), edited.

The upright profiles used in storage racks can be classified as Open Thin Walled (OTW) sections. The type of failure mechanism which determines the capacity is a buckling or instability mechanism. When analysing stability problems in OTW sections, all three approaches of Figure 5 will be required.

The general goal of the project is to find a suitable numerical approach to the critical buckling loads of thin walled profiles like the ones applied in NEDCON's scaffoldings. Numerical analysis should reduce costs of gathering results by extensive testing of new profiles. The numerical analysis will consist of application of Finite Element Method (FEM) software tools and has to be validated by the test results of actual uprights. Knowledge should be gathered about how to simulate practical similar problems entailing production errors into the Finite Element Method.

01.4. Research Questions

The research project requires to be defined by a series of sub-questions in order to solve the general objective.

01.4.1. General Question

The general objective of the research project can be translated into the following question:

'How can the bearing capacity of an upright profile be determined when exposed to pretension by diagonal bolts?'

01.4.2. Partial Questions

This general question can be boiled down to the following understandable sub-questions:

'01. What would be a suitable test setup and how can the test results be evaluated?'

Evaluation of test results will lead to the conclusion of the 'Pure Experiment' part of Figure 5. A series of tests have been carried out. This project aims add developing a new test method with the purpose of tracing the pinch tolerances.

'02. How can linear elastic buckling theorems predict behaviour of upright profiles?'

A number of theoretical, semi-theoretical and semi-numerical solutions are available; how do they compare with other methods and which ones seem applicable to the uprights at NEDCON?

'03. How can the Finite Element Method determine buckling shapes and estimate corresponding failure loads?'

The goal is to find available Finite Element formulations and investigate their suitability to buckling stability issues within uprights (OTW-sections). Collect Finite Element solutions for the problem from a chosen application. What modes and critical buckling loads do these solutions show? How do these compare to test results or theory?

01.5. Scope

In the scope, also known as 'theoretical framework', a discussion is given about the available literature of the subject. Some 'well-known' methods will be discussed quickly.

Like said in the objectives, theoretical analysis, computational (numerical) simulation and observations from laboratory experiments are made concurrently to obtain better insight in physical phenomena. The first question handles the practical experiments.

01.5.1. Experimental Approach and Evaluation of Test Results

The executed tests on actual upright profiles will be evaluated according to the Euro codes NEN EN 1993-1-8:2005 and EN 15512:2009. The assumptions stated in the test setup considering boundary conditions and failure conditions are also important for future numerical analysis. During testing and probably also simulation, one can also distinguish a different post-buckling behaviour (Yiu, 2005, pp. 13-14). This transition will by definition occur at the critical load, which is in practice the maximal load applicable to the component. Post buckling behaviour will not be studied in this research.

While considering thin-walled profiles as a geometrical shape, the thickness is assumed to be negligible compared towards other dimensions. This inevitably means neglecting changes in stresses and strains in the perpendicular-to-plane direction of the structural component. Assumptions made regarding the analysis of thin-walled profiles are stated by (Yiu, 2005) and (Slivker, 2006).

In many literature sources, in general three buckling modes are distinguished with regard to thin walled components. These mode shapes are local, global (also known as 'flexural') and distortional buckling. However, there are no widely adopted and clear definitions for the various modes. The triggered modes within the test results will be classified by observation, which is prone to subjectivity.

01.5.2. Linear Elastic Theoretical Buckling Models

Theoretical closed-form and exact solution procedures for buckling analysis of thin-walled components date back from the late nineteenth century. On the other hand, numerical techniques came up in the seventies, while the digital computer revolution took place. (Erkmen & Mohareb, 2008) give a brief summary of developments made.

Simple analysis may assume linear elastic behaviour of material. Considering buckling of thin plates, (Megson, 2014) gives a theoretical analysis. Numerical approaches entailing FEM-like discretization are innumerable. Simple linear elastic FEM-solvers are easy to write in for example MATLAB code. In their book, (Cook, Malkus, Plesha, & Witt, pp. 648-650) discuss how to formulate elements for Linear Bifurcation Buckling.

01.5.3. Finite Element Simulation of Buckling Behaviour for Thin Walled Profiles

As mentioned earlier, Erkmen and Mohareb give a list of numerical techniques that could be useful when looking at thin-walled profiles. An often used method is the Finite Strip Method (FSM), originally developed by (Cheung, 1976), which uses a finite number of strips reaching along the length of a profile. Zhanjie (Li Z. , 2009) gives the theoretical extension of the Constrained Finite Strip Method for general boundary conditions and a buckling analysis of the Finite Strip Method. (Lanzo & Garcea, 1996) describe Koiter's analysis of the post buckling behaviour of thin-walled structures by means of an asymptotic approach based on a FEM implementation. Bourezane (2012) explains the advantages and disadvantages of several methods of modelling buckling analysis in FEM. Examples are given entailing nonlinear equilibrium equations, solved using Newton-Raphson method.

FEM Software Packages Capable of Simulating Buckling Behaviour in OTW sections

The book 'Thin-Walled Structures - Advances and Developments' by (Zaras, Kowal-Michalska, & Rhodes, 2001) describes how most methods described in the previous section have been captured into software tools. Commonly used software entailing thin walled analysis are:

- SolidWorks Abaqus (by Dassault Systemes);
- Autodesk Nastran Solver;
- ANSYS US Modules;
- Solid Edge (Siemens PLM);
- COMSOL Multiphysics;
- RFEM. (Questionable if capable of handling all thin-walled phenomena.)

NEDCON employees use *Dlubal's RFEM Software*, which contains modules able to calculate stresses within thin-walled metal profiles in complete structures. However, for analysis on detailed component, the application's results might become inaccurate (van Benthem, 2015). Investigation should be carried out if RFEM or other FEM simulation tools can simulate the effect of pinching diagonal bolts on the bearing capacity, and if not what can be the reason of showing different results. Meanwhile, other FEM-packets could be used sideways, like *Dassault's Solid Works*, MathWork's MatLab, Autodesk (Nastran) or several Open Source modules including MatLab codes.

For this research project SolidWorks will be used. This application uses Solid elements, which are believed to yield satisfactory accurate results. (van Benthem, 2015) The software is available at the company and some experience is already made.

01.6. Content of the Report

For all partial questions, an explanation is given which methods will be suitable options to yield answers and results. These methods show the 'Problem Approach' for the problems. Every section references to a section of the report where the corresponding partial question will be answered.

01.6.1. Experimental Approach and evaluation of Test Results

The evaluation of the test results shall be done according to the Euro code's principles, in this case the EN 15512:2009 and NEN EN 1993-1-8:2005. According to these codes shall a component be 'deemed to have failed when either the applied test loads reach their upper limit or when deformation have occurred of such a magnitude that the component can no longer perform its design function'. For all the test samples the failure modes should be documented as well as the corresponding failure loads. The test results should then be corrected for actual material thickness and actual material yield stress observed in tensile tests compared with the design values. The characteristic loads can be determined after calculating the standard deviation and thereby ensuring capturing the "95%-fractal" at a confidence level of 75%.

An initial series of tests have been executed at NEDCON to find the reduction introduced by the pinching effect. See also section 0 for explanation of these tests and corresponding Appendix C for detailed evaluation of test results. However, the results did not yet satisfy the needs for a check on the distortional buckling effect. The results and conclusions of these tests and the reason why these tests were insufficient to solve the problem will be explained in section 0.

01.6.2. Linear Elastic Theoretical Buckling Models

Some selected FEM and Finite Strip Method (FSM) Solvers using linear Elastic theory should be deployed. Results can be displayed together with the test results for comparison. The linear elastic applications are:

- Dassault Systèmes Solidwork's Static Simulation;
- Dassault Systèmes Solidwork's Buckling Simulation;
- Several modules written in MathWorks` MATLAB;
- Dlubal's RFEM Plate-Buckling;
- Dlubal's RFEM Shape-Thin;
- Autodesk NASTRAN;
- Cornell University Finite Strip Method (CU-FSM).
- A selection out of various Open Source modules.

Suitable and available applications are SolidWorks Static and Buckling Simulation. Some Open Source programs written in MATLAB are also attractive, among which CU-FSM. The Finite Strip These programs are selected to be applied in this research project.

01.6.3. Finite Element Simulation of Buckling behaviour of Thin Walled Profiles

Underlying assumptions of the methods within the discussed literature should be found. These theoretical approaches should be investigated if suitable for simulating profiles like the ones at NEDCON. The formulations that seem to be applicable to NEDCON's uprights should be checked on usefulness.

Again a selection of FEM-Solvers should be deployed. For all options, models of the columns should be imported/drawn, loads applied, simulations executed and results visualized.

The load conditions should simulate the test samples as close as possible. For the initial displacement at the height of the diagonal (or 'spacer', displacement can be modelled by an initial stress or strain. The 'general' load in normal direction might probably be seen as a uniform load. Investigation should be done if uniform loads are a valid solution.

The source of the initial imperfections in practice is already mentioned in the introduction and has to do with the machines used to produce the profiles. In the practical tests, wedges are placed to 'imitate' all kind off effects. In this research, 'spacers' will be used to account for diagonal connection bolts. The pre- and post-tested samples should be observed to find a way of modelling. Within linear elastic FEM this could be done by either applying an initial stress or displacement to simulate the diagonal or 'wedge'. An alternative would be to design a complete spacer for placement into the model to be simulated.

Statistical analysis can be used to determine if numerical analysis correlate with the test results. A one-sample t-test could be a satisfactory way of comparing a number of test results with numerical simulation results. (IDRE, 2015) The results can be visualized with a plot of the critical load versus the initial diagonal width (the imperfection). Interpretation with regard to a general conclusion is of major concern in this part of the research.

01.7. Overview of Report Structure

Until this point, the reader was introduced to the subject and project challenges. In order to provide an overview a report structure scheme is given including the questions, methods and chapter numbers where the issues will be addressed.

Table 1. Overview of Report Structure.

Type of scientific Approach; State of the Art methods		 $f(x) = \sum_{n=1}^{\infty}\left(b_n \sin\frac{n\pi x}{L}\right)$ $N_{cr} = \frac{\pi^2 EI}{L_{eff}^2}$	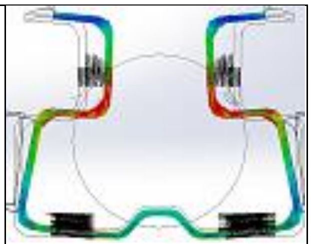 $[K]\{u\} = \{F\}$ 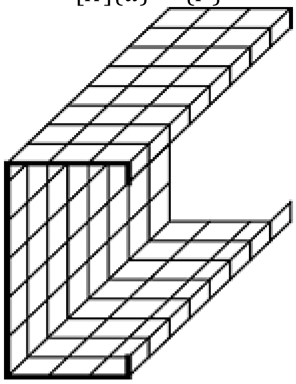
	Experiment	**Theory**	**Computational Mechanics**
Partial Question	What would be a suitable test setup and how can the test results be evaluated?	How can linear elastic buckling theorems predict behaviour of upright profiles?	How can the Finite Element method determine buckling shapes and estimate corresponding failure loads?
Applied Methods	Column Bench Press Test & Frame Bench Press Test	Megson Aircraft Structures, Gerard local Buckling Load Factor Estimation & Constrained Finite Strip Method	Finite Element Analysis executed with Solid Works
Chapter Number and Title	02. Experimental Research	03. Linear Elastic Theoretical Buckling Models	04. Finite Element Method simulation of buckling behaviour of upright profiles

02.Experimental Research

During the month of March 2015, an initial number of exploratory experiments have been carried out at NEDCON. After new insight, more test on complete frames have been executed halfway of May2015. This section will reveal what has been tested in the past, how measurements took place and most important; what results and conclusions can be deducted.

In total, there 3 types of tests were carried out. The first 2 types of setups are quite common to tests carried out many times at NEDCON, which means the company has a lot of experience with them. The last one is a rather new type of setup. The names of the setups are:

- Stub Compressive Column Test (STUB), meant to capture local buckling effects;
- Distortional Buckling Test (DTB), meant to capture distortional buckling effects;
- Complete Frame Bench Press Tests (Frame Test), also meant to capture distortional buckling.

Notice of the 2 types of setup both meant for distortional buckling. After the first (DTB) tests pointed out not to be satisfactory, the frame test was developed. The first 2 types of setups only contain a single upright and therefore these will be discussed in the first section. Table 2 gives an overview of all executed tests and where they can be found.

Table 2. Overview of tests carried out and their references. Notice that the 'classic' STUB- and DTB- tests are not within this report. References made to any STUB- or DTB-tests are with regard to the 'New' tests.

Picture in figure Figure 6	Test Name	Reference
a	‘Classic STUB’	Report # Ncon 13-300-122e (NEDCON-internal report)
b	‘Classic DTB’	Report # Ncon 13-300-123e (NEDCON-internal report)
c	New STUB	Section 02.1.1 on page 22.
d	New DTB	Section 02.1.1 on page 22.
e	Frame	02.2 Experimental Research on Complete in Frames

In the corresponding sections, the test setups will be explained in detail. The photographs in Figure 6 provide an overview of the different types of setups for now.

(a.) 'Classic' STUB

(b.) 'Classic' DTB

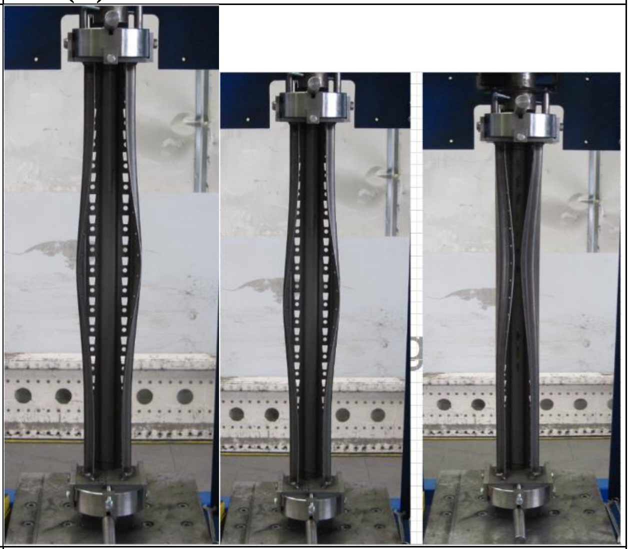

(c.) New STUB

(d.) New DTB

(e.) Frame Setup (Setup developed)

Figure 6. Overview of setups used.

02.1. Experimental Research on Single Uprights

The first tests make use of a well-known standardized test setup which is also extensively documented in the FEM-standards that apply to storage racking. (European Committee for Standardization, 2009, pp. 84-98) In this section, the previous test setup will be discussed briefly. This first test seemed to be insufficient for solving the actual problem.

Introduction

The opening of the upright usually differs from the width of the diagonal due to the production process and its tolerances. This causes deformations in the upright when the bolt for the connection between the upright and diagonal is tightened. The resulting imperfection in the upright opening flange could potentially influence the buckling capacity op the upright. To see if this is the case a series of tests will be performed.

Test Method

The first step is to do a sample test of the available upright profiles in the range of 100 to 140 mm width. The width of the profile can be found in the first 3 digits of the nomenclature of the profiles, like explained in Figure 7. If the influence of the deformed upright opening to the buckling capacity is negligible, further tests would not be required.

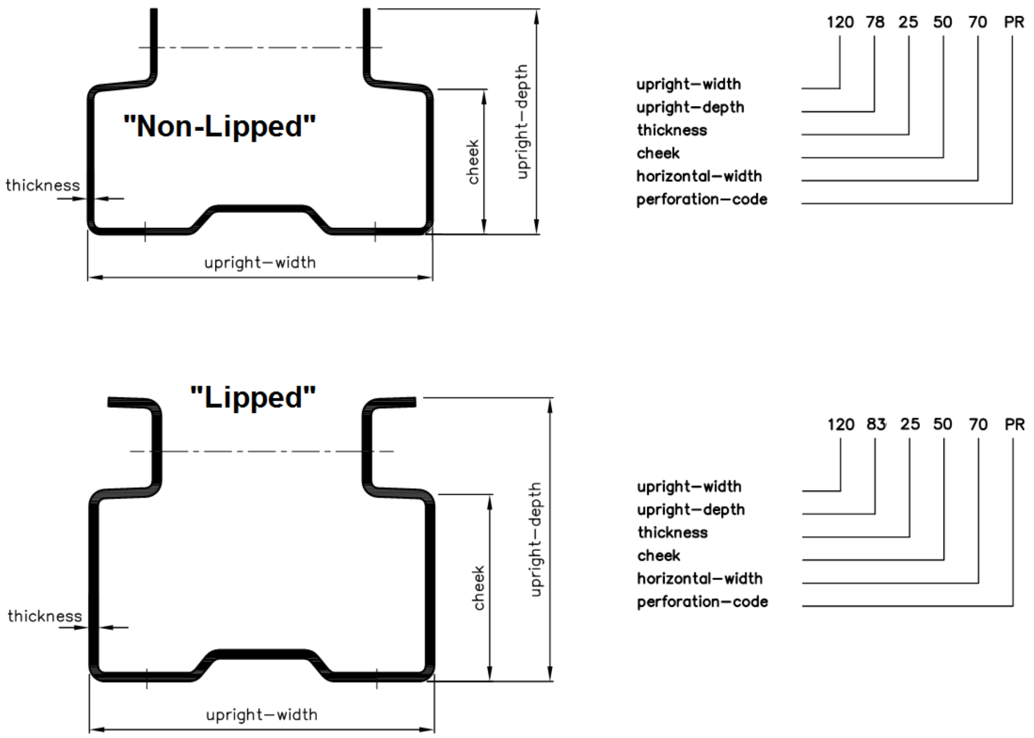

Figure 7. Nomenclature and profile properties that are believed to have substantial influence on its buckling capacity. See also Appendix D.4. for complete drawings of defined upright profiles.

The following upright properties are assumed to have the most potential to influence the buckling capacity:

- General size of the upright;
- Lipped or non-lipped (See also Figure 7);
- Thickness of material.

With this in mind the following upright profiles have been selected:

Table 3. Selected upright profiles for experiments. See Appendix F for the definitions of the upright names.

Type Upright (NEDCON classification, for definitions see Appendix F)	Lipped or Non-lipped	Thickness	Opening size and tolerances [mm]			Diagonal Dimensions and Tolerances		
			Design	Min	Max	Design	Min	Max
120 78 25 5070 PR S355	Non-lipped	2.5 mm	71	-1.0	+2.0	70	-0.5	+0.0
120 83 25 5070 PR S355	Lipped	2.5 mm	71	-1.0	+2.0	70	-0.5	+0.0

The uprights will be tested in the STUB and DTB setup (See also Figure 9) with different flange imperfections (See also Figure 8). The scope of these imperfections will be determined by the production tolerances as seen in Table 4.

Table 4. Potential remaining space between upright opening and diagonal as a result of the design tolerances.

Type Upright	Width opening upright			Width diagonal element			Total space between the upright and diagonal	
	(mm)	prod. Tollerances		(mm)	prod. Tollerances			
		min (mm)	max (mm)		min (mm)	max (mm)	min Δ (mm)	max Δ (mm)
12078255070 PR S355	71	-1.0	2.0	70	-0.5	0.0	0.0	3.5
12083255070 PR S355	71	-1.0	2.0	70	-0.5	0.0	0.0	3.5

The actual centre of gravity has to be determined first before the actual tests can be performed. It would require 3 tests to determine the optimal position, than one more test can be done at that optimal found position. At this optimal position the remaining tests with smaller spacers can be performed. An overview of all the tests executed is given below in Table 5.

Table 5. Overview of all executed tests in March. The CTC (Centre to centre) distance refers to the ball bearings at both ends of the setup and is defined in Figure 9.

Type upright	type test	L_{buc} (mm)	L_{test} (mm)	ED,M = space (mm)	# of tests	CTC Distance [mm]
12078255070 PR S355	STUB	400	400	0.0	4	560
				3.0	2	
				6.0	2	
	DTB	1000	2000	0.0	4	2160
				3.0	2	
				6.0	2	
12083255070 PR S355	STUB	400	400	0.0	4	560
				3.0	2	
				6.0	2	
	DTB	1300	2600	0.0	4	2760
				3.0	2	
				6.0	2	
					Total tests: 32	

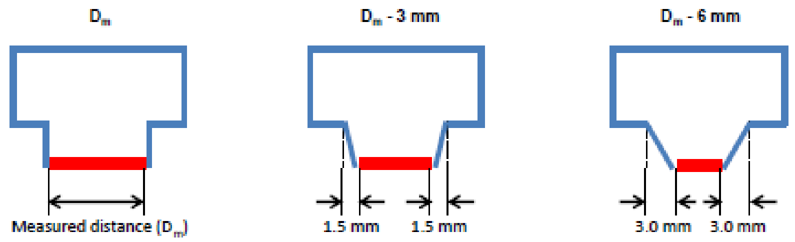

Figure 8. Variations in Flange imperfections. The diagonals in actual storage racks are replaced by spacers at the red indicated spots.

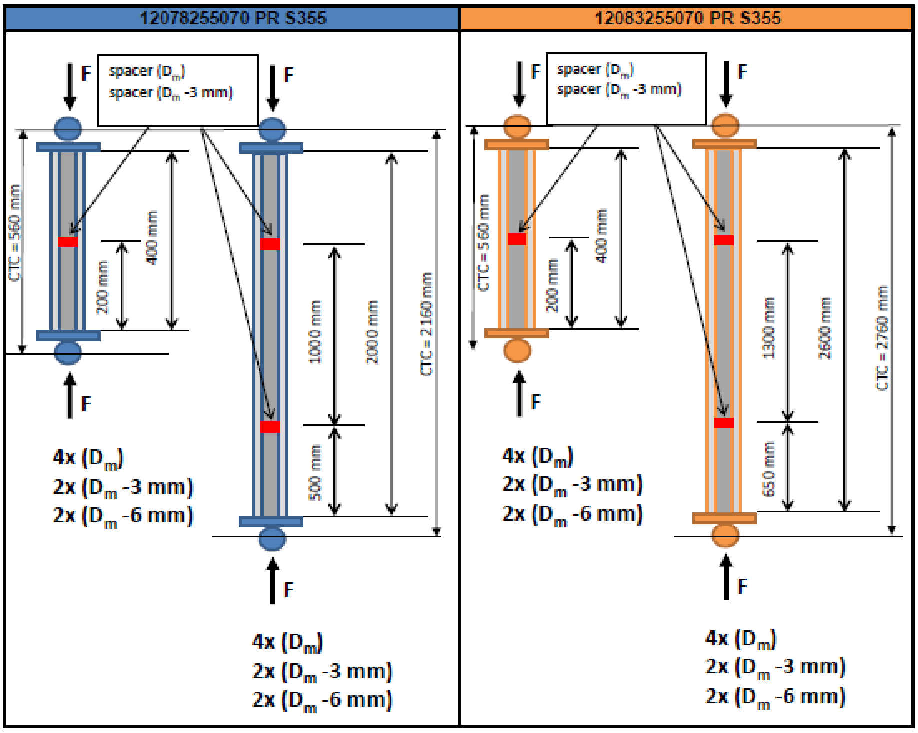

Figure 9. Schematic STUB (Blue) and DTB (Orange) test setup, according to EN 1993-1-8:2005. The goal of the STUB-setup is to access the effect of local instability and the DTB setup is meant to trigger the Distortional buckling mode. The lengths of the STUB-specimen are prescribed in the Euro codes. The lengths of the distortional buckling test (DTB) are taken conservatively at the weakest lengths for this mode. This 'weakest length' is calculated in section 03.2.

Hypothesis

The expectation of the tests is that the STUB-specimen almost certainly will fail due to local instabilities, due to the short length and therefore small change to fail flexural (global buckling). The classifications of failure modes is visualized in Figure 10. The DTB profiles are expected to fail under distortional circumstances and at lower critical loads due to the longer effective buckling length. Another failure mechanism that might be triggered is flexural buckling along the full CTC length, as defined in Figure 9. The length between the spacers is equal to the length used in earlier DTB-tests without spacers as the upright length.

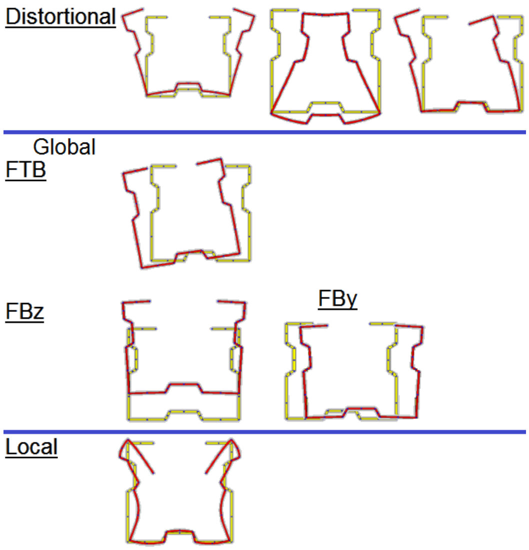

Figure 10. Overview of most common modes observed in storage rack upright profiles. In the STUB-test setup the intention is to obtain a Local failure and in the DTB (Distortional Buckling Test) the distortional buckling mode is to be assessed.

Evaluation

The reduction in initial bearing capacity has been investigated 'in the spirit of' the Euro codes. This means according to the principles of the Euro codes. References to any additional background information about the test setup have been accommodated into Appendix B; Initial single STUB- and DTB setup tests: Method of Evaluation. The detailed calculations in the evaluation can be found in Appendix C; Detailed Evaluation of Earlier Test Results. The procedure of evaluating the tests is also discussed briefly in section Evaluation of Experiments on Frames.

02.1.1. Analysis of Experimental Results of Tests on Single Uprights

As of the evaluation of the reduction in initial strength due to the pinching effect, the characteristic critical loads from Figure 11 might be deducted.

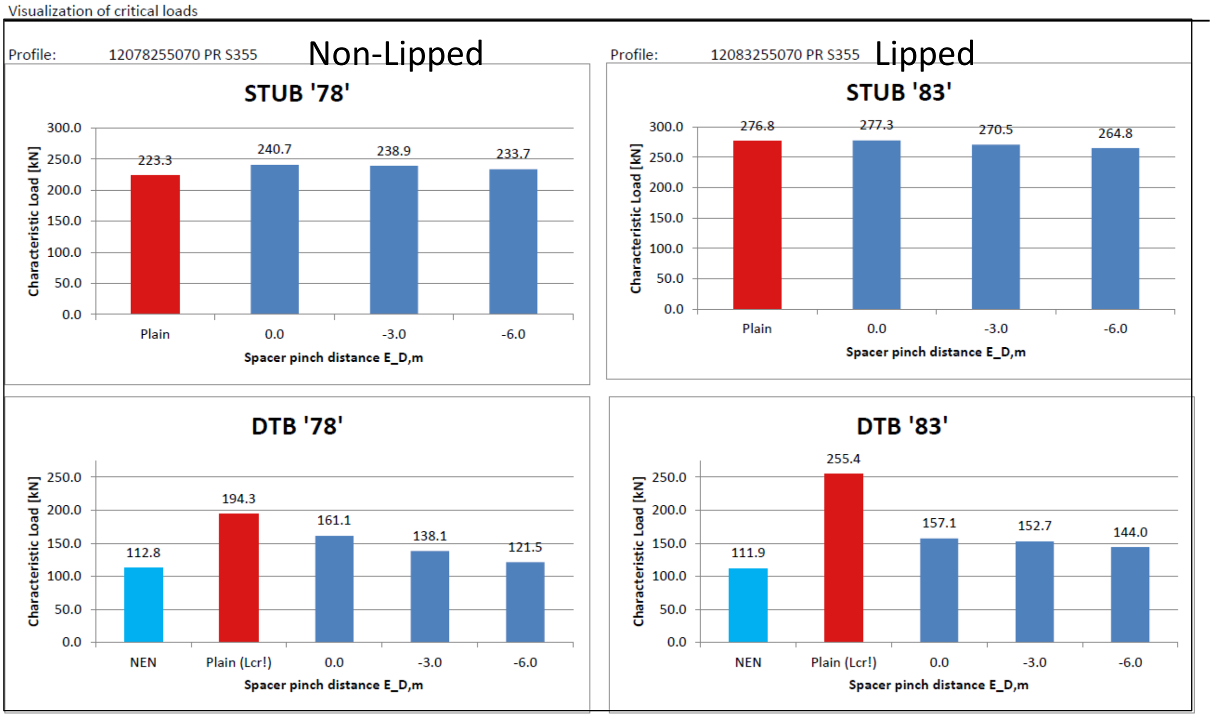

Note: The DTB-Plain values distinct from CTC-buckling lengths of 1160 and 1460 mm respectively for the '78' profile and the '83' profile. This differs strongly with the CTCs of 2160 and 2760 mm applied in the tests.

Figure 11. Characteristic Critical Loads for Upright profiles. The number of useful tests: n = 6 for every type of profile and for every type of setup. The 'Plain' test indicates the results from the 'Classic STUB' and 'Classic DTB' setup, as described in the introduction. The capacity according to the NEN is taken without any safety factors, to obtain a comparable load.

As might be expected; even in a scenario with 6 mm of pinching effect, the standards ascribe a lower resistant load to the profiles than the characteristic test results. This proves that the standard is save to use in all situations.

The profiles in the DTB tests show larger reductions in critical loads due to the pinching-effect, up to -25% at 6mm pinching for the non-lipped profile. Moreover, their initial bearing capacities are reduced due to the presence of a spacer. Especially the non-lipped profiles fail due to distortional buckling, which is intended by the DTB (Distortional Buckling Test). The spacers seems to act like "invisible" clamping constraints, as meant to be. Although the non-lipped profile in general showed the distortions the lipped profile mostly bended globally which is not the intention of the DTB (Distortional Buckling Test). The distortional behaviour of the upright was to be investigated including the effect of pinching while the Flexural buckling along the major axis is not significantly influenced by these effects. This last statement is underpinned by the 'flatness' of results. Any pinching effects do not significantly alter the situation compared with spacers at 0.0mm pinch (no-pinching situation).

All but one of the samples in the lipped profile tests failed in the flexural mode and not the devoured distortional mode. As a result, the 'plain' test and the 0.0mm pinch results do not coincide, or better to say; the 'New DTB' test setup cannot be compared with the 'Classic DTB' setup. The non-lipped profile did fail in distortional mode. However, it is clear in the photographs of the samples that the flexural mode interfered, reducing total resistance against failure. This explains why the critical loads of the ‘New DTB’ setup with 0.0 mm pinching are lower than the ‘Classic DTB’ setup. To prevent global failure, the spacers should be held in their initial horizontal position.

A failure mode that was observed in the ‘plain’ tests but did never occur in the test with spacer is distortional buckling in direction of the "front"-side with the perforations meant for the beam-end connectors. A picture of this mode can be found in Annex D of the report number "Ncon 12-300-69d". The absence of this failure mode can be explained by the normal-strain resistance of the spacer. For this same reason the spacer seemed to act like a clamping in most other profiles. Despite the results of the tests approach the expectations stated in the hypothesis (See Section 0) quite closely the effective cross sectional areas are difficult to be determined. The effective area is the area which can be used in estimating the critical buckling load of the same profiles with different lengths and steel grades, due to the elimination of these variables. This elimination could be carried out by a trial and error process. By guessing a value for the effective area and calculate the critical buckling load according to the standards, EN 15512:2009 and EN 1993-1-8:2005.

For these test setups, it seems hard to estimate the effective areas. The source of this inconvenience is that the standards do not account for any spacers within the profiles, which possibly might influence its capacity and surely the triggered modes. This is no sheer coincidence, since the objective of this research is to inquire the effect of the spacer, which is currently unknown.

The STUB-test setup do not suggest great dependence from pinching effects. As expected, performance of the uprights is slightly improved after a spacer is inserted, although this effect seems negligible for the ‘Lipped’ profile, which is already strengthened by the lips. Later Finite Element analysis also shows that the lipped profile suffers from excessive initial strains meaning the lips start acting in its disadvantage. See also section 04.5: Results: Static Study.

Further research towards the STUB-setup for local failure seems not to be necessary. The DTB-setup, which accounts for distortional effects on the other hand, does require extensive additional research. A new test setup is required to have also a ‘lipped’ profile failing into distortional mode.

To conclusion of this first series of tests can be summarized by these bullet points:

- Pinching effects are harmless to constructions in which local failure (STUB-test) is normative, this also means no additional research is required regarding the STUB tests;
- The ‘New DTB’ setup in which the upright length is twice as long as the ‘Classic DTB’ setup is not a suitable test setup for the triggering the distortional buckling effect. The reason for this is the increased slenderness which results in global failure of the profiles;
- An alternative test setup should have additional constraints. The freedom of movement for the spacers in the horizontal plane should be blocked.

02.2. Experimental Research on Complete in Frames

Earlier tests pointed out that DTB testing of single uprights with spacers did not fail in the devoured distortional mode. It is believed that testing of a complete frame including 2 uprights and 4 diagonals might give more realistic results for the critical failure loads.

02.2.1. Frame Test Setup

Selected Profiles

The following properties are assumed to have the most potential to influence the critical distortional buckling load:

- Lipped or Non-lipped;
- Size of the upright (first 3 digits of upright numbering);
- Thickness.

Practical issues entailed with testing complete frameworks could be:

- Total height of the framework, the bench press currently available has a maximum of 2620 mm between the compression-plates of the machine;
- Maximum pressure force to be generated in hydraulic pressure cylinder is 800 kN.

With this in mind, including the fact of limited availability of profiles currently in stock, the profiles in Table 6 have been selected. The presence of production tolerances from both the diagonals width and the upright opening cause a potential space between the diagonals and the upright opening. The potential space can be found in Table 7.

Table 6. Selected Upright profiles, the ideal distortional buckling lengths (L_{DTB}) are calculated by CU-FSM, see section 03.2.

Upright Profile	Steel Grade	Thickness [mm]	Lipped or Non-lipped	L_{DTB} [mm]	$L_{Upright}$ [mm]
100 68 20 4050 PR	S355	2.0	Non-lipped	1000	2250
100 72 25 4050 PR	S355	2.5	Lipped	1200	2250

Table 7. Potential space between diagonal-spacer and upright opening as a result of tolerances.

Upright Profile	Opening in Upright & Tolerances [mm]			Diagonal Diameter & Tolerances [mm]			Distance between upright and diagonal and tolerances [mm]			Potential Opening size Range [mm]	
										Min	Max
100 68 20 4050 PR	52	+1.5	-1.0	50	+0.0	-1.5	2.0	+3.0	-1.0	1.0	5.0
100 72 25 4050 PR	51	+2.0	-1.0	50	+0.0	-1.5	1.0	+3.5	-1.0	0.0	4.5

To create a clear overview of the effect of the pinching, it would require at least 3 tests at different pinching sizes, of which the last one exceeds the size possible in practice.

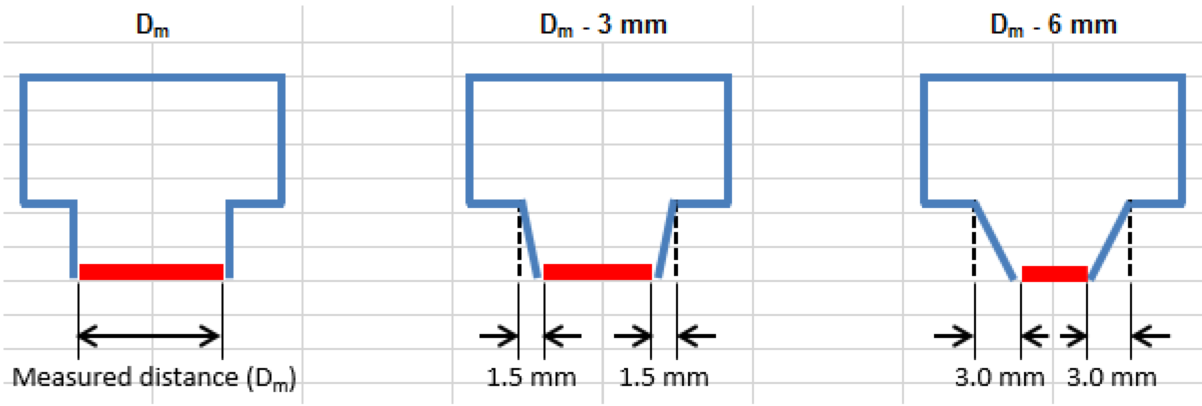

Figure 12. Visualization of Upright Opening Tolerances.

The diagonal spacers that require to be pinched are located at positions B, C, D, E, F and G in the sketch of the setup, see Figure 13 and Figure 14.

Table 8. Number of tests at different pinching Distances. Notice that the total number of tests required is: 12

Profile:		PR 100 68 20 4050	PR 100 72 25 4050	Final Outer Size of the diagonal including spacer [mm]
ED,M =	0.0	2	2	50
space	-3.0	2	2	47
(mm)	-6.0	2	2	44
Number of test in a statistical family of n samples:		6	6	

Required Materials

A rough ‘Bill of Materials’ is given in Appendix I to indicate the most important components of the Frame Test Setup.

Setup of Complete Frame Test on PRF 100 68 20 4050 PR S355

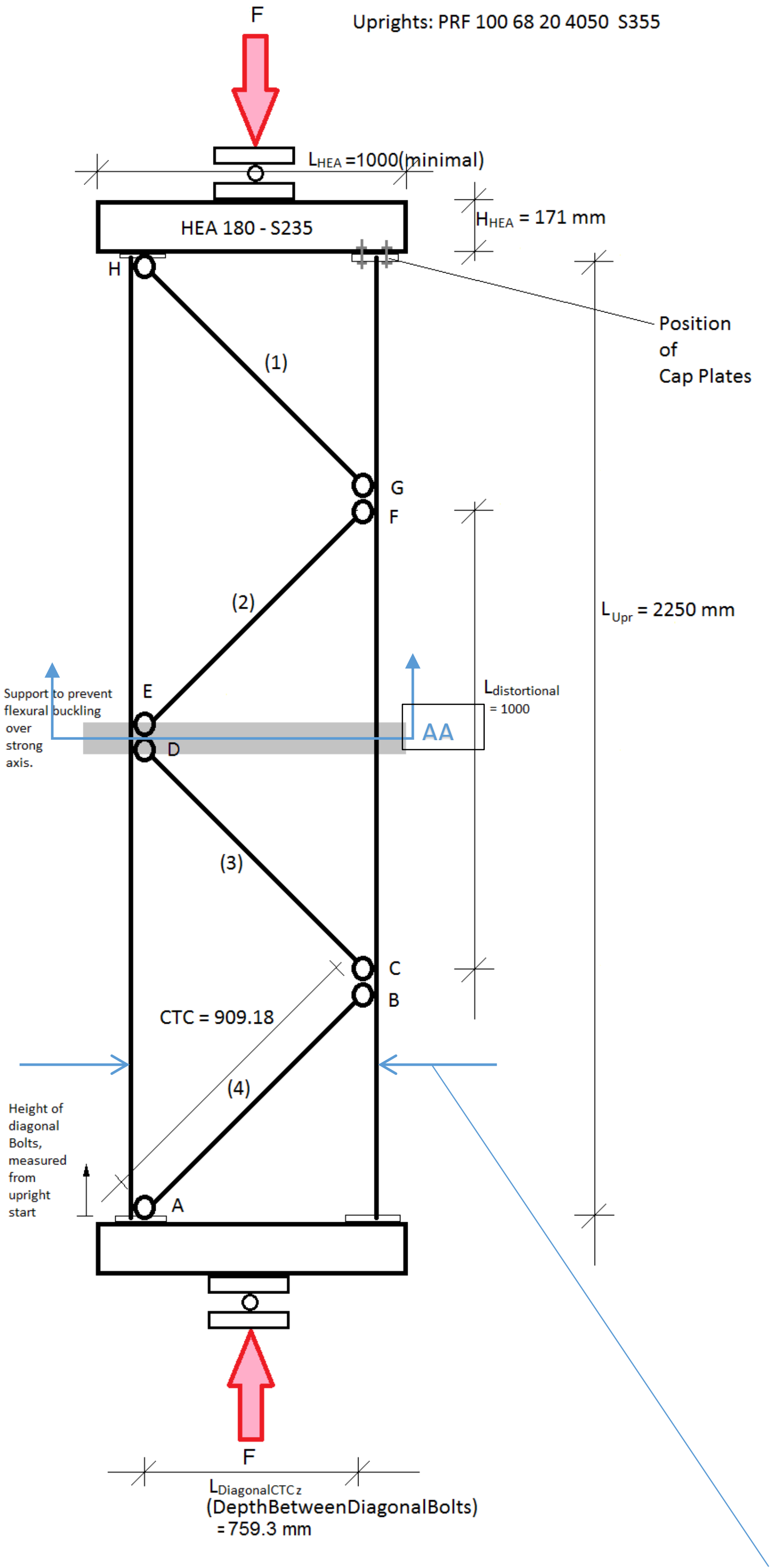

Table 9. Locations of diagonals, measured from bottom of the upright.

Heights of diagonal bolt Connections:			
	A	64	mm
	B	564	mm
	C	614	mm
	D	1114	mm
	E	1164	mm
	F	1664	mm
	G	1714	mm
	H	2214	mm
L_Upright =		2250	mm

Table 10. CTC of the diagonals. The type of diagonals used is 503015, the CTC-lengths is 909.18 mm. For this frame, no diagonals require to be shortened.

Diagonals:		
CTC (inner 2&3):	909.18	mm
CTC (outer 1&4):	909.18	mm

Depth of Frame; uprights outer distance: $L_{DiagonalCTCz}$ + 2*55mm = 870 mm.

Figure 13. Setup of Frame Test on Non-lipped upright profiles. Cross section AA can be found in Figure 15.

Setup of Complete Frame Test on PRF 100 72 25 4050 PR S355

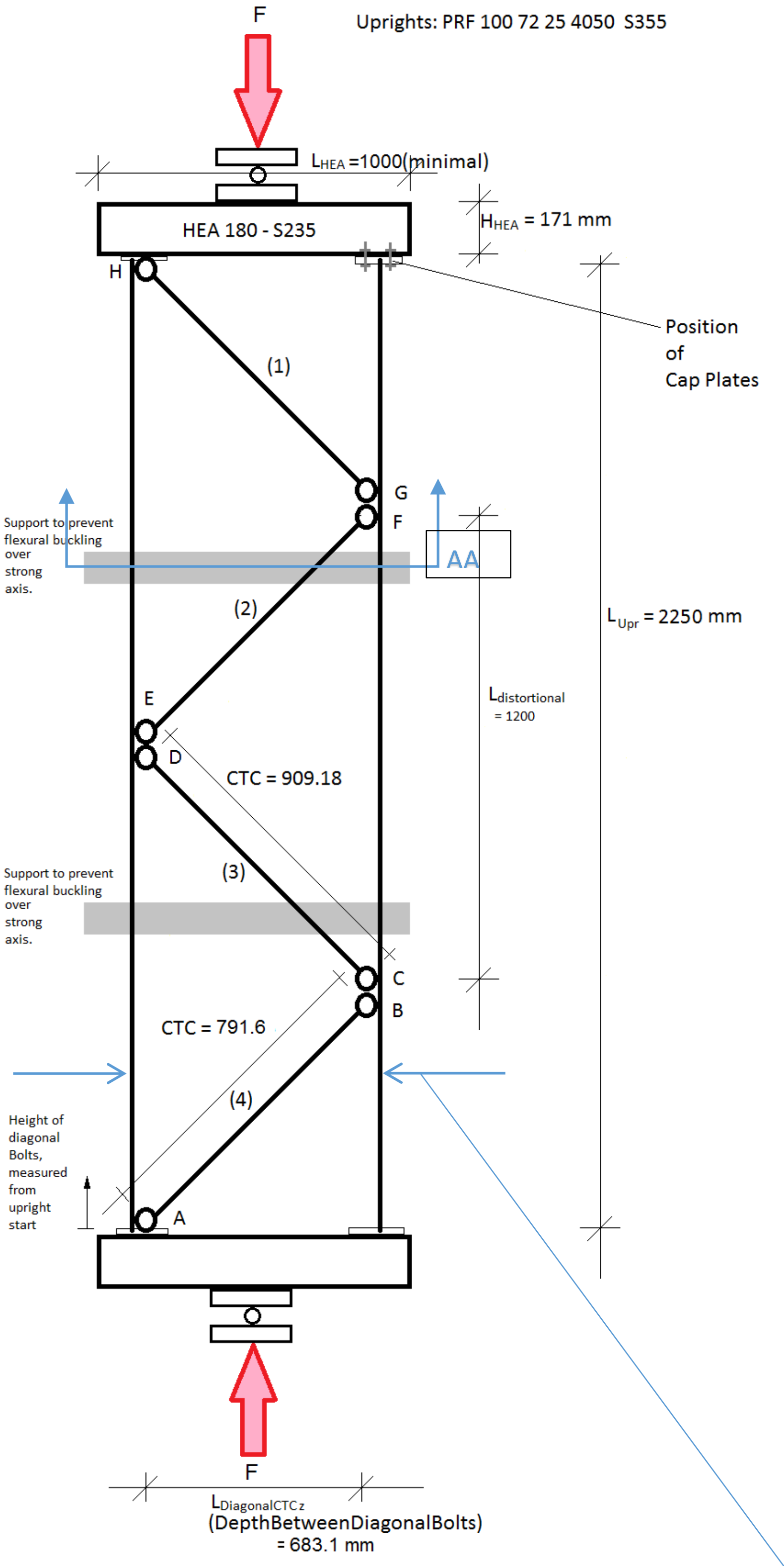

Table 12. Locations of diagonals, measured from bottom of the upright.

Heights of diagonal bolt Connections:			
	A	64	mm
	B	464	mm
	C	514	mm
	D	1114	mm
	E	1164	mm
	F	1764	mm
	G	1814	mm
	H	2214	mm
L_Upright =		2250	mm

Table 11. CTC of the diagonals. The type of diagonals used is 503015, the CTC-lengths is 909.18 mm. For this frame, the outer diagonals will require to be shortened by 84 mm.

Diagonals:		
CTC (inner 2&3):	909.18	mm
CTC (outer 1&4)	791.5859	mm

Depth of Frame; uprights outer distance: $L_{DiagonalCTCz}$ + 2*55mm = 793 mm.

Figure 14. Setup of Frame Test on Lipped profiles. Cross section AA can be found in Figure 15.

Roll Supports

Calculations have pointed out a substantial chance of flexural buckling along the major (y-)axis. To prevent this from happening, some additional roll supports have to be added in the middle of the frame. The type of support is the same for the no-lipped and lipped uprights frame. The same type of support can also be used to prevent torsional buckling about the upright its own axis and about the vertical middle-axis of the complete frame.

After several trials on the non-lipped profiles frame, the best configuration for the supports was finally found to be most realistic and is therefore expected to yield accurate critical buckling loads. Notice that the test setup did indeed change mid-way of the test, which caused the results for the non-lipped profiles frame test to be inconsistent and containing external effects that could not be corrected in the results.

The roll support can be made out of any simple profile available, on precondition of having sufficient stiffness and buckling capacity. Rough calculations indicate the stiffness of the profile in depth-direction of the frame to be at least I = 1.2e6 mm^4 against horizontal bending. A suggestion could be a cylinder 80x80x4 or heavier. The rod profile can be made out of any simple profile that is available, on precondition of having sufficient resistance against buckling. This would make L-profiles quite attractive for application.

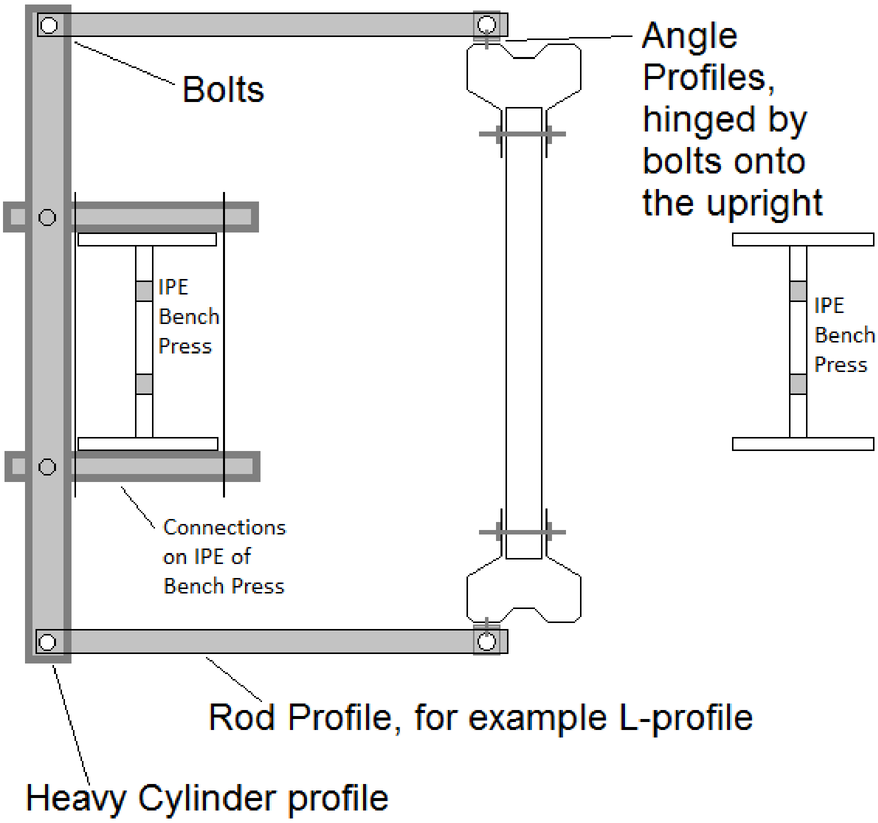

Figure 15. Cross sectional view AA (Top) from support at half-height of the frame. Supports can be mounted at the IPE profiles of the bench press. Rod profiles can be made out any profile in stock, L-profiles are suitable. In the actual setup, three supports are required, see also Figure 16 for the positioning of these supports. For the "Heavy Cylinder Profile", probably an 80x80x4 profile will meet requirements of bending stiffness.

Notice the rod profiles are bolted between the rod which is "fixed" at the IPE and, on the other side at angle profiles resulting in a roll-hinged connection restraining no degree of freedom but the one of displacement in the longitudinal direction of the rod. Adding this restrained will block out the mode of flexural buckling over the major y-axis as well as flexural-torsional buckling about the upright its own axis. The supports also prevent the complete frame from uncontrolled rotating and twisting which is in terms of safety a good addition.

The supports are expected not to initially interfere in the test setup. However, in cases of expressions of unwanted modes, the supports fulfil their job by opposing displacement in this direction and therefor only handling the 2^{nd} order effects. This is also the reason why the stiffness of these components is allowed to be small compared to the actual components to be tested.

The IPE-columns of the bench press would be a suitable place to mount the supporting profile onto. This connection can probably be made with clamp screw tools or a threaded rod.

For both the 2 type of frames to be tested 3 supports are required for the non-lipped- and lipped uprights frame. In Figure 16 the final positions of the supports are visualized.

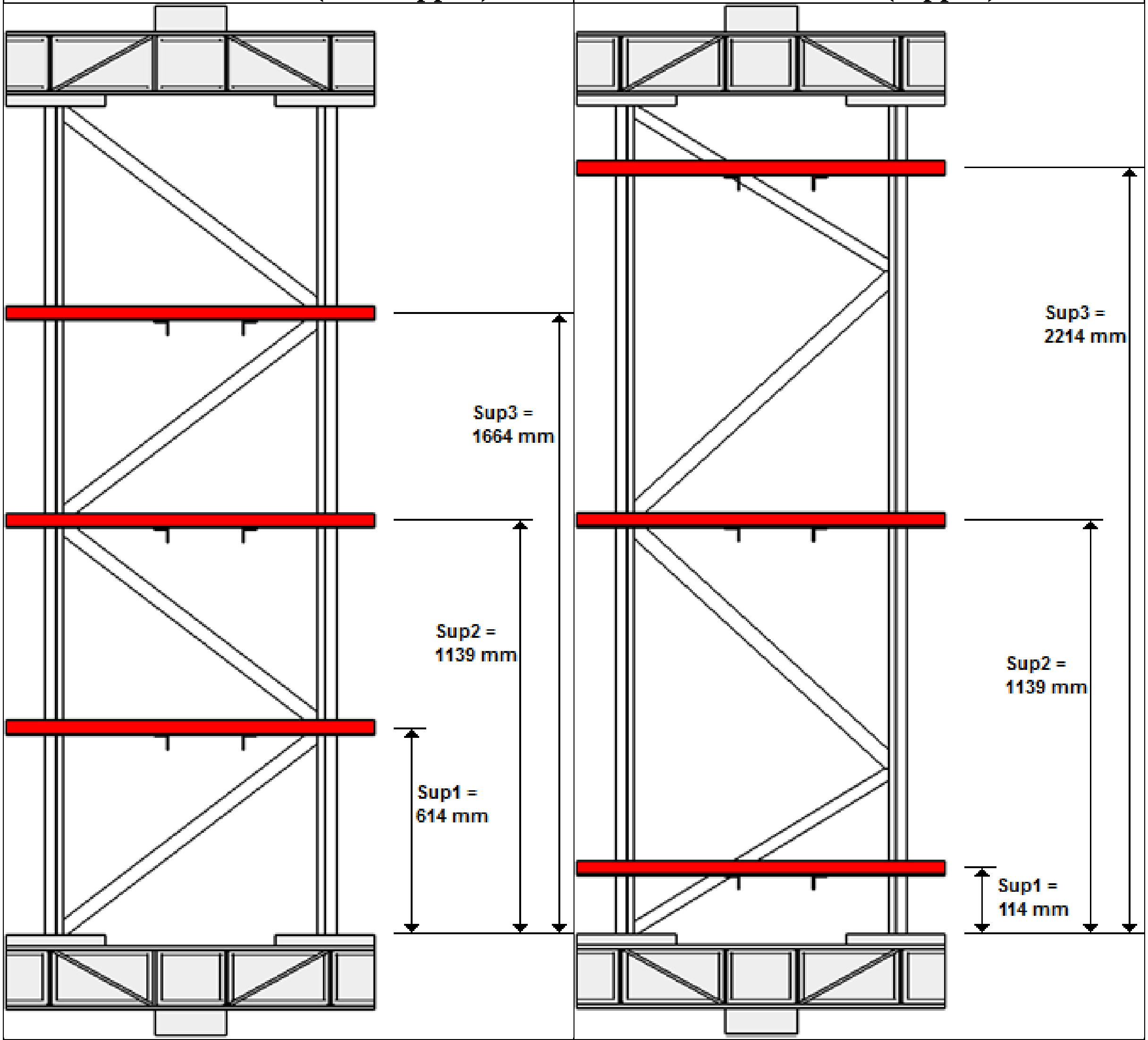

Frame 100-68-20-4050 (Non-Lipped)	**Frame 100-72-25-4050 (Lipped)**
Sup 1: 614 mm (Diagonal bolt C) Sup 2: 1139 mm (Middle) Sup 3: 1664 mm (Diagonal bolt F)	Sup 1: 64 mm (Bottom) → 114 mm Sup 2: 1139 mm (Mid) Sup 3: 2214 mm (Top) → 2114 mm

Figure 16. Positions of supports, heights measured from bottom of upright.

The supports will therefore coincide with the diagonals in both frames, which have different dimensions in the non-lipped profiles frame and the lipped profiles frame. Moreover, the frame is stabilized against twisting and flexural buckling. It is expected that the current support type for the lipped profiles frame results in the most realistic behaviour. Take notice the slightly changed placement of the supports. This change was done after the testing of the non-lipped profile and before the test series for the lipped profile. The change in setup is taken into account into the evaluation by a minor change in eccentricity.

02.2.2. Evaluation of Experiments on Frames

The evaluation of test results is carried out according to the Euro Codes EN 1993 and FEM 15512:2009 likewise the earlier DTB & STUB column compressive tests. The global idea of the progress is given in this section.

The rough output of the test setup is a datasheet per sample containing the applied load versus the total displacement, measured on top with a strain gauge along the upper Ball Bearing. Additional information can be found in photographs made before and after testing. In order to check the actual mode shape at the failure point (Ultimate load), a video recording was made.

Sidelings' of the frame test setup, a tensile test was taken out of a part of the undamaged uprights after they were tested. In the tensile test the actual yield strength and thickness of the sheet metal was measured.

The results of the frame test setup are evaluated in a similar way as the earlier tests on the DTB and STUB column compressive tests. This evaluation has roughly the following pattern:

- Sorting and selection of the rough test results on the basis of expressed failure mode according to photographs and therefore determine validity of test results;
- Apply a correction factor for the observed material yield point compared with the design yield point;
- Apply a correction factor for the observed material thickness of the sheet metal;
- Plot the corrected failure loads against the varied pinching distances and employ the method of least squares to fit a 2^{nd} order polynomial to the data points;
- Normalize the corrected test results with the so 'fitted' polynomial function value at that point;
- Find standard deviation of the 'normalized' data and apply a statistical evaluation to assess the 95% fractile at confidence level 75% which should led to the characteristic loads which could be compared mutually;
- This characteristic value could be used to find the effective area with an iterative technique using trial-and-error estimates of the effective area compared with their corresponding resulting failure force. The reduction in effective area could also be compared among each other and with the 'reference' situation of no spacers. These last value should theoretically be the same although the frame test setup contains slightly more flexibility in constraints. The actual constraints allow for many more degrees of freedom in practically all directions at the point of the spacers which was taken as a 'reference' to the 'fixed world'.

Detailed evaluation of results can be found in Appendix D: Frame Test Evaluation.

02.2.3. Analysis of Experimental Results of Frame Tests

Characteristic loads and effective areas can be extracted from the evaluation and compared among each other. Beside actual performance of the profiles the failure shapes are quite important in explaining internal behaviour of thin walled profiles and interacting between modes and corresponding load factors.

The observed failure modes were practically all the same for the same profiles. The non-lipped profile failed in symmetric distortional mode, with the opening in the middle of the profile growing larger. The lipped profile on the other hand showed a combination of Flexural Torsional Buckling (FTB) and A-Symmetric Distortional, with both flanges buckling in the same direction.

From the evaluation of the test results characteristic ultimate loads can be determined. These are shown in Figure 17.

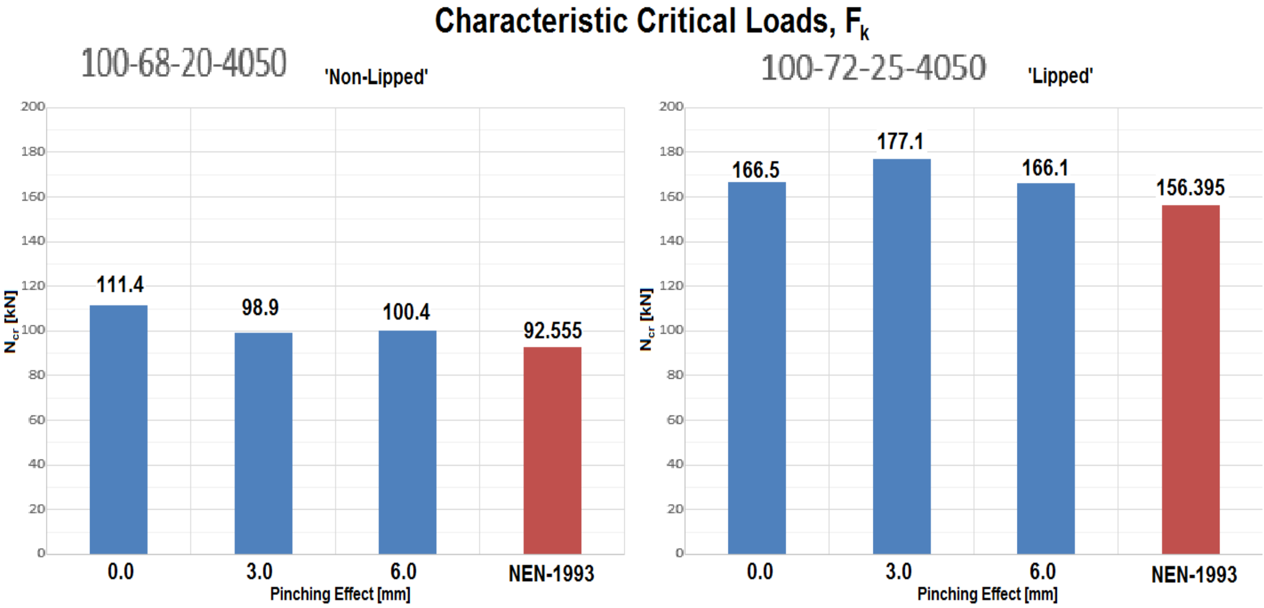

Figure 17. Characteristic Ultimate (=Critical) Loads for the Non-Lipped and Lipped uprights. The number of useful samples for statistical evaluation are n = 4 for the Non-Lipped profile and n = 5 for the Lipped profile.

At first sight, the reduction in capacity does not seem dramatic and in all cases performance meets the ones which the standards ascribed to the profiles. According to FSM and FEM simulations as explained in the chapters 03.2 and 04 respectively worst cases are reached for the non-lipped profile. Anyway, for the lipped profile this is proven to be not the case. The simulation results show different types of modal expressions and it was dubious what the effect could be of the combination of a-symmetric distortional and flexural torsional mode after pinching. The results show both an increase and a reduction in strength. The increase in failure load can be the results of the pinch effect which ‘pulls out’ the distortional mode, leaving only the flexural torsional mode to be able to have the profile failing, which increases the total resistance. The decrease could be the result of bending of the diagonals. In this way, the diagonals give way to the development flexural torsional mode meaning the actual effective buckling length in the FTB mode is a little longer than the earlier assumed distance between the collective geometric centroid of the two sets of diagonal spacers. At heavier pinching effects, also the resistance against the FTB mode reduces, which seem to neutralize the consolidation from the banned distortional mode.

The capacity ascribed by the standards is calculated without any safety factors. Although the non-lipped profile shows a decrease in capacity after pinching effect are applied, the characteristic strength of the profile is still larger than the capacity ascribed by the standards. This means that the pinching effect is relatively harmless for non-lipped profiles.

It is clear to see that the lipped profile shows an actual increase in strength after pinching. This might be caused by the diagonals, which have a larger stiffness for the 3.0 and 6.0 mm pinch frames than the 0.0 mm pinch frame. The normative mode of failure in all situations in the lipped profiles was Flexural Torsional Buckling (FTB), whereas the non-lipped profile tended to buckle in the Distortional mode. Diagonals with a larger stiffness increase resistance against failure in FTB mode. The reason for the differences in diagonals was practical convenience. Applying pinching effects by compressing ‘standard’ NEDCON diagonals resulted in deformations of the web of the diagonal, resulting in complications at assembly of the frame. The solution to this problem was application of u-profiles

(40x40x3) and adding extra washers of thickness 1 mm until the devoured total diagonal width is reached. Moreover, an increase in strength might be the reason of the pinching effect, which will be explained in Chapter 04.

Effective areas

Because of the large reductions in total stiffness of the frame test setup, also the effective area are reduced. When the finite stiffness of the setup environment is taken into account, all of the resulting effective area would significantly improve. However, it is hard to prove the presence of certain stiffness in any arbitrary direction and their influence on the actual results. In future tests the constraints applied should be made as stiff as practically possible and other degrees of freedom assumed non-stiff should be ensured of free movement.

Table 13. Effective areas and their reductions of the 0.0-pinch with respect to the 'plain' situation and the -3.0 and -6.0 pinch relative to the 0.0-pinch situation.

Profile		100-68-20-4050 (Non-Lipped)		100-72-25-4050 (Lipped)	
		A_{eff} [mm^2]	Red. factor [-]	A_{eff} [mm^2]	Red. factor [-]
Pinch [mm]	No Spacer	472.0	0.822	707.6	0.765
	0.0	388.1	1.000	541.1	1.000
	-3.0	334.5	0.862	582.0	1.076
	-6.0	340.4	0.877	539.7	0.998

Recommendations for Frame Bench Press Setup

This type of complete frame compressive test setup experiments are relatively new. This means new insight can be gathered after every single test on a sample. During the first test on the non-lipped 68-profile, many adaption were made resulting in insufficient useful samples to meet a complete statistical evaluation according to the Euro Codes. To create a more ‘standardized’ test setup the following bullet points might be of interest.

- The top beam of the setup was previously taken as a HEA-180 S235 profile and should have just slightly larger than largest expected failure force, based on a 95% fractile at 75% confidence. Better option would be to use a HEB- or maybe even better a HEM- profile and include a safety factor of 1.5 and probably increase this to 2.0 if deflection seems still large.
- Moreover, the expected displacement and angle of rotation at the connection of the upright should be checked for acceptability. If expected introduced rotation exceeds a bending resistance capacity of 5% and probably less if future tests show heavy reductions in 0-pinch situation compared with no-spacer DTB tests or simulation expectations;
- Before testing the final setup Finite Element Analysis should have pointed out that a symmetric distortional mode only is expressed. Modal analysis could be used to assess load factors for at least 3 modes and probably more to check for close concurrence of neighbouring modes. In case of undesired modes with close encountering load factors, adaptions could be considered to be applied. It is advised to first consider changing the length of the potential distortional length;
- The failure mode most likely to reduce the capacity most after pinch is shown to be the symmetric distortional mode. This mode should therefore in all cases be the simulation result of the test;
- The supports to prevent flexural buckling over the major axis of the profiles (FBy) are preferred not to be placed within the domain of the profile that is meant to deform

distortional. The number of supports should be at least 4 with one of the support at the lower and one at the upper diagonal joint's centroid. The other two should be placed at the highest and lowest point respectively to prevent complete rotating or torsion of the frame. Moreover the clamped situation within the upright is ensured;
- Supports should be connected with angle profiles into the round holes of the front perforation pattern of the upright. The angle supports might be considered to have some rotational resistance or not, although the most important function of the supports would be to prevent displacement. This will mean that backlashes in bolts should be prevented as much as possible;
- Always use the same diagonal profiles for all sample tests within a family to ensure allowance for comparison of samples within a family, even in case of discovering an unexpected A-Symmetric or Flexural Torsional Buckling expression after initial tests or deeper simulations.

Conclusions from Experimental Research

The experimental research should answer sub question 1:

'What would be a suitable test setup and how can the test results be evaluated?'

- Pinching effects are harmless to constructions in which local failure (STUB-test) is normative, this also means no additional research is required regarding the STUB tests;
- Pinching effects can have significant impact on capacity of constructions in which distortional buckling effects are normative;
- The Frame test setup seems to be a suitable test setup to test uprights exposed to pinching effects;
- Evaluation of results can be done according to the standards, similar to the evaluation of the 'classic' tests on single uprights.

03.Linear Elastic Theoretical Buckling Models

In the literature a number of standardized techniques can be found to access the buckling shapes and critical loads of thin walled profiles. The most sensible methods are carried out here. The first method is a rather simple semi empirical and theoretical approach, based on linear plate buckling as stated in his book by (Megson, 2014). This method will be used to find comparative data for STUB-column test data. The effect of distortion will be approached with the Constrained Finite Strip Method, discussed afterwards. This method contains numerical as well as theoretical characteristics.

03.1. Linear Plate Buckling Theory

An estimation formula derived from aeronautical design of stiffened panels for aircraft hulls to find the local buckling load factor is explained here.

Plenty of estimation techniques have been developed on the basis of experiments and research. Values of local buckling stress have been determined by Boughan, Baab and Gallaher for buckling in stiffened panels. (Megson, 2014) Extensive summarizing can be found in works of Gerard, which resulted in a semi-empirical solution which will be assessed here. (Gerard & Becker, 1957) Although their models are optimized for stiffened panels and columns, upright profiles are assumed to act likewise in local failure behaviour.

The expectation is that this formula will not give a really helpful tool for estimating of actual failure load for thin walled profiles prone to premature post-plastic buckling behaviour. Nevertheless, the estimation technique could show give a quick estimate to compare several design among each other and probably estimate performance after pinch effects. This kind of estimations could be used as an educated guess for comparing the effect of geometric changes that potentially alter local buckling behaviour. For derivation of the method see (Megson, 2014) and (Gerard & Becker, 1957).

$$\frac{\bar{\sigma_f}}{\sigma_{cy}} = \beta_g \left[\left(\frac{gt^2}{A} \right) \left(\frac{E}{\sigma_{cy}} \right)^{\frac{1}{2}} \right]^m \qquad \text{(Eq. 1.)}$$

Where:

A = Cross Sectional Area of the column;

B_g & m are empirical constants; Experiments on simply supported flat plates and square tubes of various aluminium and magnesium alloys and steel show that b = 1.42 and m = 0.85 fit the results within ±10 percent up to the yield strength. Corresponding values for long clamped flat plates are b = 1.80, m = 0.85. For the uprights b = 1.42 can be taken.

g = number of cuts required to reduce the cross-section to a series of flanged sections plus the number of flanges that would exist after the cuts are made, see also Figure 18;

t = material thickness (varies between 2 – 4 mm for most profiles);

E = Elasticity modulus of material = 210 GPa for steel;

σ_{cy} = compressive yield strength of the material in this case this can be taken as the tensile yield strength which is 355 MPa for structural steel S355.

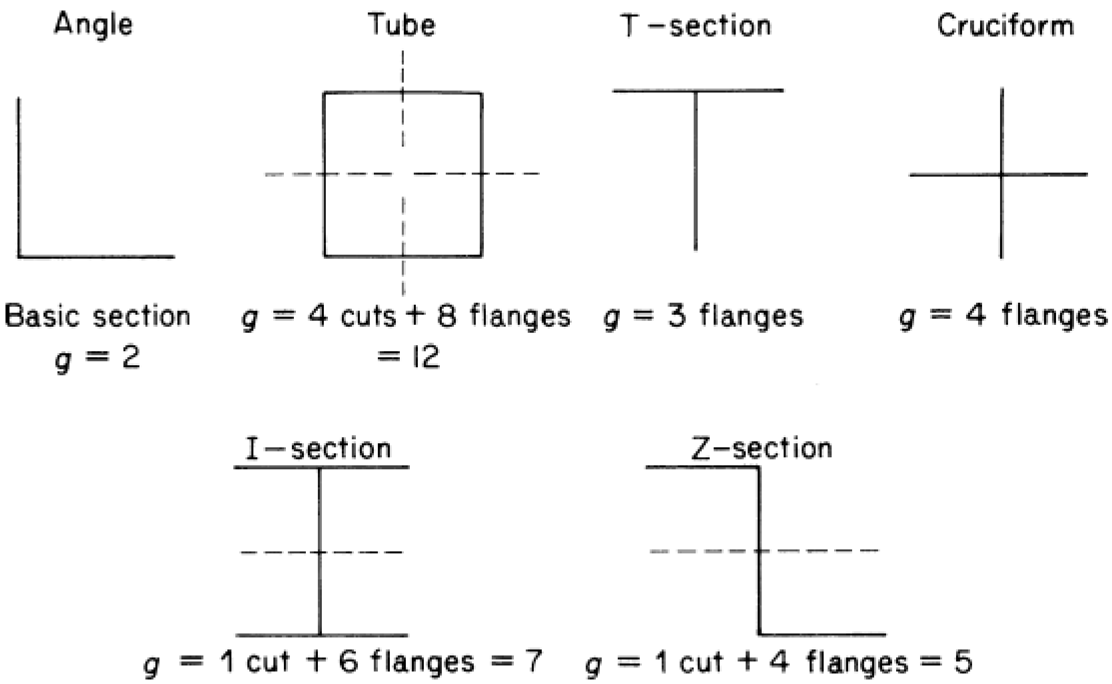

Figure 18. Number of cuts required to reduce the section to a series of flanged sections. Source: (Megson, 2014).

The attending reader may have already counted some upright profile corners and should be able to observe the number of cuts and resulting flanges.

Table 14. Number of cuts and flanges for a 'standard' storage rack lipped- and non-lipped profile.

Profile	Non-Lipped	Lipped
# Cuts Required	5	7
# of resulting flanges	12	16
g = cuts + flanges =	**17**	**23**

The calculation of the estimated load factors for a non-lipped and a lipped profile is extracted in Table 15.

Substituting the terms of the formula with the values stated shows the following load factors:

Table 15. Calculation of estimated local buckling critical failure Load Factor.

Type:	Non-Lipped Profile	Lipped Profile
Full Definition:	PRF 120-78-25-5070 S355	PRF 120-83-25-5070 S355
Base Material, before cold forming (Steel Strip) =	305 × 2.5	340 × 2.5
Empirical Constant, g =	17	23
Included spacer g =	26	32
Material thickness, t [mm] =	2.5	2.5
Cross Sectional Area [mm^2] =	762.2	850
$\frac{\bar{\sigma_f}}{\sigma_{cy}} = \beta_g \left[\left(\frac{gt^2}{A} \right) \left(\frac{E}{\sigma_{cy}} \right)^{\frac{1}{2}} \right]^m$ No Spacer	4.0	4.7
Spacer	5.8	6.3
Increase in buckling load after having a spacer:	+43.5 %	+32.4 %
Increase in strength by the lip of the profile	+ 17.9 %	

The increases after placement of the spacer is quite substantial. This is reason is of course that the spacer is taken as a full set of flanges, which is quite progressive. In the experiment, the rest of the STUB-column where no spacer is present the actual profile has a lower empirical ‘g’-constant meaning a much lower resistance against local failure.

This estimation method seems legit when it comes to comparing situations among each other. Anyway, for deeper analysis involving prediction of modal expression or failure loads more complex models are required.

03.2. Constrained Finite Strip Method

In this section the semi-theoretical method of the Constrained Finite Strip Method (cFSM) will be discussed. The finite strip method approaches the buckling modes of thin walled profiles using a number of finite strips, reaching over the full length of the profile. The constrained finite strip method is also used for determining the most optimal buckling lengths for the distortional buckling tests.

The goal of the DTB test is to find the critical torsional buckling load. To obtain conservative test results it is important to choose the length of the profile that is most sensitive to deform distortional. The obtained distortional buckling upright test length is tested in the stub column test setup described in Annex A of EN 15512:2009. In Distortional buckling, changes in the cross sectional geometry results in failure of the profile. Distortional buckling can be recognised by the collapse or widening of the end flanges over the whole length, like displayed in pictures (b.) and (d.) in Figure 6 (see page 17).

The normative length for the distortional buckling can be found by testing a large number of arbitrary lengths and find the minimum failure force, this is a rather expensive and time consuming activity. Another alternative could be to simulate various options with Finite Element Solvers, which requires a lot of computing power and also takes a long time to run.

A better alternative would be the Finite Strip Method (FSM) as described extensively in the book 'Finite Strip Method in Structural Analysis' by (Cheung Y. , 1976). This model, which models thin walled profiles as a number of strips with variable thickness and width but all with equal lengths has the same characteristic as the Finite Element Method (FEM). It is basically a simplified version of the FEM. The difference between FEM and FSM is also visualized in Figure 19. A practical application of the FSM is the Cornell University Finite Strip Method (CU-FSM). This application originates from the University of Cornell (Ithaca, United States) and is extended by many others, among a large share from Professor Ben Schafer's Thin-Walled structures research group at the Johns Hopkins University (Li & Schafer, 2010) is CU-FSM.

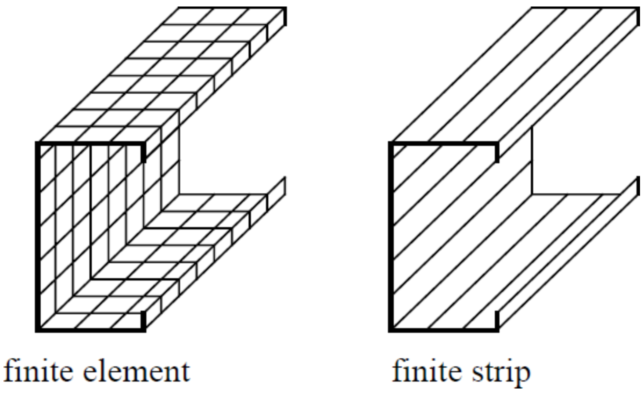

Figure 19. Finite Element and Finite Strip discretization. Source: (Schafer, 1998).

For the prediction of the distortional buckling lengths and the degree in which certain modes are expressed, the software CU-FSM v4.05 is deployed. CU-FSM is open source software, written in Matlab code. An important consideration to keep in mind is that the Constrained Finite Strip Method (cFSM) cannot account for changes in cross sectional geometry or half-way initial stresses and strains like diagonal spacers. This application of FSM can only be used to estimate the triggered modes of the 'plain' profiles.

03.2.1. Boundary Conditions

The modelled boundary conditions should apply with the ones of the test setup. Within the test setup, the upright is welded on 10 mm thick cap plates which are themselves supported by ball bearings. The centre of the ball bearings is located 80 mm in total from the end of the upright. The cap plates are simply connected while the upright itself is 'clamped' onto the cap plate. This boundary conditions is not available within CU-FSM.

The flexural buckling can occur freely over the clamped part, but the distortional buckling will experience a 'clamping' due to the welding at the flanges. The pinned connections are believed to have negligible influence on the distortional buckling modes, and for this reason the clamped boundary condition in CU-FSM will be reasonably accurate. Earlier research at NEDCON and by (Casafont, Pastor, Roure, Bonada, & Pekoz, 2011) also stated this as a valid solution to similar problems. In the boundary conditions input, the "clamped-clamped" option is applied. The model input can be found in Figure 62 in Appendix J.

An issue that needs to be kept in mind, is that the boundary conditions are only valid for the actual distortional buckling failure criteria and not for other mode types. Because distortional buckling is the failure mode of interest, the "clamped-clamped" boundary condition will hold.

03.2.2. Cross Section geometry

Earlier research at NEDCON also pointed out that the detailed modelling of corners within the cross section does not have significant influence the results, see also ' (Assink & Horácek, 2014, pp. 16-17)'. In CU-FSM, the cross section is for this reason simplified the sense of number of element-entries.

The number of elements is a compromise between accuracy of results and saving computation time. In earlier tests, every notional side (important upright cross section part, web/flange) was divided in 4 elements. Carrying out the calculation for 8 elements per important side seems not to yield significant differences in results, although it shows the potential different degrees of modal expression at small intervals of lengths. This is shown in Appendix H. CU-FSM Analysis of the uprights applied in the Frame Test Setup, also, due to the creation of singular stiffness matrices results might become inaccurate. This actually means that more elements yields worse results. Running the same simulation with less elements, namely two elements per side, results in nearly the same values as with 4.

Applied External Load

The external load can be specified along with the nodal coordinates. The applied load type is the same as for the STUB and DTB test setup, it is a uniform compression load. CU-FSM uses linear buckling theory (Assink & Horácek, 2014) and therefore it is advised to take the upright yield stress as the external equivalently distributed load. The material of the uprights in the test setup is S355JR.

03.2.3. Perforations

The actual profile does not have a constant cross section but has perforations. However, Finite Strip Models are limited to strips of constant thickness. The only way to somehow include perforations is by applying a reduction factor and in this way obtain the equivalent element thickness.

A possibility for inclusion of the reduction is to look at the bending stiffness of the perforated and the non-perforated part. The bending stiffness of the modelled non-perforated profile with reduced thickness should be the same as the perforated profiles. The derivation is as follows;

Let 'L' be the perforation pitch length (see Figure 20), and;

'L_{np}' the length of the non-perforated part (see also Figure 20), and;

I_1 The moment of inertia of the non-perforated part, and;

I_2 The moment of inertia of the perforated part, which is of course equal to zero.

Then calculate the thickness as:

$$I_{eq} = I_1 + I_2 = I_1 + 0 \quad \text{(Eq. 2.)}$$

$$\frac{1}{12} * L * t_{eq}^3 = \frac{1}{12} * L_{np} * t^3 \quad \text{(Eq. 3.)}$$

$$t_{eq}^3 = \frac{L_{np}}{L} * t^3 \quad \text{(Eq. 4.)}$$

Where

$$L_{np} = L - L_{perforation} \quad \text{(Eq. 5.)}$$

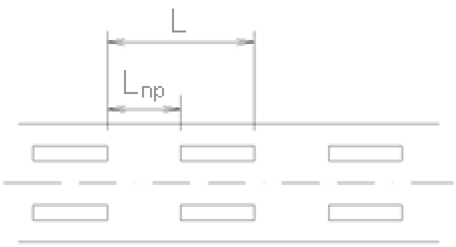

Figure 20. Perforation pitch and length of non-perforated part.

Casafont improved this formula by adding an extra safety factor of 0.9. While using this formula, the CU-FSM model approaches the distortional buckling slenderness within a range of 3%. The formula of Casafont which is finally employed in the input of the model looks like:

$$t_{red} = 0.9 * t * \left(\frac{L_{np}}{L}\right)^{\frac{1}{3}} \quad \text{(Eq. 6.)}$$

When using this reduction of elements, it is necessary to make sure the width of the perforation should be equal to the average width of the perforation. This means when the perforations have variable widths, which is the case in trapezoidal and round shapes of the –PRF- coded profiles, the reduction factors should have a linear match with the widths along the perforations.

03.2.4. Upright lengths

The lengths at which modal analysis is required should contain the complete range of upright lengths used in NEDCON's structures, which is between 300 mm and at least 3000 mm. Another requirement is that the maximum length simulated in the model does not fail under distortional circumstances. The flexural buckling will become normative for the longer lengths. The step size should not be too large to prevent concealing strong local pits in Load Factor against Length Curve. The chosen step size is 50 mm, which coincides with the perforation pitch and is therefore the standard possible variation of applied profiles in NEDCON's structures.

03.2.5. Example of Input

For one of the non-lipped profiles, the input is displayed here. First, the cross sectional geometry is shown in Figure 21, including the applied load at all elements equal to 355 MPa. Some additional tool in CU-FSM calculates several static properties of the cross section, see Figure 22.

120 78 25 5070 PR

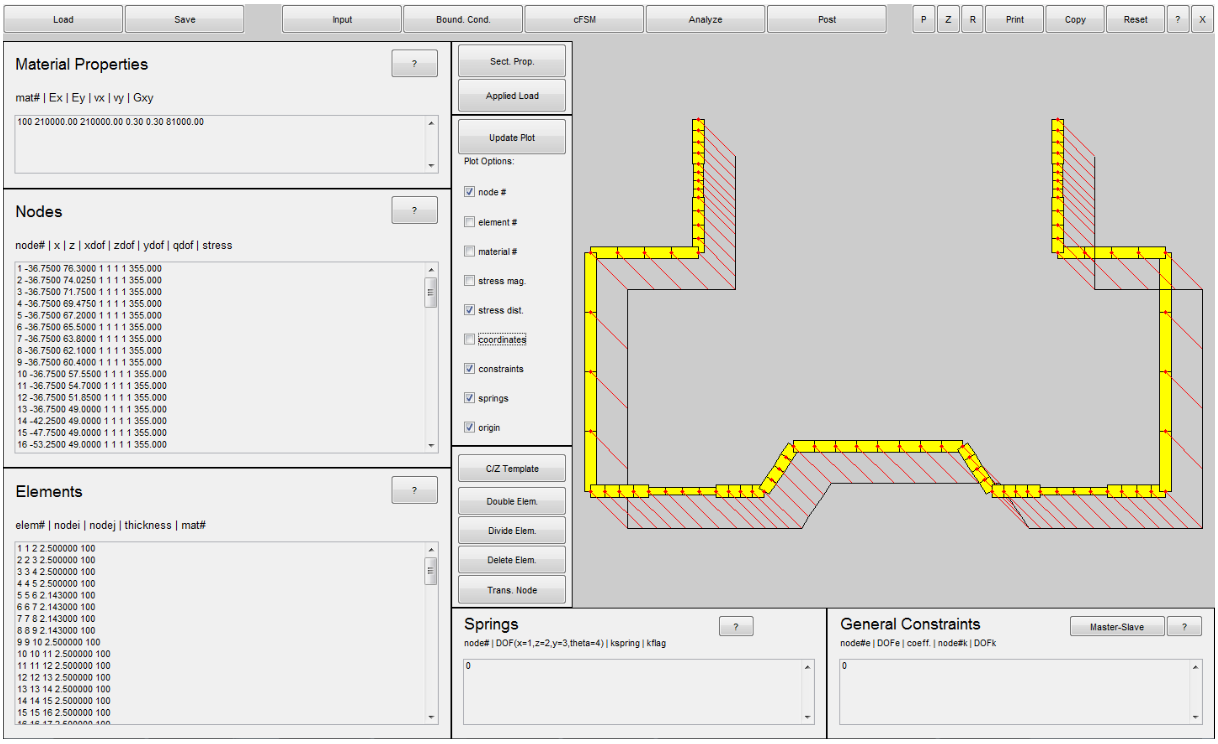

Figure 21. Example of input of the non-lipped profile.

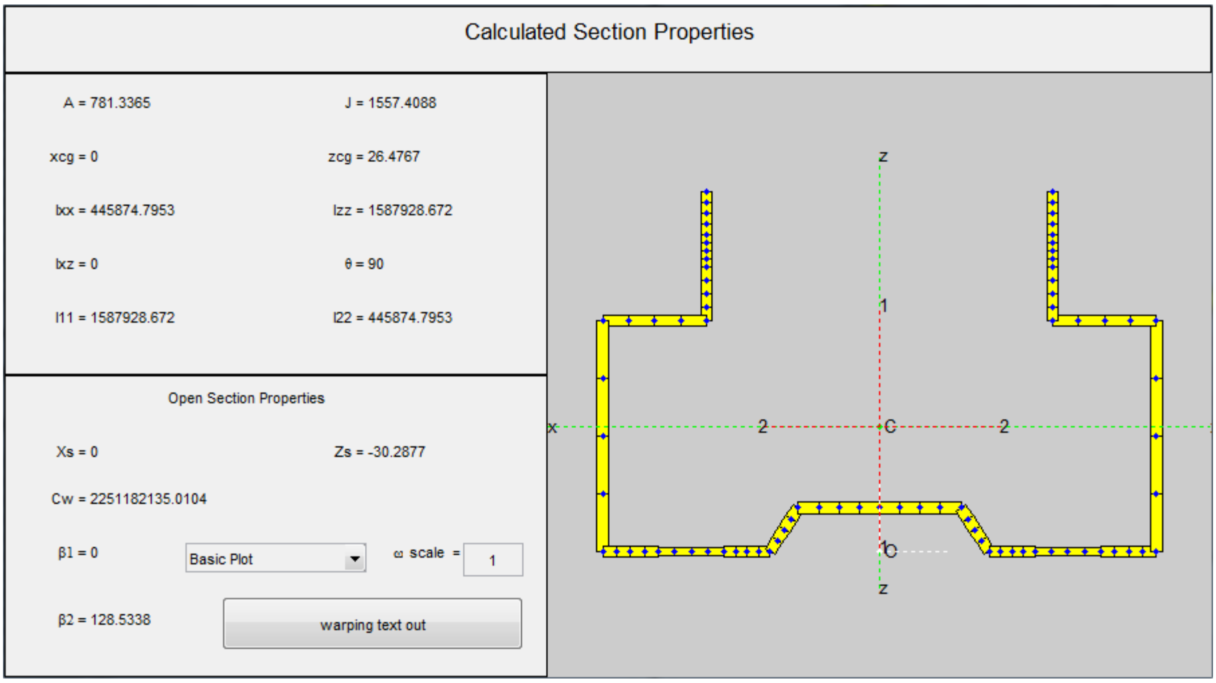

Figure 22. Intermediate results: Section Properties.

The input for other profiles investigated can be found in Appendix H.3. for the 100-68-20-4050 profile and Appendix J for the 120-83-25-5070 profile.

03.2.6. Constrained Finite Strip Method

The intermediate results show the shapes of the possible modes. In general there are three kind of modes which are likely to be normative; the global, distortional and local modes. Within all kind of modes several sub-modes can be distinguished. In theory, the number of possible modes is infinite and for this reason only the most important ones are shown in Figure 23 and Figure 24. The modes most likely to occur are the Distortional- (symmetrically outwards) and the global Flexural Torsional Buckling (FTB) modes D1 (in Figure 23) and G1 (in Figure 24).

120 78 25 5070

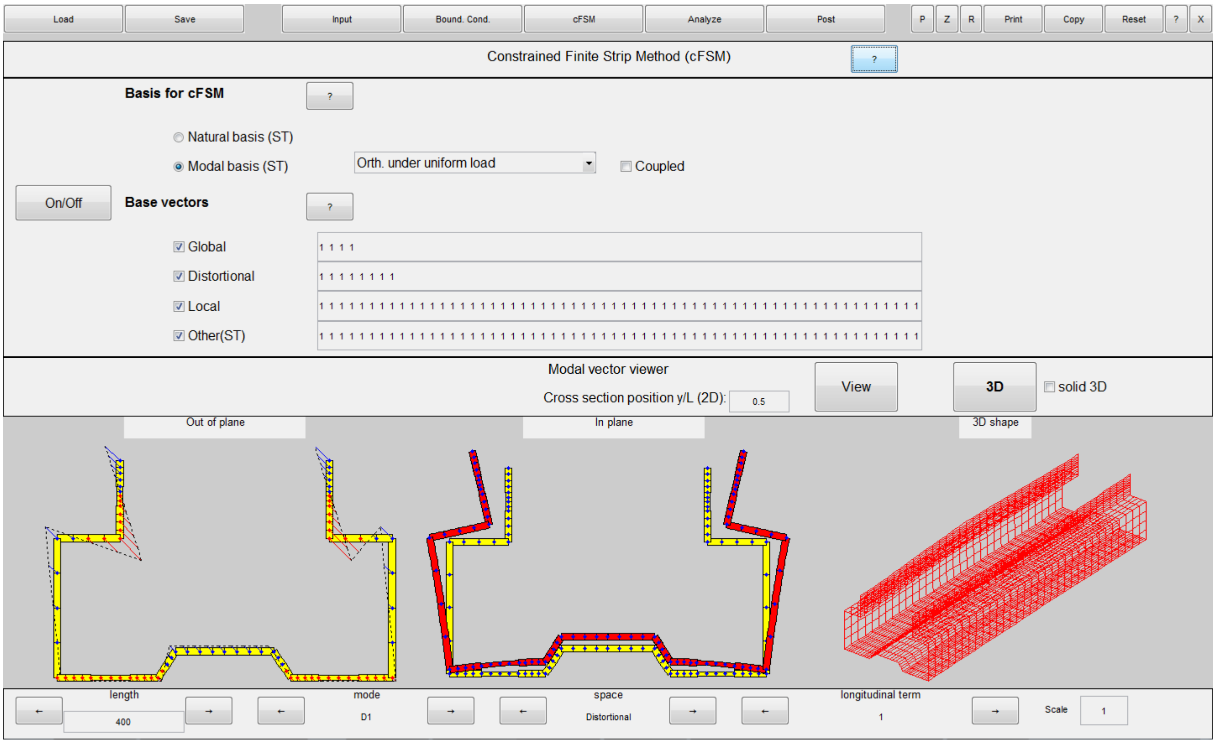

Figure 23. First distortional mode (outwards bending of flanges)

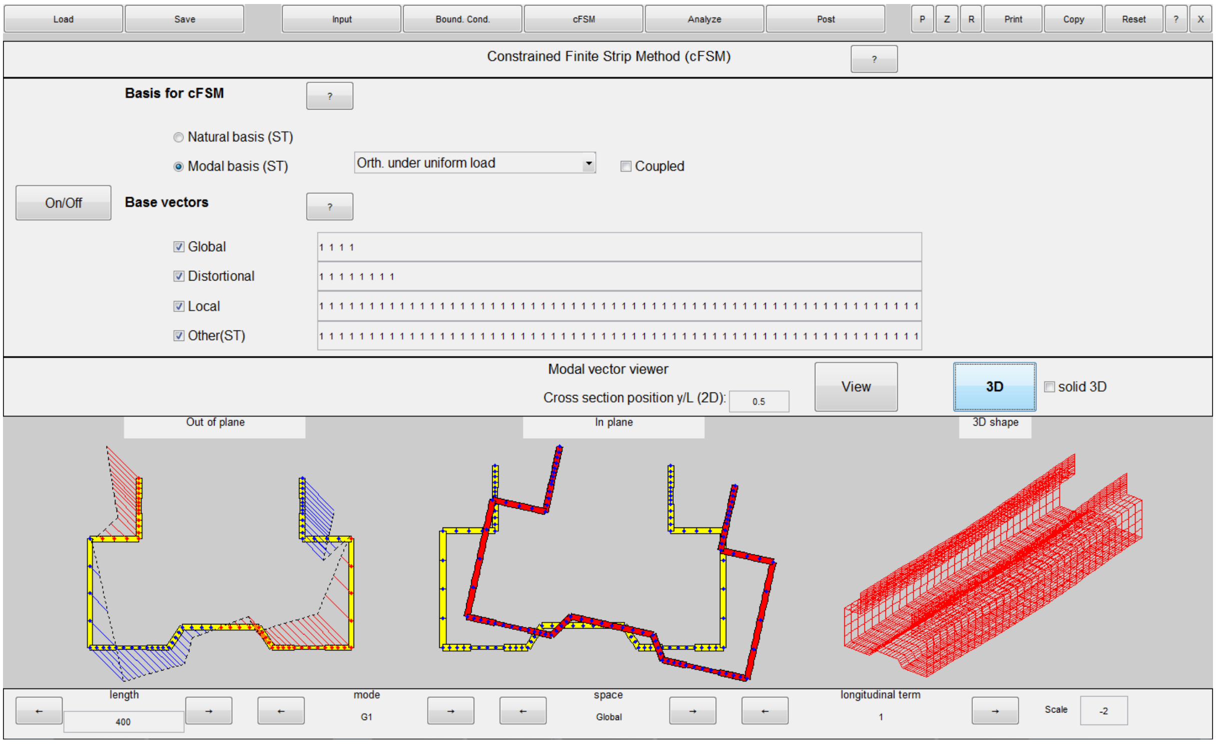

Figure 24. First global buckling mode (Flexural-Torsional, along full length)

03.2.7. Example of Results

An example of possible results is displayed here, according to a non-lipped profile. Other results of its lipped brother can be found in Appendix J.

The most important result is the Load Factor Length Diagram, like displayed in Figure 25. In this diagram, the (linear elastic) load factor is plotted against the input lengths of the profile. Colours are used to classify the modes. Multiplying the load factor with the applied load should give the critical load for linear elastic buckling. In a real world situation, the profiles will fail under lower critical forces, because of (non-linear) yielding in the material.

120 78 25 5070 PR

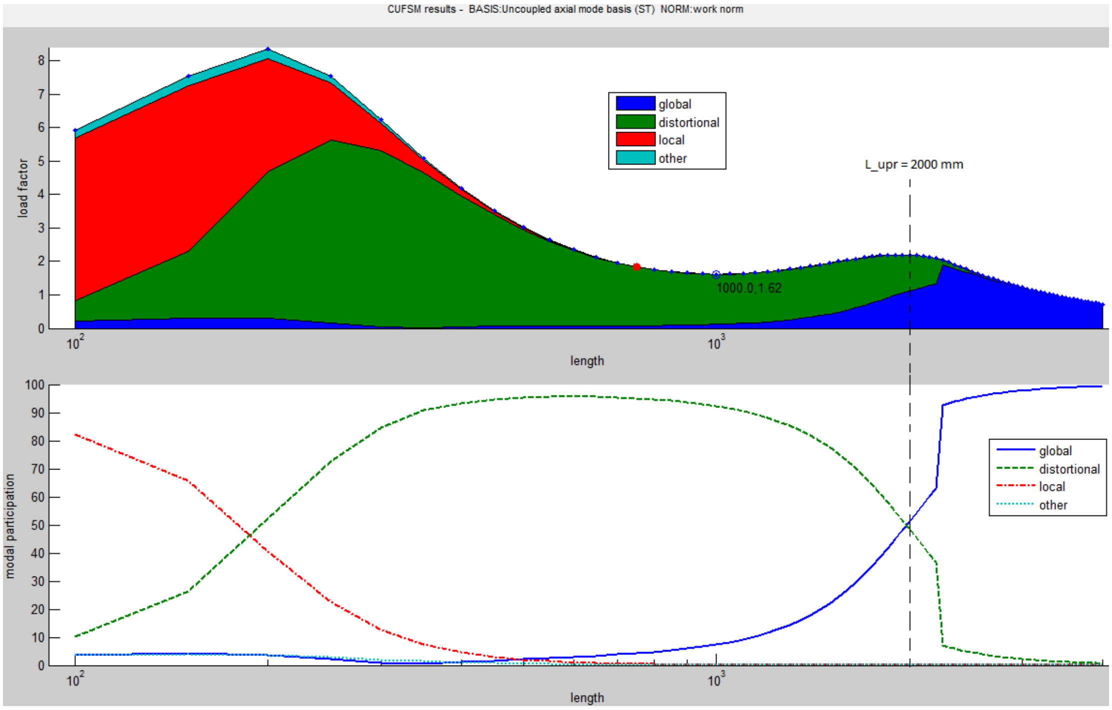

Figure 25. Load factor versus Length diagram. The colours indicate the degree of expression of a mode. The black dotted line indicates the applied 2000 mm upright length applied in the DTB tests with spacers. It is difficult to say which mode is dominant, is seems nearly 50-50 change of flexural or Distortional buckling. Most of the tested samples failed in the distortional mode. However, recalling the boundary conditions are specified as "clamped-clamped" it can be noticed that these boundary conditions are not valid for the flexural buckling area.

Modes at various upright lengths can be calculated with CU-FSM for detailed analysis, see Figure 64 in Appendix K. A closer look to the shape of the distorted cross sections can help to find scenarios in which pinching effect will become crucial.

A gradual transition from symmetric Distortional buckling towards Flexural buckling over the minor axis (FBz) can be recognised in the upright length range of 1 400 to 2 200 mm, see the figures at various upright lengths in Appendix K. After 2250 mm a sudden 'modal switch' to the Flexural Torsional Buckling mode (FTB) is revealed.

The CU-FSM results of the non-lipped 100-68-20-4050 and lipped 100-72-25-4050 profiles can be found in Appendix H. 'CU-FSM Analysis of the uprights applied in the Frame Test Setup'.

03.2.8. Conclusion

For the situation in which the finite strip method applies, without spacers, it is likely that the profiles will fail under flexural (-torsional) behaviour at the lengths used in the experiments. Although this conclusion seems obvious, one should consider the boundary conditions in the model do not match the ones in the experiment. When the distortional area is finished, longer lengths of the non-lipped profile will show flexural buckling over the weak (z-)axis, while the lipped profile shows flexural-torsional behaviour. When even longer profile lengths are used, (L_{upr} > 2250 mm), also the non-lipped profile will be prone to the flexural-torsional mode. The effective length for this flexural-torsional mode in the model is half of the upright length while the actual effective length is equal to half of the Ball-Bearing-CTC-length. As a results, the CU-FSM results will draw the border of the green-blue indicated transition between distortional and flexural-torsional behaviour a little more to the left. This is because the modelled profile has slightly more resistance to the torsional mode even at longer lengths, than the actual profile in the experiment which has a longer effective length in is therefore 'weaker'.

Although this minor uncertainty in borders of the distortional buckling area, it can be stated that the real-world non-lipped upright profile will fail in distortional mode, if the upright length is 2000 mm. The lipped profile at a length of 2600 mm will fail in a flexural-torsional shape.

These conclusions show some minor conflicts with the actual experiments executed on single uprights in DTB-setup. The actual experiment showed the lipped profiles to be failing into flexural buckling and flexural-torsional at the same time. It is unclear which mode was dominant in the experiment while the semi-theoretical CU-FSM programme states a nearly 'pure' flexural-torsional mode. Absence of the flexural buckling over the weak (z-)axis might lay in the 2nd order effects. While the constrained finite strip method only the mode most likely to follow, it assumes the mode will also expressed rather this way. In the real world there will be 2nd order effects that 'push' the profile in the flexural-buckling over-the-weak (z-)axis shape after the flexural-torsional mode expression had 'weakened' the resistance in this other global mode.

The test setup for further tests on the lipped profiles should have additional constrains to limit effects of both flexural modes.

Conclusions from Linear Elastic Theoretical Research

The theoretical research should answer sub question 2:

'How can linear elastic buckling theorems predict behaviour of upright profiles?'

- The linear elastic Finite Strip Method (FSM) can be used for modal classification of upright profiles;
- The linear elastic load factor calculated by the FSM tends to overestimate the critical load of the profile. Real world profiles will yield before the linear elastic critical load is reached, causing significant lower failure loads;
- The load factors themselves can still be compared among each other. This means the load factors can be used to determine which failure mode will be normative and which lengths of the upright profile will have the critical buckling load.

04. Finite Element Method simulation of buckling behaviour of upright profiles

The experiments have been simulated in SolidWorks simulation. FEM discretization was also used to predict the framework test outcome and access the required stiffness of the top beam. In this section is discussed how the input of the model was defined.

04.1. FEM Formulations applicable to Open Thin Walled Profiles

Firstly, an overview for formulations of elements is given to clarify the system behind the model.

The types of elements available in SolidWorks 2014 Premium are 1st and 2nd order tetrahedron and triangular shells. For the analysis of complex shapes like uprights the 2nd order tetrahedral solid elements like in Figure 26 are used. Actual upright profiles might show more flexible behaviour than 'only' solids but this is neglected for convenience. Nevertheless, the use of shell elements in SolidWorks introduces some difficulty in input for the model and might also neglect local through-the-thickness effects which will possibly means neglected significant changes in stress distribution near pinched areas.

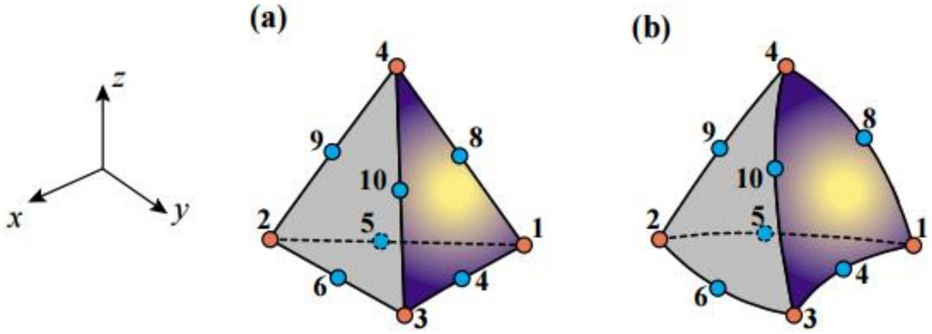

Figure 26. Actual Quadratic (10-node) Tetrahedron. (a): Element with planar faces and side nodes located at side midpoints; (b): Element with curved faces and sides. (Source: (Carlos Felippa, 2013, pp. 10-4))

Visualization of a single element gives an insight in the way of calculating stresses and displacements of a complete model as seen above. To simplify the picture, an actual tetrahedron is shown Figure 26 and a (2D) quadratic triangle is shown Figure 27 with the directions of displacements at the nodes.

$$u = a_1 + a_2 x + a_3 y + a_4 x^2 + a_5 xy + a_6 y^2$$
$$v = a_7 + a_8 x + a_9 y + a_{10} x^2 + a_{11} xy + a_{12} y^2$$

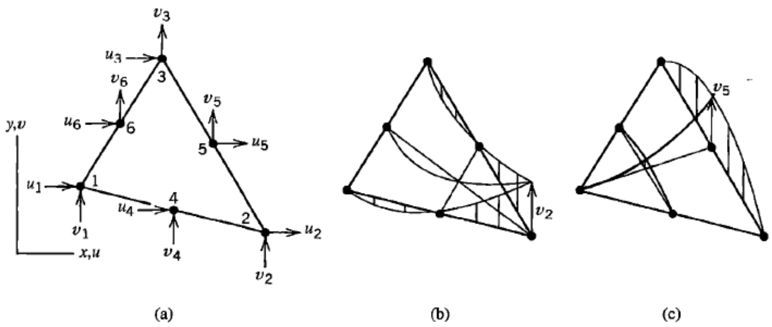

Figure 27. (a) Quadratic Triangular element with 6 nodes and 12 modal d.o.f. (b, c) Displacement modes associated with vertex and side d.o.f. (Source: (Cook, Malkus, Plesha, & Witt, p. 95))

04.2. Overview of simulations

The earlier experiments executed as well as the planned experiment as described in the test setup requires a numerical approach. This paragraph will give an overview of all simulations executed in SolidWorks.

Table 16. Overview of numerical 'Buckling' simulations. Greyed out cells mean non-possible configurations due to absence of the diagonal spacer. The 'nL' and 'L' behind the abbreviated profile name stands for Non-Lipped (nL) and Lipped (L).

Configuration and upright lengths [mm]	Profile Type (Abbre-viated):	Type of fixture at the diagonal spacers in z-and x-direction, if present	Amount of initial pinching applied in the spacer			
			<No Spacer>	0.0 mm	-3.0 mm	-6.0 mm
STUB, 400 mm	78 (nL)	"Free"	X	X	X	X
STUB, 400 mm	83 (L)	"Free"	X	X	X	X
DTB, 2000 mm	78 (nL)	"Free"	X	X	X	X
DTB, 2300 mm	83 (L)	"Free"	X	X	X	X
DTB, 2000 mm	78 (nL)	Roll-support in z-direction		X	X	X
DTB, 2300 mm	83 (L)	Roll-support in z-direction		X	X	X
DTB, 2250 mm	68 (nL)	Roll-support in z-direction		X	X	X
DTB, 2250 mm	72 (L)	Roll-support in z-direction		X	X	X
Complete Frame	68 (nL)	Pin-Pin Diagonal		X		
Complete Frame	72 (L)	Pin-Pin Diagonal		X		

The complete overview of SolidWorks simulations used for this research is shown in Table 16. The type of fixtures at the diagonal spacer is an important boundary condition in this analysis. To save computation time, no complete frames with pinching effects of 3.0 and 6.0 mm have been calculated. The results of the complete frame calculations should match the 'cut out' single uprights simulation results.

04.3. Input

SolidWorks offers the possibility to run static and buckling analysis on complete assemblies constructed out of a number of parts, also known as components. In this section the process of creating these components and assemblies is described. The final assemblies will be loaded with various boundary conditions and, most importantly, a series of initial displacements (imperfections).

04.3.1. Geometry of Parts

The definitions of upright profiles are documented in DWG drawings which can also be found in Appendix F. Additional information about the perforation type used can be found in Appendix F.6.

Modelling of engineering devices within SolidWorks happens using a practical application of the parametric modelling principle as discussed also in (Eastman, Teichholz, Sacks, & Liston, 2008) in their book about BIM-Modelling. When modelling parts, sketches are used to define cross sections and detailing for extrusions and extruded cuts.

First, a cross section is sketched of the actual profiles, see also picture Figure 28. This has to be done for a 'lipped'-profile and one of the 'non-lipped'-profiles. When for example a non-lipped profile 100-68-20-4050 is sketched, the larger version 120-78-25-5070 non-lipped profile can be obtained by changing the parameters and edit features like material thickness.

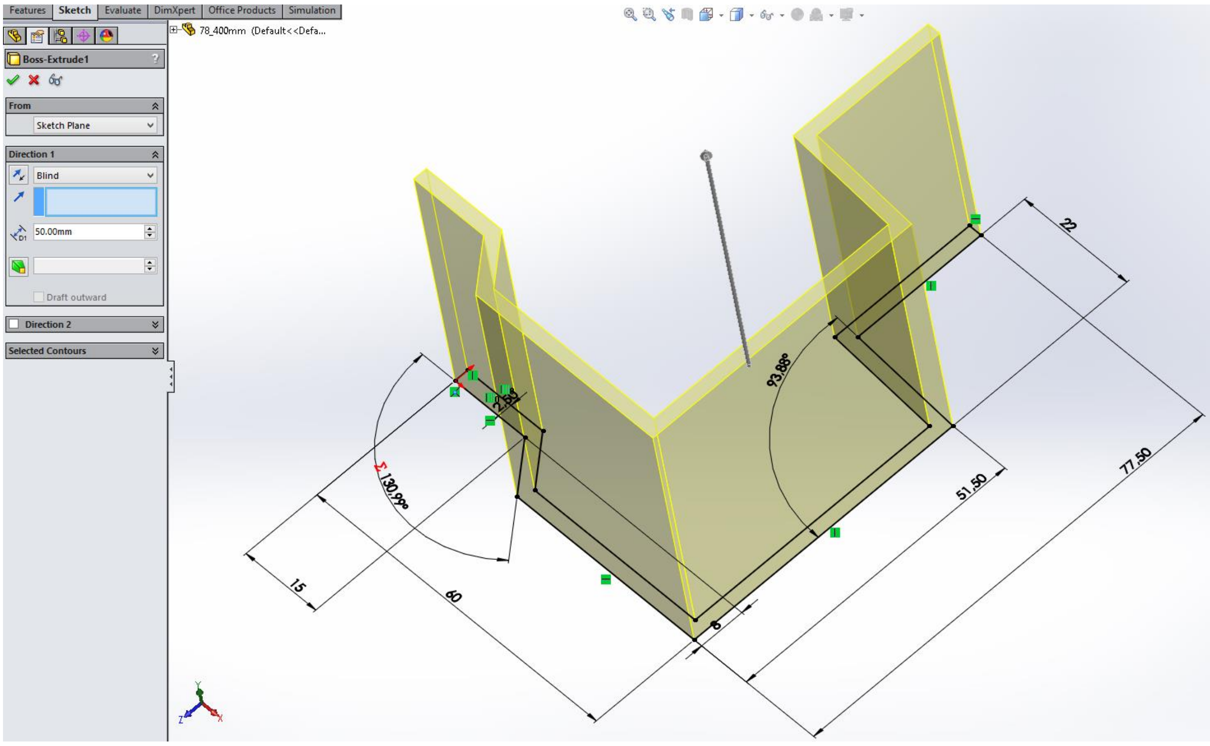

Figure 28. Extrusion of a sketched cross-section. This sketch shows the properties for the 120-78-25-5070 profile, changing the dimensions of the sketch could convert the profile into a 100-68-20-4050 profile or any familiar shape. For this analysis the profile is split over its axis of symmetry in order to reduce calculation time. Later on, the full cross section was used for analysis.

The so called 'Smart Dimension'-tool is employed in order to adapt the parameters as discussed earlier. After sketching a given profile's cross section geometry and extrusion is applied. The minimum extrusion distance is 50 mm, which is equal to one perforation pitch, and can be increased by equal steps of likewise distances.

After the extrusion of the cross section is applied the perforations can be sketched, see also picture Figure 29. This perforation is sketched at one side of the upright and then inserted with the 'extruded cut' feature. This is done for one of the flanges and copied to the other flange using the linear pattern feature. Simply adding a direction and perforation pitch in the same linear pattern feature results in the creation of perforations all over the profile, as shown in the picture below.

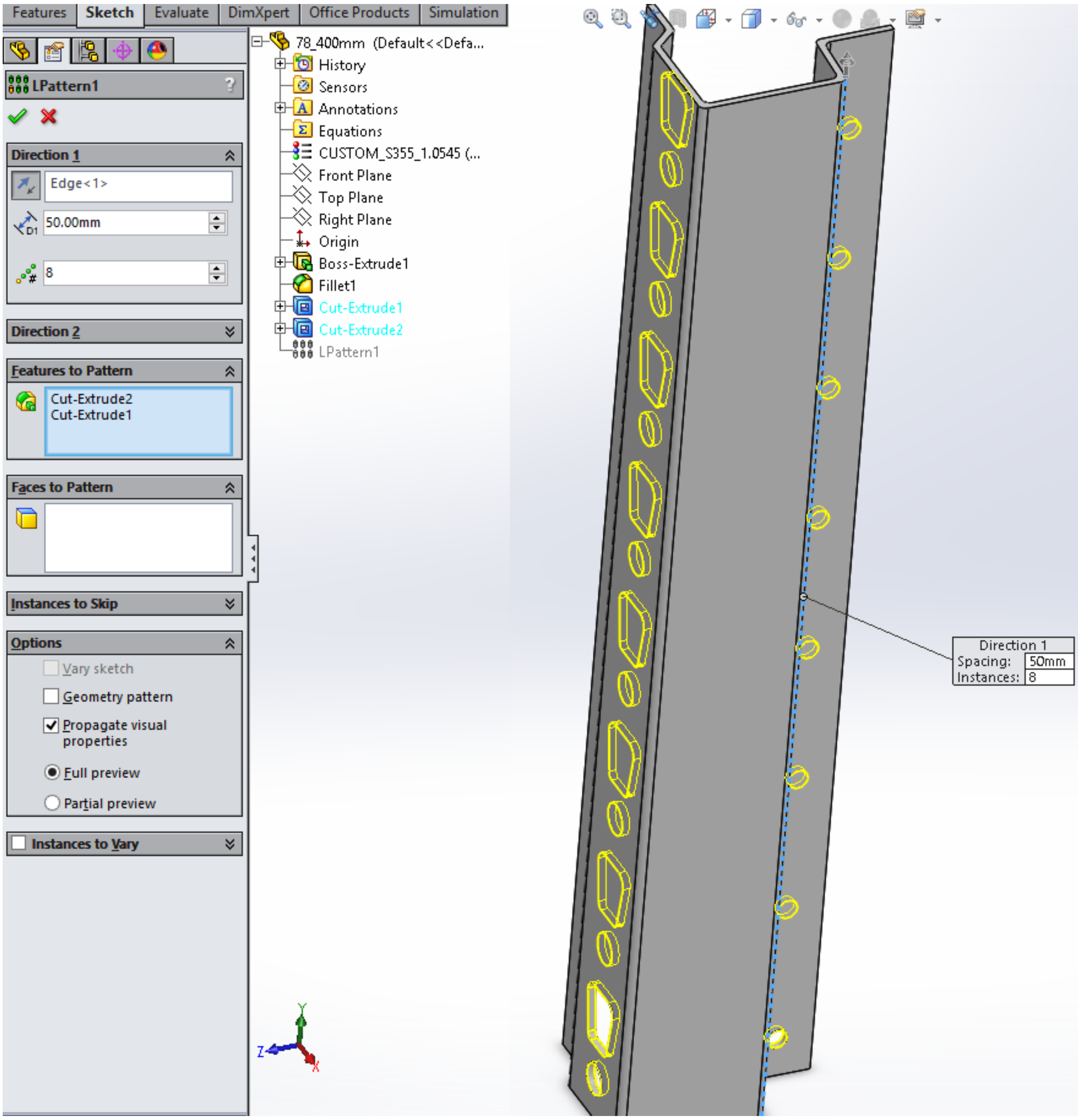

Figure 29. Pattern for perforations. In case of a fully sketched profile including its symmetric other halve, the same pattern-feature could be used to 'pattern' the perforation to the other halve using the 'Direction 2'-property.

The diagonal holes are added and copied likewise.

The actual profiles produced are made out of bend sheet metal and therefore still contain the bended profile edges. The rounded edges can be obtained by introducing ‘fillets’ at the corners of the profile. The fillets have a radius between 4 and 5 mm, depending on material thickness.

The length of the profiles in the configurations differs depending on type of upright profile and its most vulnerable distortional buckling length. Changing components lengths can easily be accomplished by changing the parameters used in the design involving the extrusion lengths and perforation repeating.

Sheet Metal Features

Here is where an alternative way of modelling is introduced: Sheet Metals, as visualized in Figure 30. SolidWorks software offers a range of features to create and edit 'sheet metal' components. This kind of modelling allows fast and realistic sheet metal shapes to be virtually folded faster than the method described earlier. However, modelling thin walled features in this stadium of design prevents using more complex welding providing 'clamping' support of the sheet metal onto a potential cap-plate into Finite Element Analysis. This is the reason that modelling occurred with full sketching, extruding and filleting as described earlier.

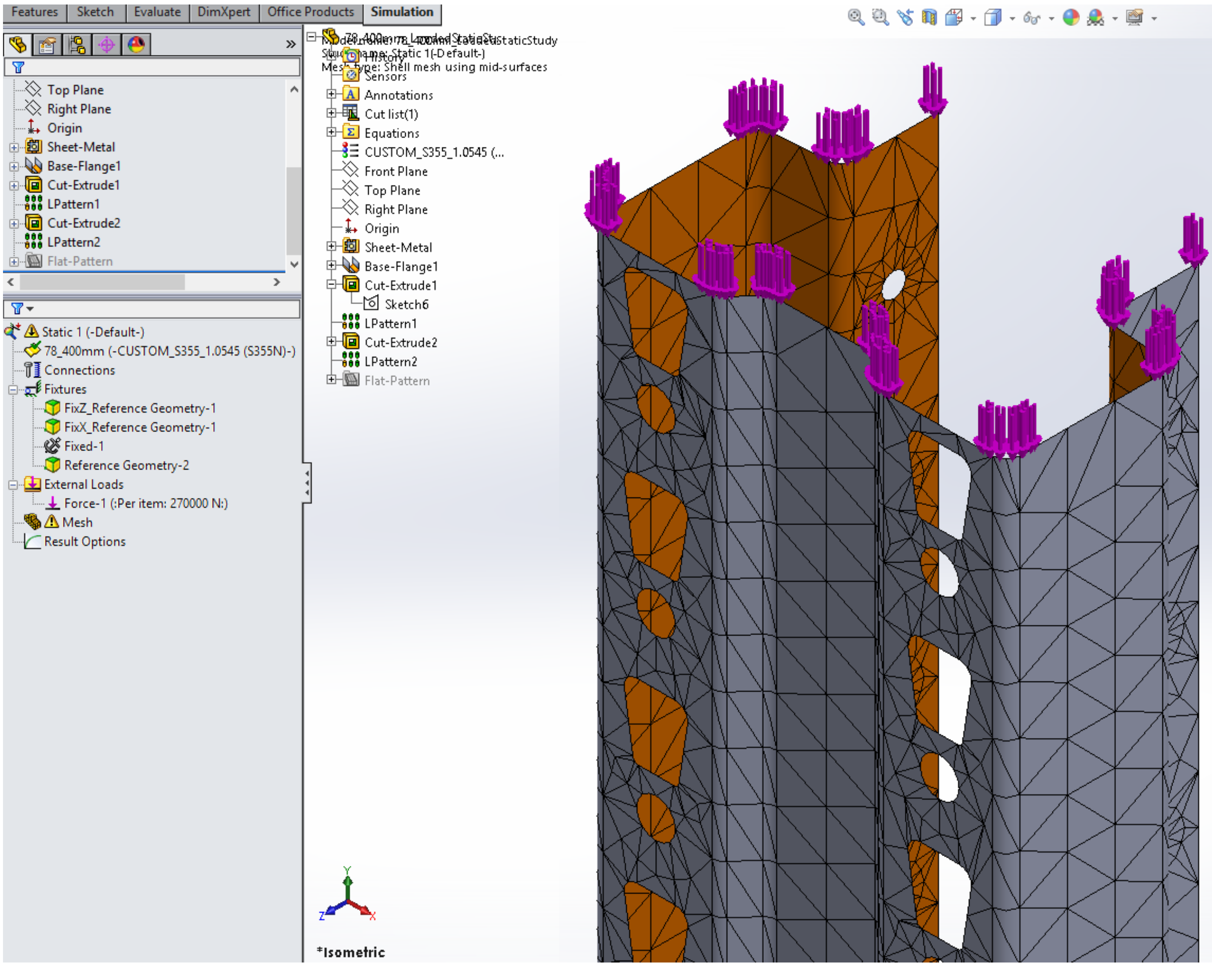

Figure 30. Alternative modelling in SolidWorks with the use of 'Sheet Metal'-feature. This method will save calculation time and probably modelling time but adding constraints had limited applications and simulations results might be less accurate, since some through-the-thickness effects (variation in stresses/strains) will probably have significant influence on the distortional mode.

Additional Parts

To simulate the experiments as close as possible some additional parts are inserted in an assembly. The 'standard' STUB- and DTB-test setups both have basically the same layout. Both setups use 'Cap plates' at the end of the uprights with dimensions 160x120x10 mm. The ball bearings are also sketched to approach the actual boundary conditions at the ends as close as possible. The diameter of the ball bearings is 60 mm and the distance from the upright-end to the centre is 80 mm, as seen earlier in the test evaluation of the single uprights.

Preliminary simulation and theoretical results showed that most of the upright profiles in DTB-setup showed flexural-torsional behaviour. In the actual experiment this mode is prevented by a torsional constraint, which can be seen on the right of Figure 32. In the Finite Element method, this constrained is intercalated by restraining the lower Cap Plate end from torsional motion, more on this in the section 04.3.2: Boundary Conditions.

For the test setup entailing the complete frame, the top beam is an important additional construction part. The top beam will be made out of an HEA-180 profile with some adaptions. The beam will require extra welded plates to prevent the middle web from buckling. The Cap Plates from the upright will be bolted onto the HEA. The HEA can be clamped to the Cap Plates of the Bench Press.

The diagonal spacers will mostly only be designed with initial displacements at the holes meant for bolting diagonals onto the profiles and not with actual spacer-parts that are inserted into the assembly, which is difficult to accomplish in SolidWorks.

Assembly

All parts discussed before require assembly into an assembly-file in SolidWorks to run the actual study on buckling. The STUB- and DTB- setup can be made out of the selected upright-part and two cap-plate-parts.

The complete framework is more complex to create and computation time will increase likewise. To avoid spoiling hours of time, complete-framework Finite Element Analysis was only executed for the case of 0.0 mm pinching in the spacers. When this result matches with the single-upright setup, no further research is ought to be required.

All components in the complete framework test as well as the STUB- and DTB-setup should be connected with their respecting neighbouring-components using for example ‘smart connectors’ or ‘mates’, with preference to the last due to computation time issues. The more advanced ‘smart connectors’ are not necessary because the Cap Plates are in relative simple ‘compression’ connection with the HEA-profile as well as the uprights. Friction between bolts is not of any relevance to the problem and tension in connection is unlikely to occur. Moreover, the interest grows towards the failure modes of the upright between the spacers and not towards effects occurring in the HEA-profiles, save for the HEA its stiffness and capacity.

The assemblies for the STUB- and DTB-setups are completely connected with mates, while the Framework test setup consists of 2 separate top-beam-assemblies, 2-upright-with-cap-plates-assemblies and no diagonals. How the effect of the diagonals was taken into account can be found in the next section, 04.3.2: Boundary Conditions. When no mates or alternative connections are inserted in the assembly, Finite Element analysis will fail due to the possibility of the components to move over large displacements while the results of the analysis is only valid for small displacements relative to the notional component dimensions.

04.3.2. Boundary Conditions

A new buckling study can be started as soon as the assembly of a test setup configuration is complete and geometrically fixed in the sense of no components capable of unrestrained large motion.

Upper Ball Bearing

Obviously, there have been created a number of additional parts to establish the right boundary conditions. The ball bearings of the constructions are halves of spheres. The one on the top is connected onto the hydraulic press, which resists torsional rotation but of course is able to move in longitudinal direction. To realize this type of restrained two advanced fixtures can be used. One restrained is the movement of the sphere in z-direction, the other in y-direction, see also Figure 31 showing the upper Ball Bearing.

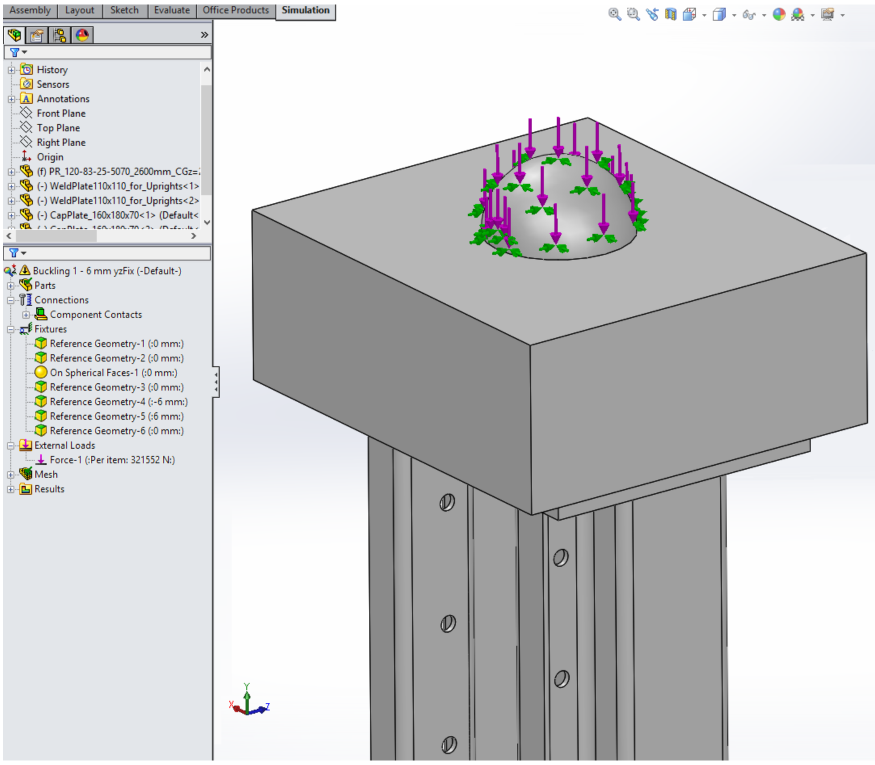

Figure 31. Boundary conditions at the top of the upright profile. The distance from the end of the upright to the centre of the Ball Bearing is 80 mm. The hydraulic press resist rotation which is modelled as restrains on the Ball-geometry in all directions but the direction of the bench-press force, which is equally distributed over the ball bearing.

Lower Ball Bearing

The lower ball bearing is nearly symmetrical. This ball bearing is a ball that is practically able to rotate freely about all axis, but no displacement in any direction is allowed. This type of boundary condition is visualized in Figure 32 next to the actual boundary condition in the experiments. Calculations made in the test evaluation of the first experiments have pointed out that the profile is likely to fail in Flexural-Torsional mode. According to the Euro Code EN 15512 a torsion restrained should be added at the baseplate to prevent this mode to be triggered. In SolidWorks, this restrained can easily added with only one ‘advanced fixture’ which locks one side of the Cap Plate of moving in its own plane and perpendicular to the upright-direction. However, this kind of restraining might cause non-legislated resistance in bending and that is why a more complete model of the lower Cap Plate was created.

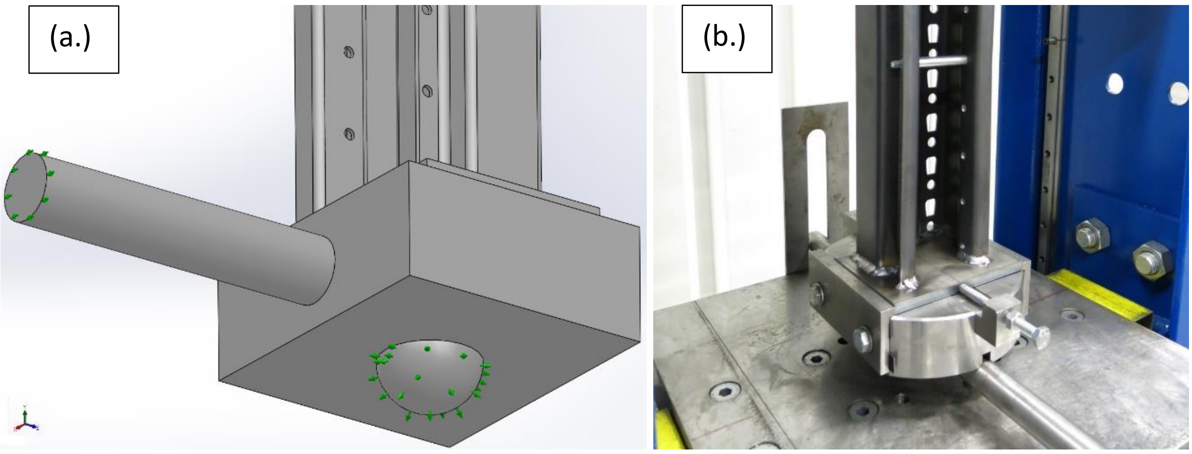

Figure 32. Lower Ball Bearing and restrained on torsional mode in (a.) SolidWorks model and (b.) as applied in actual experiment. A simplified way to model the torsion-constrained would be to apply the boundary condition directly onto one side of the Cap Plate instead of adding the cylindrical extension. Having constrains like pictured left in (a.) will ensure no additional interfering rotational-resistances are introduced.

This constrains in Ball Bearing is valid for the STUB- and DTB-setup, as well as the Ball Bearings in the complete frame test setup.

Diagonal Spacers Simple Setup

As already mentioned in the section 'Additional parts', modelling of the complete diagonals seemed not to be a reasonable solution. Within SolidWorks, a fixture or reference geometry can have an initial displacement. In practice, this will connote that the indices of the {u} vector corresponding to the degrees of freedom at selected nodes already contain non-zero entries before calculation. This type of fixtures will be employed at all the perforated holes in the upright where the diagonals should be inserted in the actual framework, see also Figure 33. The direction of the initial displacement is in the y-direction (major axis) and in inside-opposite direction simulating the actual spacer as close as possible. Only the diagonal spacers in the middle are exposed to 'pinching' by initial displacements. The 'end' diagonal spacers at 64 and 36 mm measured from respectively the lower and upper upright end will not be subjected to initial displacements. However, like all the diagonal spacer positions, movement in horizontal direction (both major and minor axis) is still restrained. This means the upright opening is held constant in z-direction, which simulates a spacer of constant size but also stabilizes the upright in the in-depth-direction. In the experiment with single uprights, actual spacer are still allowed to move.

In the frame test setup, the actual diagonal spacers are held in the same position using actual diagonals which have a finite stiffness. Therefore, a more sophisticated way of modelling would be to use 'springs'. But doing so will 'soften' the diagonal spacers to a finite stiffness and also make it harder to apply the pinching effect. Pinching should be accomplished by an external force. To keep things simple, the boundary conditions around the diagonal spacer perforations are made with translation fixed reference geometry as displayed in Figure 33.

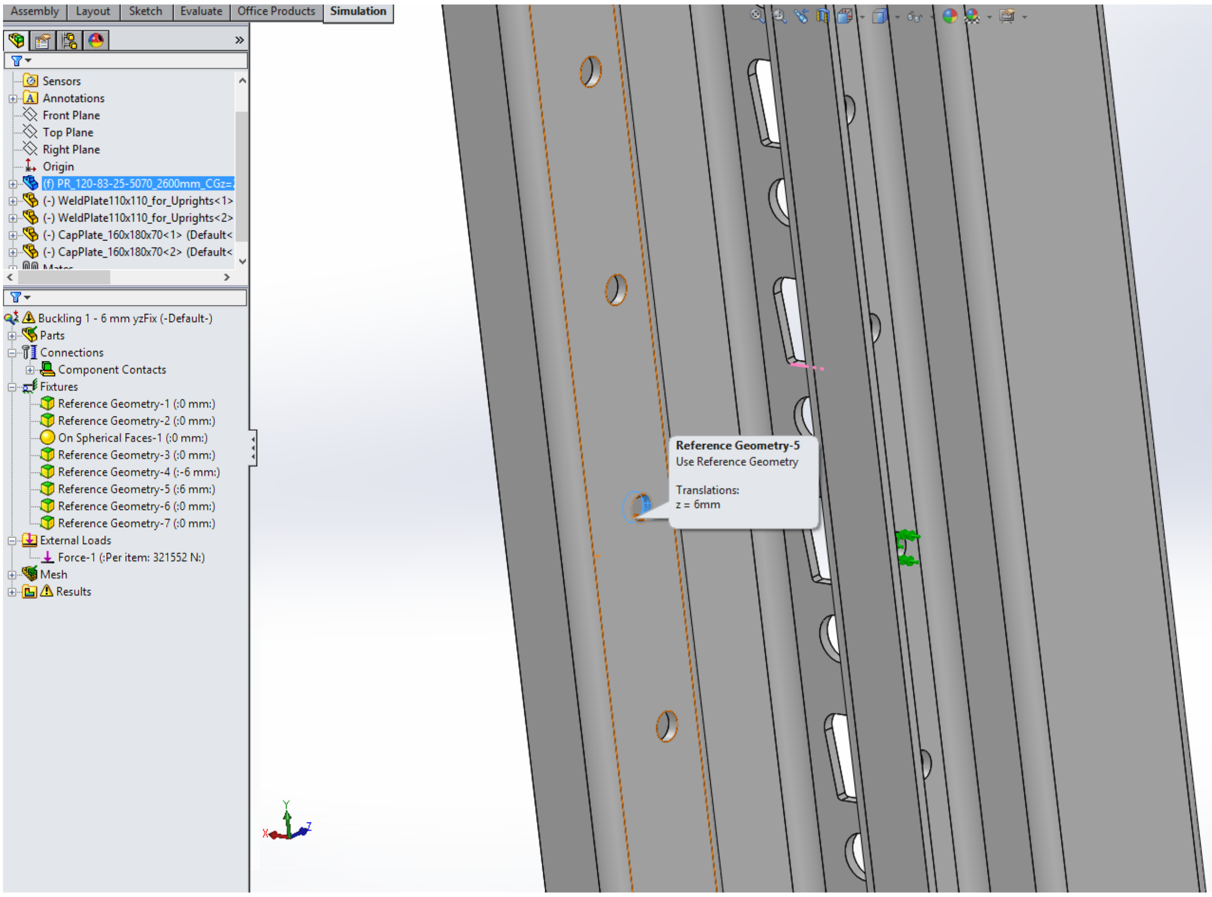

Figure 33. Boundary Conditions at the diagonal spacer. The geometry is given an initial displacement towards the inside. After the displacement the geometry is still able to move over all other degrees of freedom, including rotation over any axis.

Diagonal Spacers Complete Framework

Within the complete framework test, diagonals are handled a little different. Actual diagonals are relatively simple components, when seen as parts of the whole framework. A diagonal fulfils its function by acting as a rod in pin-pin connection with the spacers.

The most realistic way of simulating the experiment is completely model the diagonals including spacers and bolt-connections. This approach will take many hours of modelling and computation time. Furthermore, this method completely ignores the relative simplicity of the pin-pin connection meaning it is definitely not the smartest choice.

One option in the simulation settings is the ‘pin’-feature which can be found under ‘Connections Advisor’. The disadvantage of the ‘pin’-feature is the two nodes required to be specified for a pinned connection. These nodes are only available if the complete diagonal spacer is sketched including a number of nodes necessary to satisfy a rigid-diagonal assumption. There are 4 pin-pin relations needed for every diagonal to establish a rigid diagonal; one between the front-ends of the spacers, one between the back-ends of the spacers and two positioned cross-over, see also the most right alternative of Figure 34. This means a complicated modelling process for yet a not quite accurate system since the actual diagonal is not connected to the endpoints of the spacers-bolts but at the outer spacer located between the upright openings. Moreover, using pin-pin relations at fully modelled spacers will make it even harder also simulating the situations with pinching-effects included. Note that the current situation to be investigated is with spacers, but without a pinching distance.

A better solution would be to employ the 'rigid connection'-feature, which makes selected faced rigid and forces them to move together instead of unbound of each other. Within the Finite Element Method, this means that all the indices in the displacement vector of nodes within those fields have the same values. The disadvantage of modelling the boundary condition in this way is that the faces themselves are, as part of their feature definition, rigid. In the actual experiment, hinge-like rotation will be small and therefore the difference between a connection that can rotate freely and the rigid one shall be negligible.

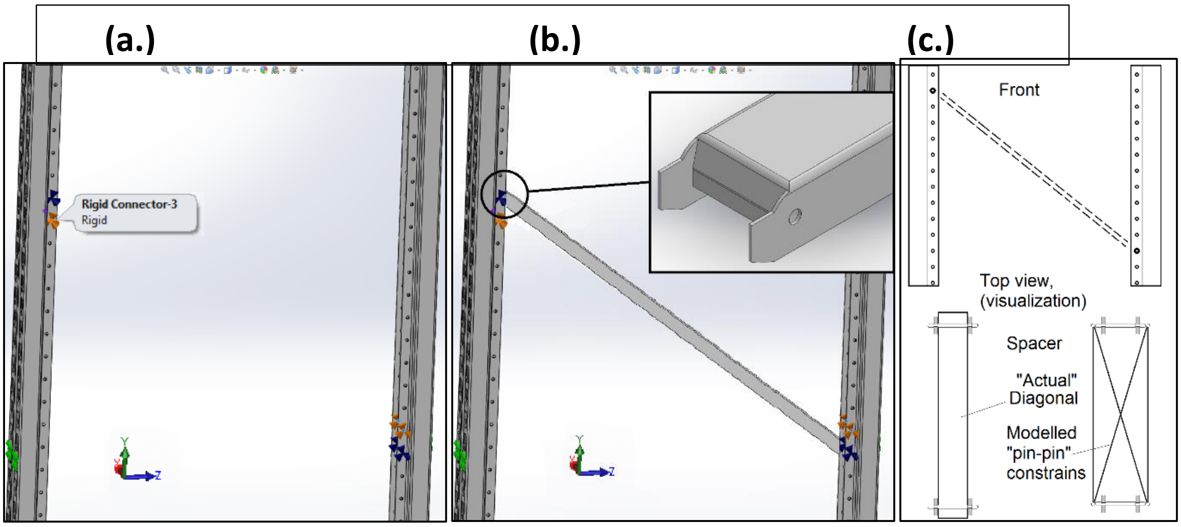

Figure 34. Three alternatives for modelling of diagonals in FEM discretization. The first (a.) makes the geometry around the spacer perforation rigid, the second one (b.) is an actual diagonal mounted in bearings and the third one (c.) uses 4 pin-pin connectors to imitate the solid diagonal rod.

04.3.3. Loads

The critical failure force is applied in parallel direction of the uprights, with the resultant force in the exact centre of gravity of the uprights cross section. In the SolidWorks Assembly, the force will be applied onto the Ball Bearings while their centre lays in the same line as the uprights cross sections. The magnitude of the force applied is the same as the "theoretical" maximum when the profile is in case of an infinitely stable profile, which is its cross sectional area times the yield stress of the material. For the complete framework test this force is simply doubled to account for both profiles. For convenience, the loads are rounded to whole Newtons.

Imperfection Loads

Several imperfections are present in the upright profiles. In general, SolidWorks does not really have options to initial alter the stiffness matrix with a slight change in coordinates of the nodes. When imperfections are taken into account, the best implementation would be to apply a variable force along a face or line of the upright body. The static analysis containing only that imperfection load could be used to determine magnitude and type of function. In this project, relatively simple data tables was used to describe a single sine functions in order to vary an imperfection load in the most unfavourable way. For more advanced structures, a complete Fourier-series containing multiple terms might be adopted.

04.3.4. Mesh

For the calculation, the Finite Element Method requires a defined mesh for location all the elements within the analysis. A mesh is a combination of nodes and links that practically constitute a large number of triangles. Analysis approaches an accurate solution when the number of elements used becomes sufficiently large, although the more elements the larger computation time becomes. Besides total element count, the aspect ratio of links within the mesh is a suitable parameter for mesh quality.

The standard mesh engine in SolidWorks uses an adapted type of algorithm based on the Delaunay triangulation to obtain the lowest aspect ratio of elements. (Peterson, 2014) In SolidWorks it is possible to apply 'mesh controls' which control the mesh in selected parts in the sense of ensuring larger or smaller elements. For the frame setup, this was used to vary element size of the top beam to be 'simple' and large and the uprights to be rather complex and small.

The visualization in Figure 35 indicates a relatively simple mesh using sufficiently small elements to carry out a structural analysis.

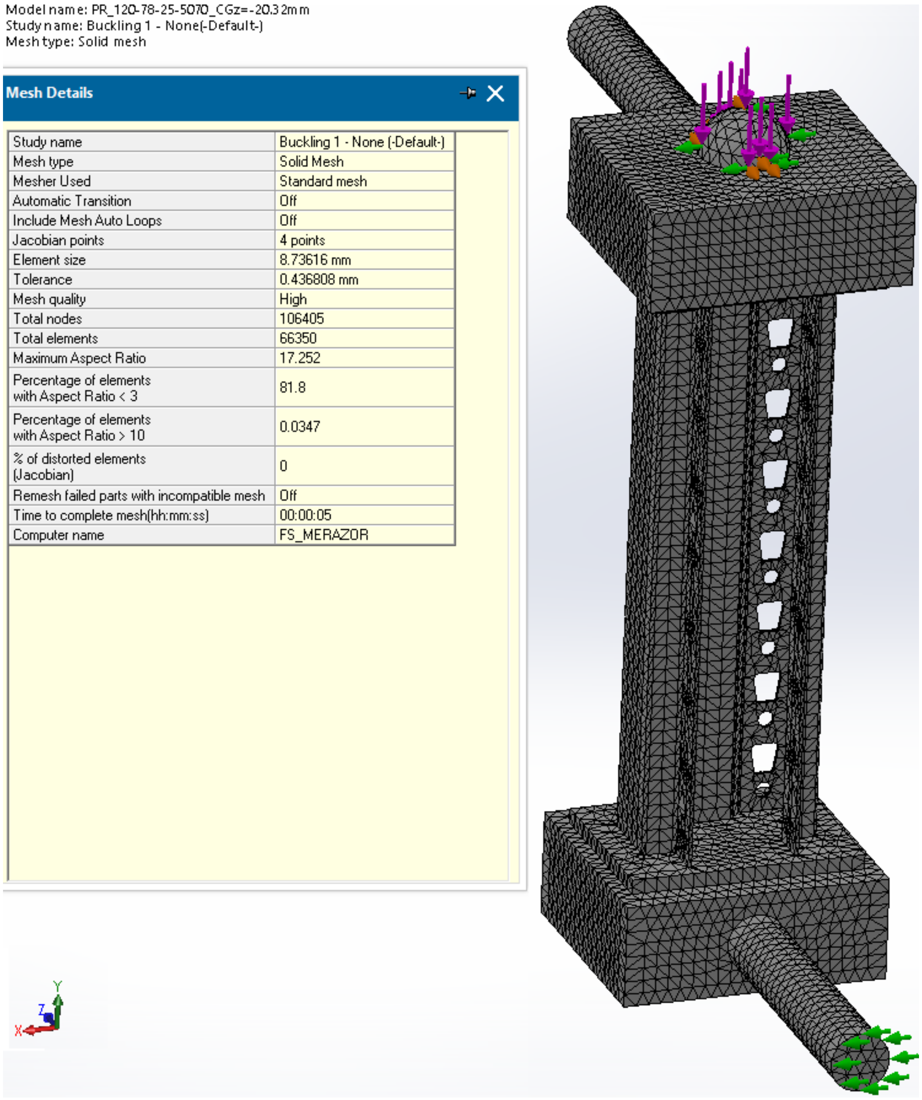

Figure 35. Example of a mesh. Elements with an aspect ratio larger than 10 are 'bad' elements while smaller than 3 means 'good' elements. An aspect ratio of 1 means an exactly equal sized triangular element.

04.4. Simulation Settings

The type of studies executed are known in SolidWorks as the 'Static', 'Buckling' and 'Non-Linear' study. This section will briefly explain which assumptions are made, how the model generally works and what could be the added value of carrying out the simulation studies.

Within buckling analysis of structural components, globally two issues of interest exist. The first one is the shape of failure and the second the corresponding amount of work or force which the component should be able to withstand.

04.4.1. Static Study

The static study is quick and not really helpful in simulating complex post-plastic buckling behaviour. The study is in reality excellent to estimate displacement effects of initial imperfections introduced by diagonal spacers, constrained displacements or 'small' external forces meant to imitate initial imperfections.

04.4.2. Linearized Buckling Study

The Linearized Buckling study in SolidWorks calculates the mode in which the sample is supposed to fail in case of elastic buckling. Elastic buckling ignores the yield stress (f_y) nor the ultimate tensile strength (UTS). The study also yields a series of load factors, for a desired number of modes which can be compared among each other. Actual upright profiles tend to show plastic buckling behaviour, driven by imperfections which means actual profiles will probably not even closely reach this load factor. The goal of the buckling study is therefore purely modal classification.

The failure modes calculated by the Finite Element method are of great significance to the validity of test results. When the failure modes of the numerical model and the theoretical model match, no further simulations are required. Second most important is the critical failure force, or stress, at which the specimen are ought to fail. Recognising which mode is triggered will be highly subjective, like also announced in the introduction to the Constrained Finite Strip Method, in section 03.2.

04.4.3. Non-Linear Static Study

The non-linear Static study can finally be applied to assess the actual failure force by an iterative estimation method. The input of the Non-Linear static study is the geometry of the model loaded with the full combination of all expected present initial imperfections in the form of forces. After applying a normal-load of the profile its cross-sectional area times the yield strength of the material, a certain point in time will show a ratio of plasticity that proved to fail in an earlier test. This 'rate-of-plasticity' can be found by 'imitating' an earlier test of a profile most similar. The estimation technique is a rather time consuming process and not really accurate.

This last line states exactly why the Finite Element method is excellent for modal analysis but lacks convenience for ultimate load assessment. Within this project, the actual ultimate load can be found be experimental observations.

04.5. Results: Static Study

The static study is employed to apply for several imperfections without normal loading. Central in this project is the distortional mode triggered by the pinching effect. A static study was carried out to find the shape and stresses in the sections with pinch but without applied load.

The 'linear static study' in SolidWorks is based on linear theory that cannot be used to find failure forces. Actual real world profiles show non-linear behaviour before the ultimate load is reached, see also section 03.2.7. However, the static study can still be used for relatively simple analysis on uprights exposed to pinching effects but not exposed to the normal loads that causes actual buckling. This analysis can predict order of magnitude of stresses in areas in the component and the deformed shapes of the profiles. Isometric views of analysis of uprights as part of a frame are displayed in Figure 36 and Figure 37.

100-68-20-4050 (Non-Lipped); Scale of deformed shape: 3.0x

Selected Upright Profile in complete Frame:	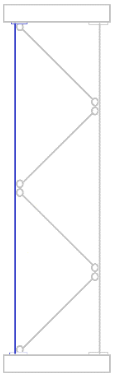 "Left"	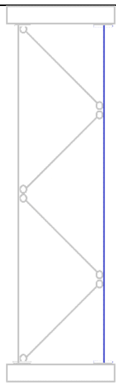 "Right"
Pinch -3.0 mm (2* -1.5 mm)	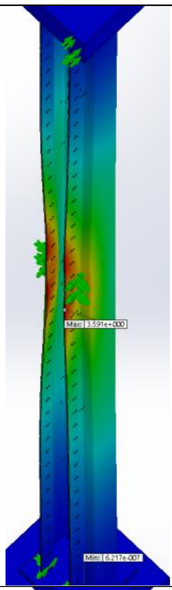	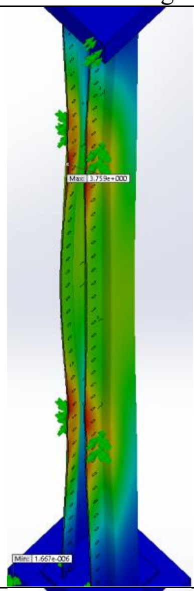
Pinch -6.0 mm (2* -3.0 mm)	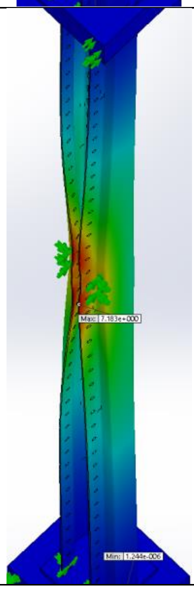	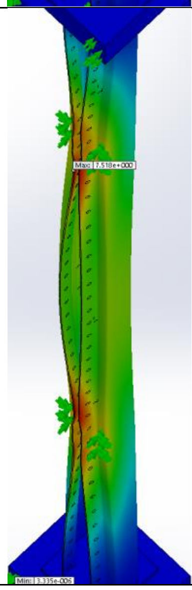

Figure 36. Pinching Only Results of the non-lipped profile 100-68-20-4050. The deformed shapes are scaled with 3 times actual size.

100-73-25-4050 (Lipped); Scale of deformed shape: 3.0x

Selected Upright Profile in complete Frame:	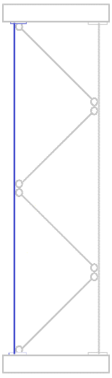 "Left"	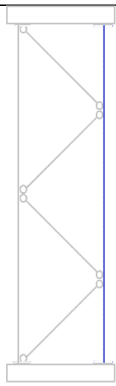 "Right"
Pinch -3.0 mm (2* -1.5 mm)	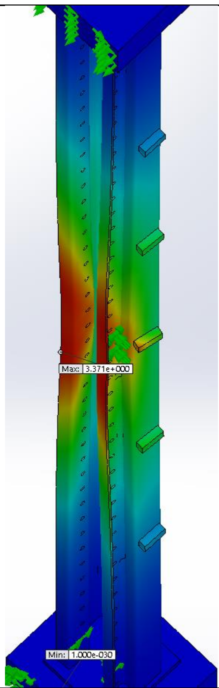	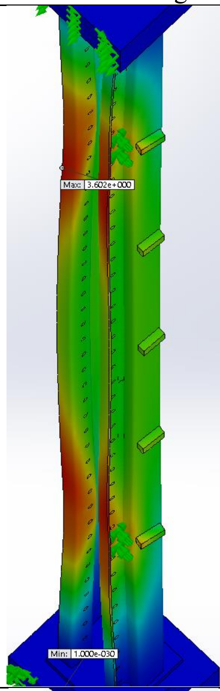
Pinch -6.0 mm (2* -3.0 mm)	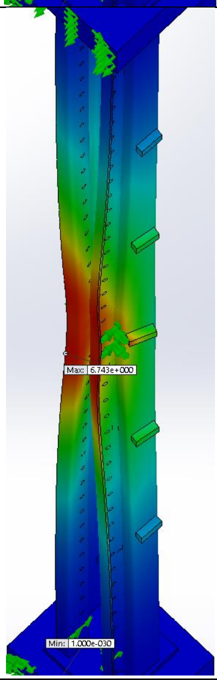	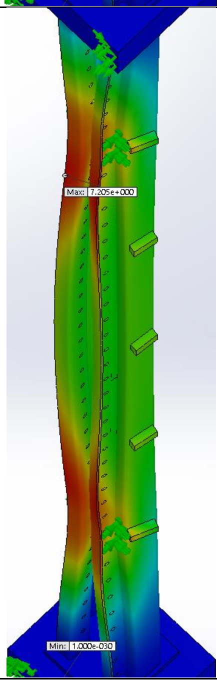

Figure 37. Pinch Only Results of the lipped profile 100-72-25-4050. The deformed shapes are scaled with 3 times actual size.

Cross Section Stresses

The cross sections in the profile at the height of the diagonal spacers might be interesting for further analysis. The table of Figure 38 shows the stresses in the cross sections.

	Non-Lipped Profile PRF 100-68-20-4050 S355	Lipped Profile PRF 100-72-25-4050 S355
Pinching -3.0 mm	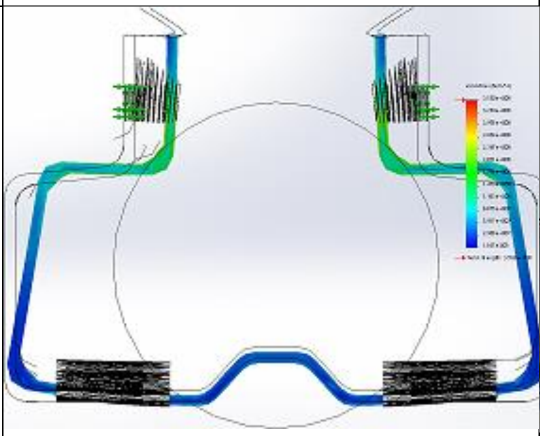	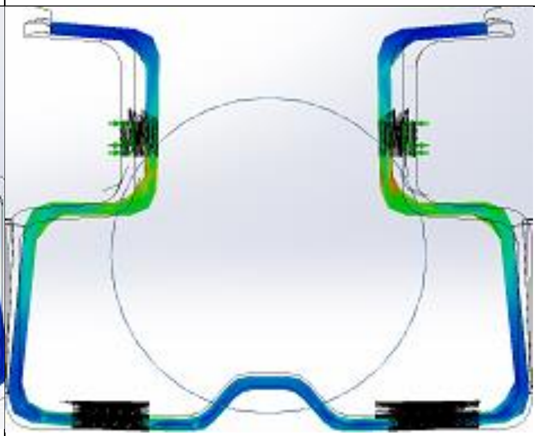
Pinching -6.0 mm	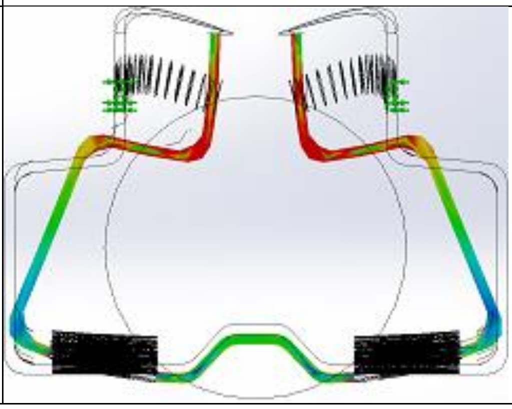	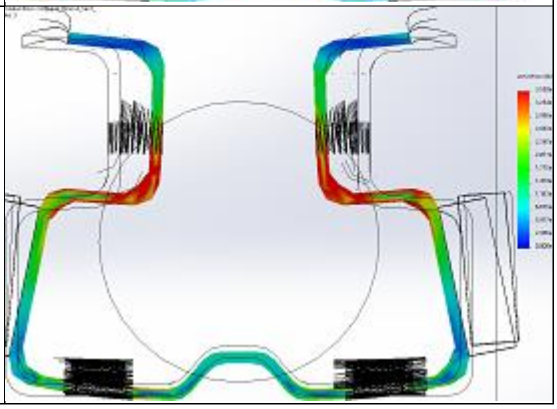

Figure 38. Static study of the cross sections at the height of the diagonal spacers, where the pinching effect is applied.

The static Finite Element Simulation with only pinching effects reveals the “disadvantage” of having lips in case of pinching effects. The lip prevents the upright’s web containing the diagonal bolt perforations from rotating, meaning the corners will suffer an excessive internal bending moment. The non-lipped profile shows less resistance against distortion of the cross section (rotating of end-flanges), resulting in a more ‘equal’ distribution of pinching stresses. This explains why the STUB column tests of the lipped profile showed a larger decrease in ultimate load after pinching, compared with the non-lipped profile.

04.6. Results: Buckling Study

Results of all configurations are listed ordered per profile and type of test setup. The dominating failure mode is described to trace the significance of the pinching effect best. For convenience, the y-displacement (along strong axis) is indicated by the colours, while the deformation of the final resultant shape (failure mode) is shown.

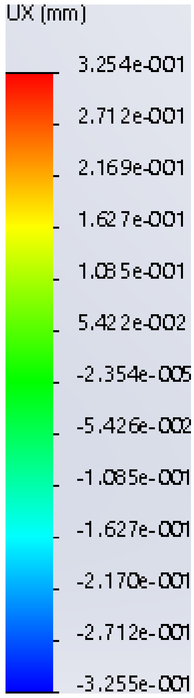

Legend

The first 4 models are the counterparts of the first experiments with the single uprights. Most of the models are displayed in ISO-view after total resultant deformation, unless other representations are ought to be more suitable to show the shape of the specimen. All deformations have been scaled with a factor 30 – 50 to obtain a clear picture of the effect. The legend in Figure 39 indicates what the colours mean. The actual values of resultant displacement distances are not important, since continued loading of the profile after failure will automatically lead to larger displacements. Nevertheless, the shape and relative magnitude of the displacements are still valuable information for modal classification.

Figure 39. (Right) Legend of result plots. Note that the colours only indicate the displacement in direction of the spacer (strong axis, A.K.A. y-axis), to visualize the distortional mode as best as possible.

STUB Non-Lipped (120-78-25-5070), "Free movement of spacers in y- and z"			
No Spacer	$E_{D,m}$ = 0.0 mm	$E_{D,m}$ = -3.0 mm	$E_{D,m}$ = -6.0 mm
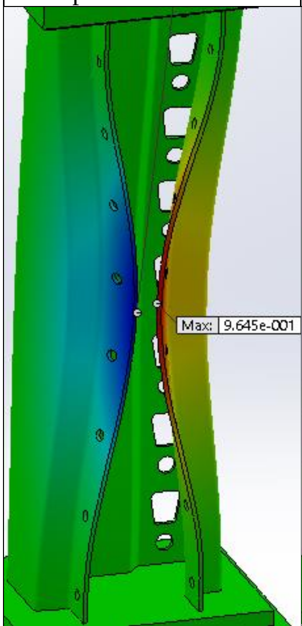	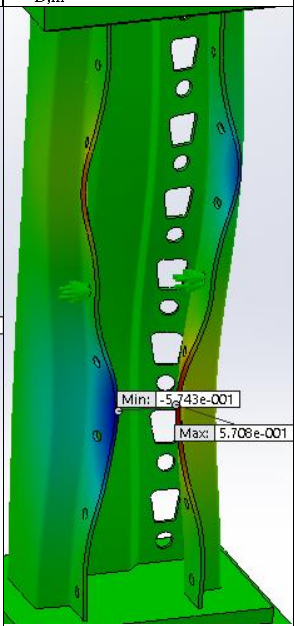	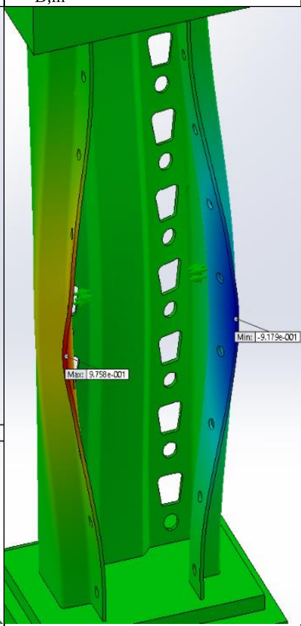	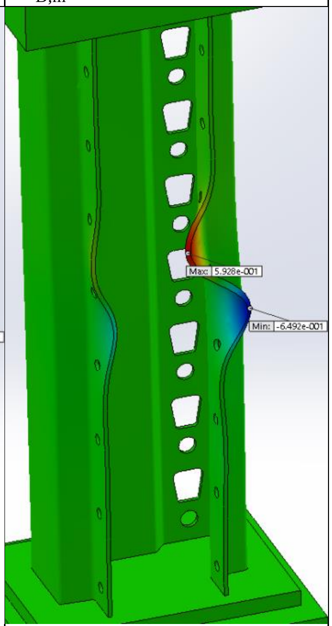
Distortional/Local	Local	Local, DTB	Local

Figure 40. Results of numerical analysis of non-lipped STUB-test setup.

STUB Lipped (120-83-25-5070), "Free movement of spacers in y- and z"			
No Spacer	$E_{D,m}$ = 0.0 mm	$E_{D,m}$ = -3.0 mm	$E_{D,m}$ = -6.0 mm
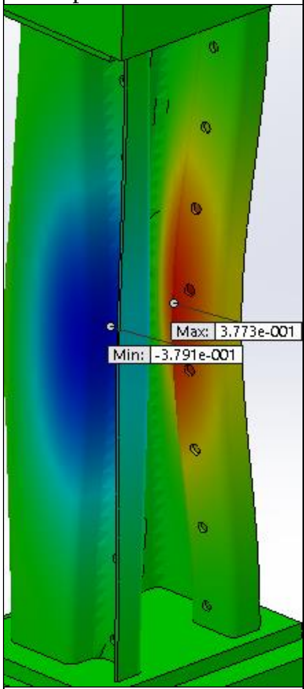	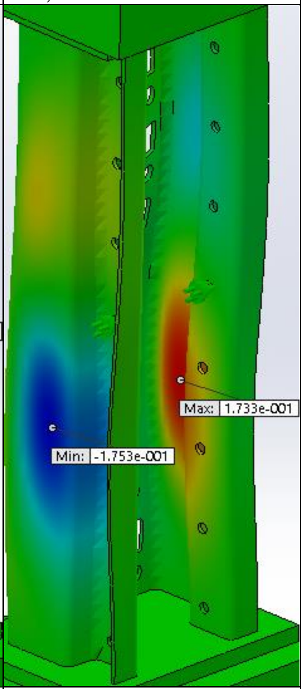	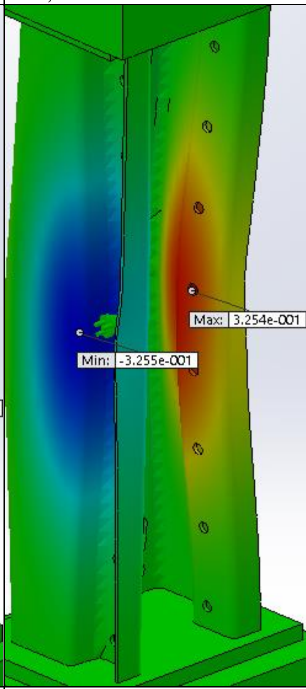	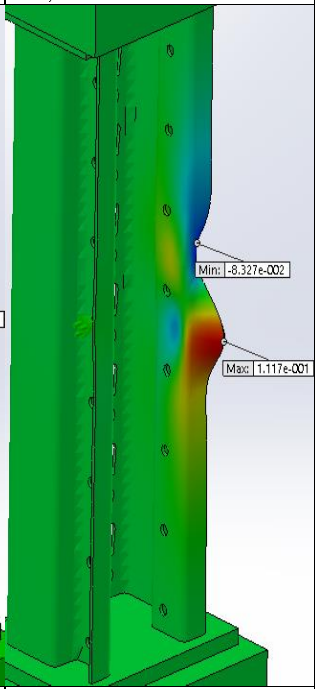
Local, web	Local, web	Local, web	Local, end-flange (lip)

Figure 41. Results of numerical analysis of lipped STUB test setup.

In general, the resulting failure modes of the simulated STUB tests (Figure 40 and Figure 41) look quite similar to the ones observed in the experiments. However, the linear elastic study tends to overestimate the load factor, like also encountered in the FSM model in section 03.2.

Distortional Buckling Test, Single Uprights

The simulations of the 'New DTB' setup with extended lengths is shown in Figure 66 and Figure 67 in Appendix L. The results show a symmetric distortional mode for the non-lipped profiles and clear evidence of flexural (global) buckling can be found in the lipped profiles. Apparently, SolidWorks simulations seem to approach the test results closely.

Simulation results after restraining movement of the spacers in the horizontal plane are visualized in Figure 42 and Figure 43. The idea of keeping the spacers in the same horizontal direction would tend to approach a frame setup.

The reduction in degrees of freedom as a result of actual diagonals in a frame can be modelled in innumerable alternatives. One way to model this into SolidWorks is simulating a single upright and adding constrains to disable movement in the horizontal plane (against flexural failure, any axis).

DTB Non-Lipped (120-78-25-5070), "yz Restrained"		
$E_{D,m}$ = 0.0 mm	$E_{D,m}$ = -3.0 mm	$E_{D,m}$ = -6.0 mm
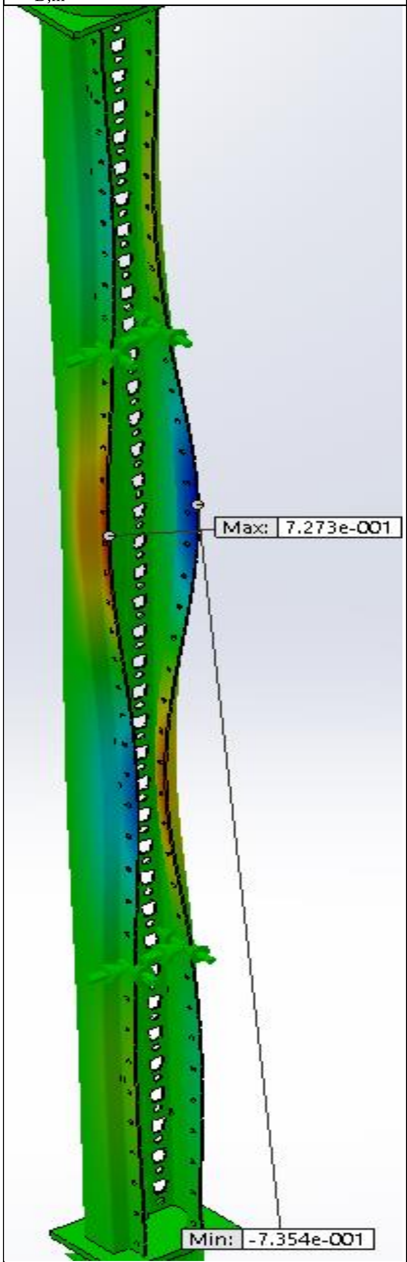	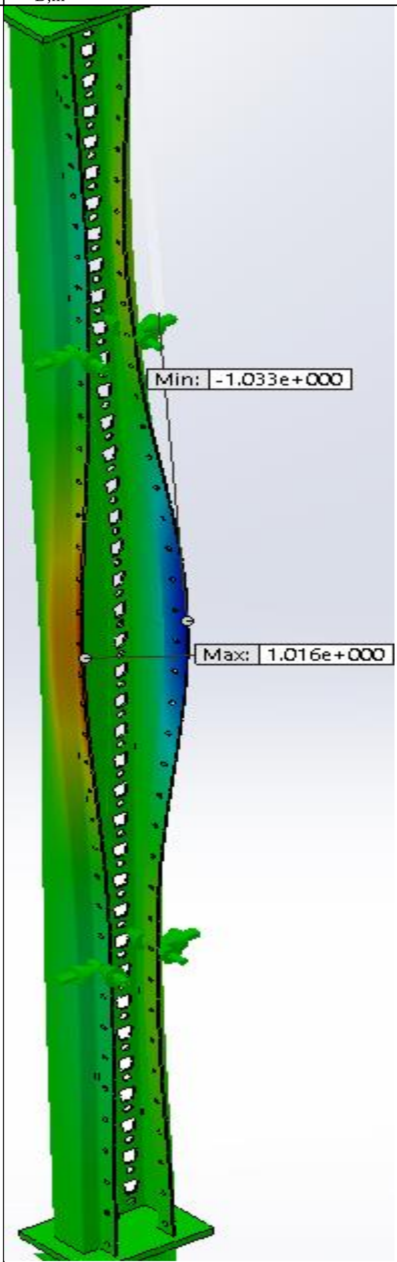	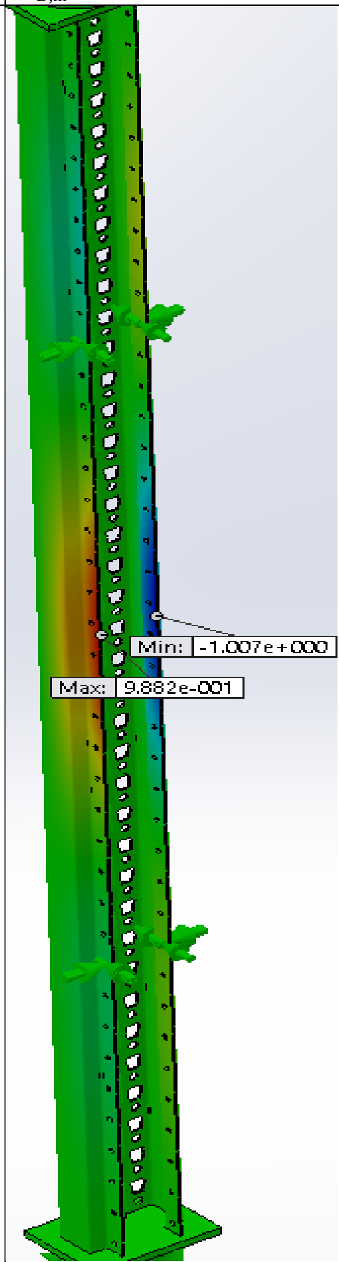
Distortional	Distortional	Distortional

Figure 42. Distortional buckling test of non-lipped profile, after restraining movement of the spacers in horizontal direction.

DTB Lipped (120-83-25-5070), "yz Restrained"		
$E_{D,m}$ = 0.0 mm	$E_{D,m}$ = -3.0 mm	$E_{D,m}$ = -6.0 mm
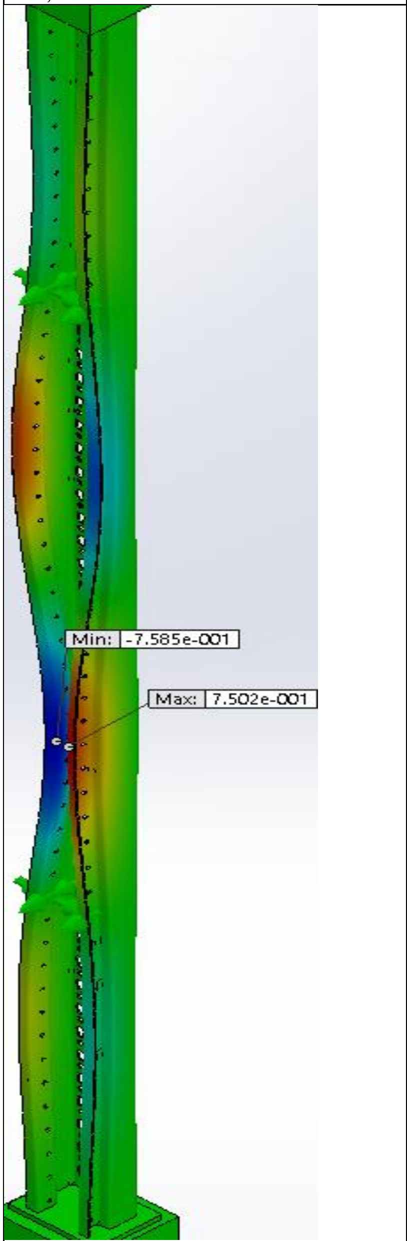	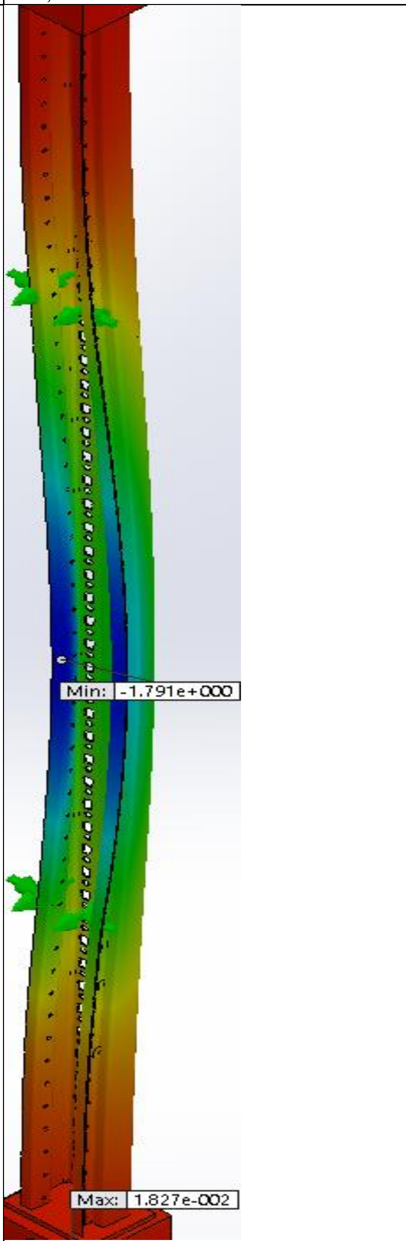	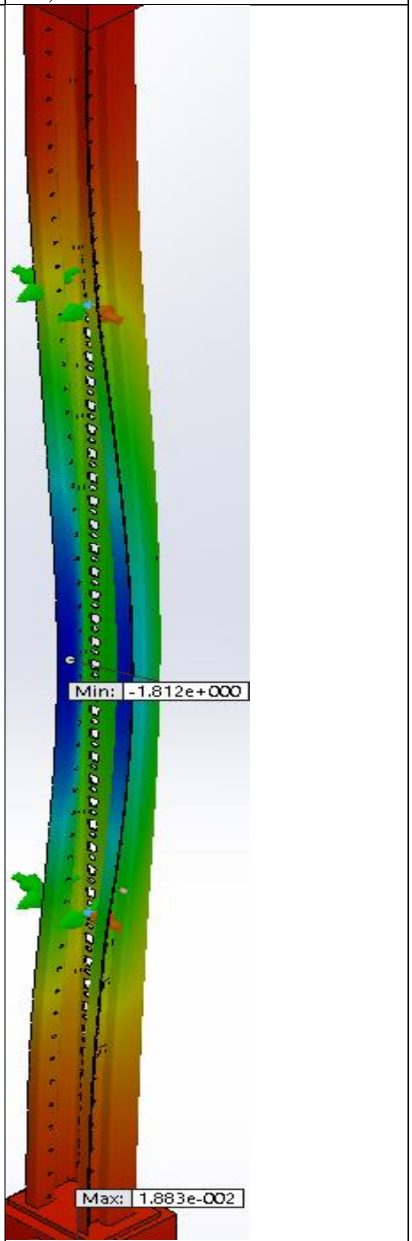
Distortional	Flexural-Torsional / Distortional	Flexural-Torsional / Distortional

Figure 43. Distortional buckling test of lipped profile, after restraining movement of the spacers in horizontal direction.

When the spacers are kept in the same horizontal position the flexural- (global) buckling effects are largely eliminated. The load factors show significant increases of about +50%, which reveals the increase in strength after adding stiffness. Despite Flexural Buckling effects over the minor (z-)axis (FBz) is eliminated, another global mode shows up: Flexural Torsional Buckling (FTB). Against expectations, the pinching effect 'blocks' the distortional mode and the first mode hereafter is the FTB mode.

Single Uprights used in Frame setup

The types of uprights profiles used in the frame test setup are simulated using boundary conditions according to the ones expected in a complete frame.

The results of analysis on the ‘cut-out’ single uprights used in the frame setup can be found in Appendix L, Figure 70 and Figure 71 and for detailed view including cross sectionals; Figure 72 and Figure 73.

To access the validity of modelling the full diagonals as simple constrains around the diagonal spacer perforations some simulations on full frames have been executed and results are visualized in Figure 44. When the results on the full frame simulation match the corresponding ‘single-upright-DTB’ setup, no further research is required.

<table>
<tr><th>Frame Setup (Non-Lipped)</th><th>Frame Setup (Lipped)</th></tr>
<tr><td>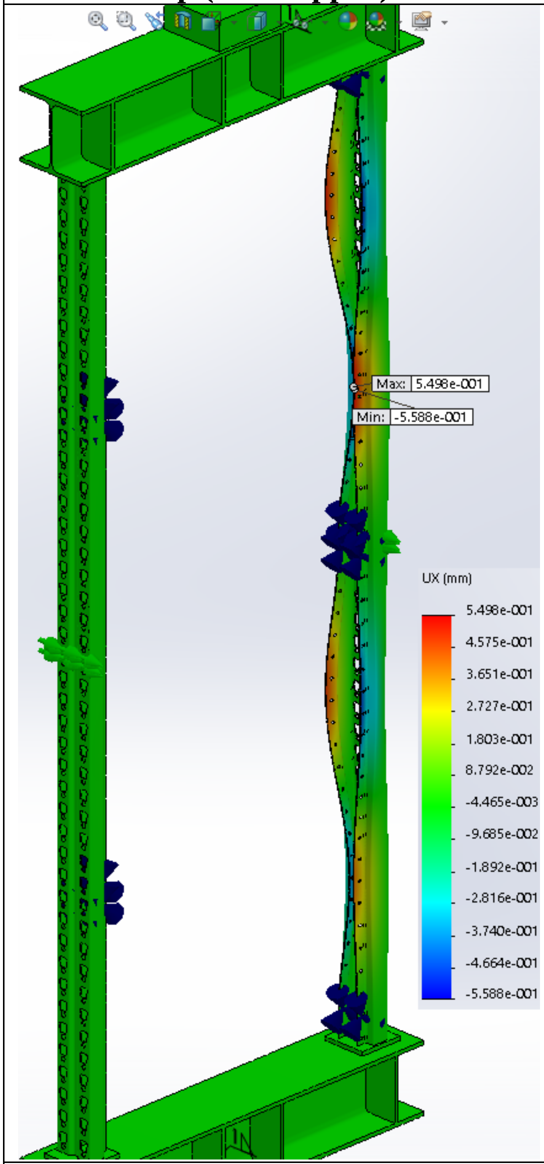
</td><td>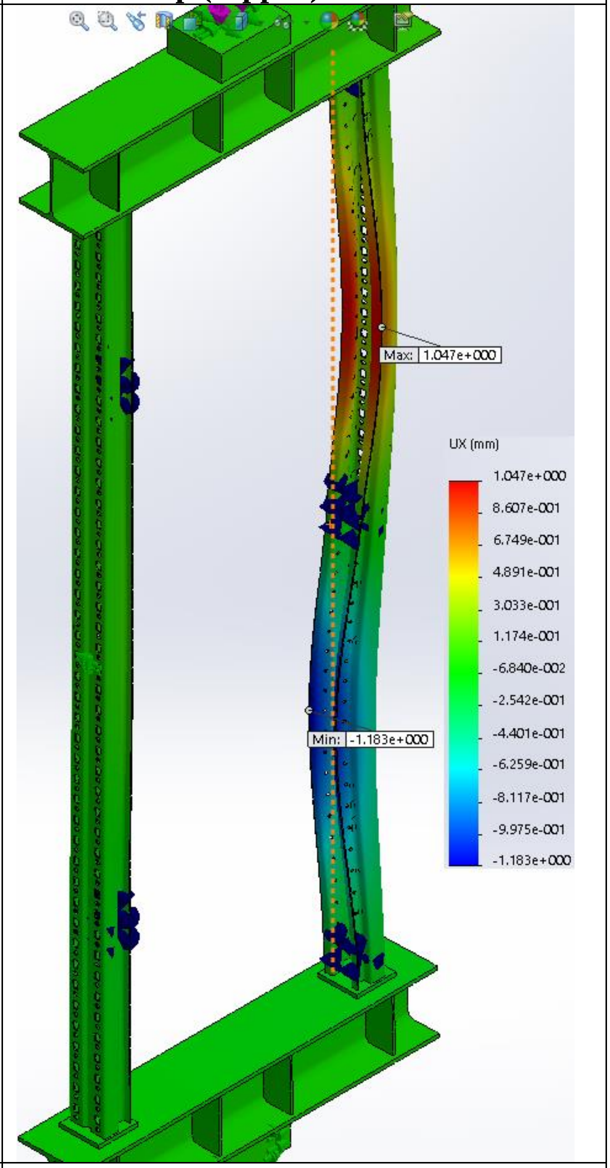
</td></tr>
<tr><td>Distortional</td><td>Flexural-Torsional / (Subordinate) Distortional</td></tr>
</table>

Figure 44. Results of numerical analysis of complete frames, using pin-pin diagonals. Notice similar behaviour as simulation of single uprights. Because the behaviour is similar, no additional simulations of complete frames are necessary.

04.7. Results: Non-Linear Analysis

After several buckling and static studies have been carried out, estimates of failure modes and imperfection forces are generated. These can be used in the Non-Linear study to estimate failure load.

First step in the progress of estimating the bearing capacity is finding reference criteria for the point of failure. Standard SolidWorks FEM simulation will not directly give an answer for the ultimate load point. The reference model could be based on a former experiment carried out. In this reference model, the earlier test should be rebuild as close as possible. This means that previously observed material yield point should be adapted, and if available all registered initial imperfections.

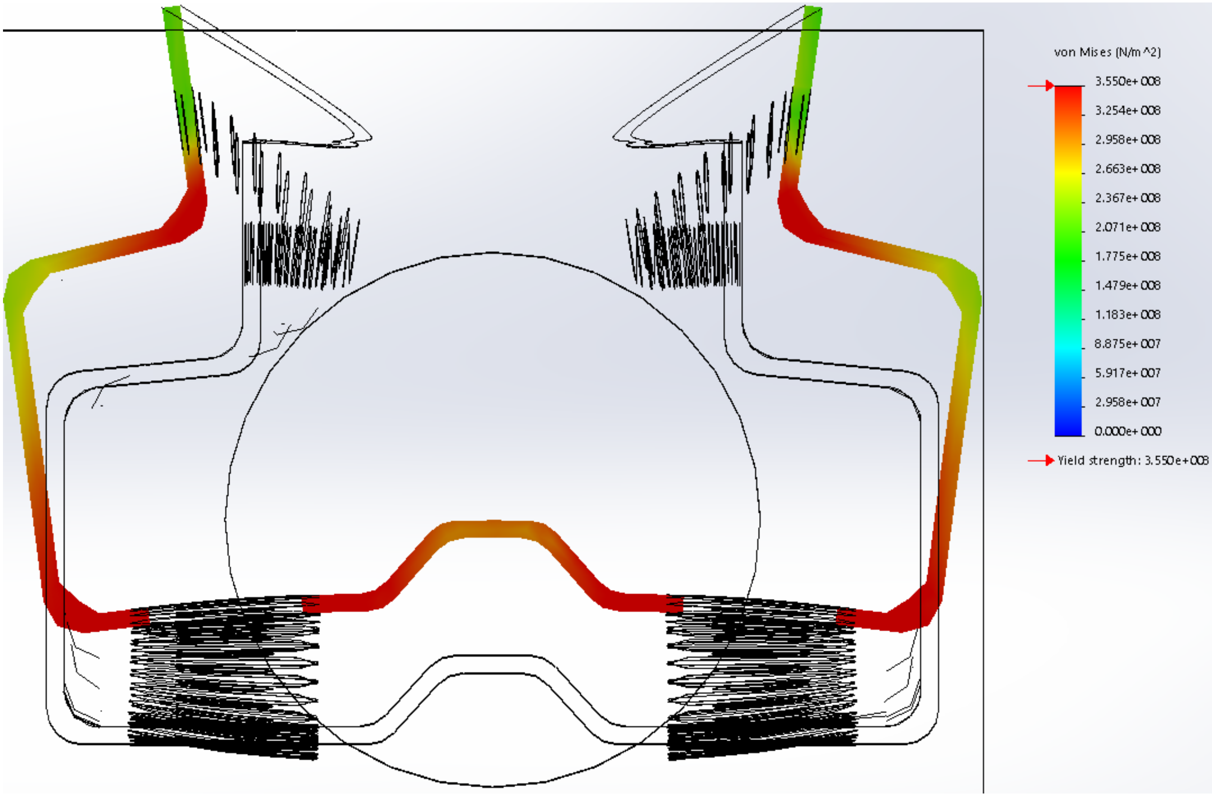

Figure 45. Non-Linear Study at the point of failure in a non-lipped 100-68-20-4050 profile. The percentage of area which is plastic could be used as a criteria for failure in other sections at varying pinching amounts or probably also other imperfection effects.

The reference situation shows that samples will fail when the percentage of the cross-sectional area in plastic state reaches around 55 and 64 percent respectively for the non-lipped and lipped profiles. Sadly enough, acquisition of more significant digits will cost valuable computation time and also requires better approximation of the reference percentages in failing cross sections. For an estimation of the load factor, no more additional digits than 2 are calculated. The percentage of plastic area allowed is in fact a value of major interest, since this can also tell more about what kind of profile classification the profile could potentially be assigned.

Conclusions from Numerical Research

The results of the numerical simulation research should answer sub question 3:

‘How can the Finite Element Method determine buckling shapes and estimate corresponding failure loads?’

- Linearized elastic buckling models can be used to predict failure mode shapes;
- Running a simulation model is a relatively simple and easy job. However, finding boundary conditions which simulate the real-life profiles closest can be tough and requires deeper insight;
- Estimating actual failure forces with a non-linear analysis is rather ‘guessing’ than exact calculation. The estimation technique can be used to find order-of-magnitude of the failure forces. Nevertheless, the linear elastic load factors can be used to compare situations among each other to find out if applied effects are favourable or unfavourable for the failure load;
- Numerical Simulation can be used to reduce the number of tests required, but cannot substitute experimental research.

05.Conclusions & Recommendations

As a result of the research process the most reasonable comparison would be between the experiment and the Finite Element model simulation results.

05.1. Conclusions concerning Pinching Effect

Results of all studies and analysis, effect on local, A-Sym- & Sym-Distortional (DTB) modes.

05.1.1. Modal Expression

The DTB-setup experimental and numerical analysis results seem to match, emphasizing the statement made earlier entailing required restrains on flexural buckling over the weak axis. When the degrees of freedom are reduced in y- and z- direction (in cross-sectional plane) the results are better, although the pinched profiles seem to switch to the flexural-torsional mode. It could be possible that the pinching ‘locks out’ the distortional mode by exactly opposing the distortion somewhere in the bulged part of the flange, reversing its effect and increasing resistance to this mode.

When considering full frames to be tested, again the non-lipped profiles buckle distortional like expected. However, the lipped profiles tend to fall back in the flexural-torsional mode. Obviously, even more supports are necessary to prevent this behaviour.

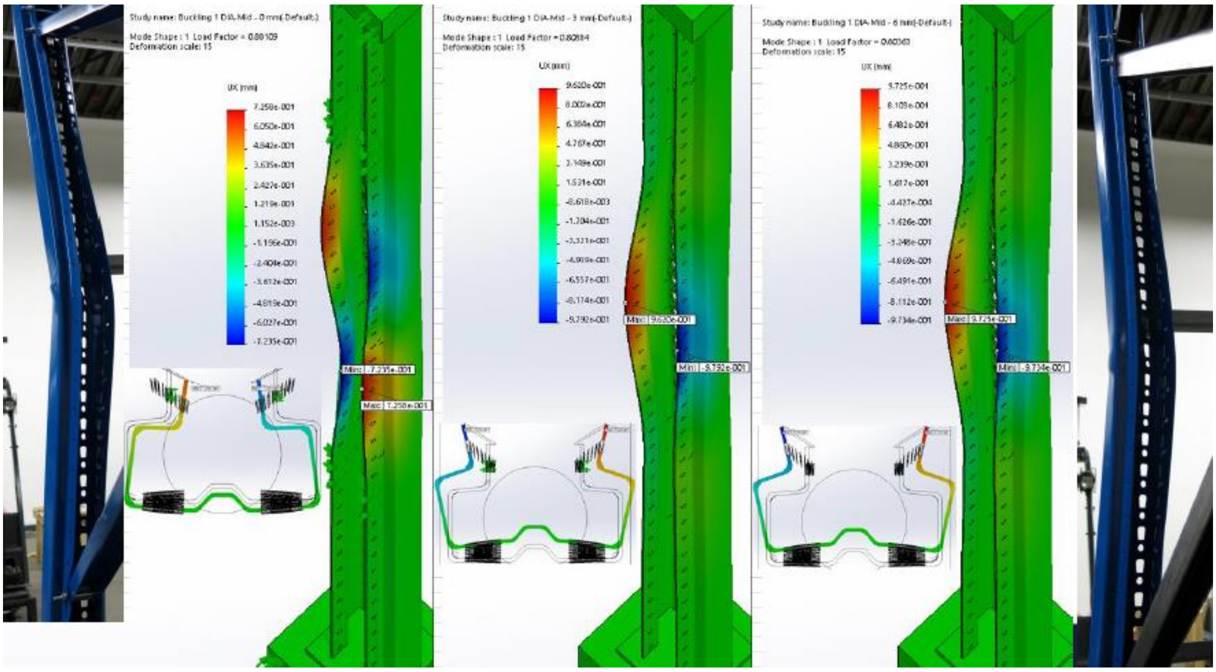

Figure 46. Frame test experiment versus simulations, non-lipped profile. Notice the model switch after pinching effect is introduced. This switch is explained by the cross-sectional resistance against distortion which cannot uphold the large moment introduced by the smaller spacers.

Besides distortional failure, a portion of global buckling over the mayor axis of the frame was exerted. This was because the supports to prevent this type of buckling where weak. During the first tests some minor changes to these support were made. As a result, the number of remaining tests is not enough to statistically exclude potential presence of other phenomena.

All samples failed under symmetric distortional circumstances but in a setup with decreased flexural resistance. This caused the failure loads to be quite low averaging between 250 and 300 kN, while 300 to 350 kN was predicted in a full only-distortional setup.

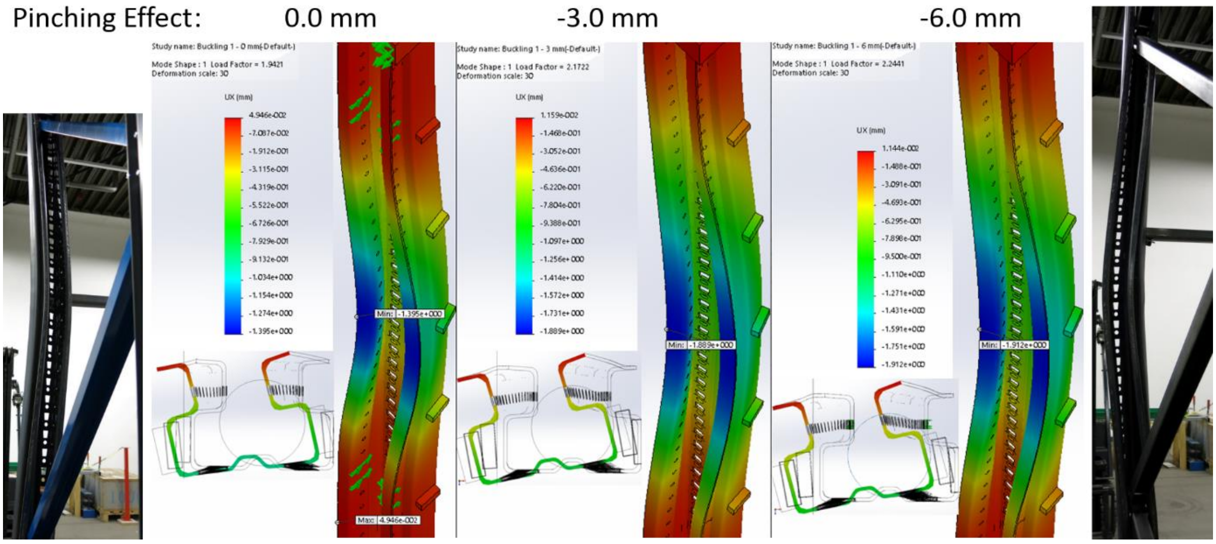

Figure 47. Frame test experiment versus simulations, lipped profile. Effect of pinch strengthens the profile.

In Simulations, a combination of Flexural-Torsional and Distortional buckling can be recognised. After pinching, the Distortional mode is blocked (or pinched out) and the FT-mode remains. Anyway, the total stiffness increases because the only way of failing is FT-mode which forms only a part of the total expressed deformation.

In actual experiment, Flexural-Torsional is also dominant in the no-pinch situation. This is the results of having actual diagonals with a finite stiffness and having rigid restrains in the numerical SolidWorks model.

05.1.2. Ultimate Loads

After analysis with the Non-Linear study the actual failure loads can be estimated and compared with experiment results.

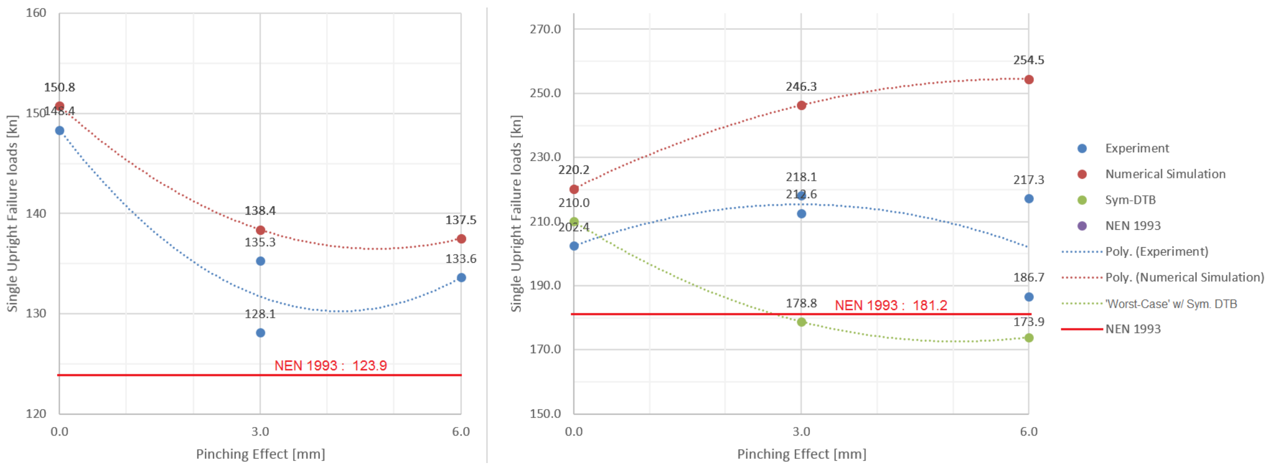

Figure 48. Ultimate loads: Comparison between Numerical estimation, Experiment observations and the standards.

Non-Lipped profile

Experiment has lower critical loads which is the result of the weak supports. The general shape of the effect seems quite legit, although insufficient number of tests for a statistical valid evaluation. The reduction in capacity at 6mm is 9% in the simulation and 10% in the experiment.

Lipped profile

Experiment shows lower critical values as a results of reduced resistance against Flexural Torsional buckling. The diagonals have a finite stiffness allowing the profile to show more FT-mode. After excessive pinching, the profile is automatically forces to move more into FT-mode. If this mode has lower resistance (bending diagonals) the experimental results drop in comparison with the Numerical Simulation. The increase in capacity at 6mm is 16% in the simulation and in the experiment turns out to be practically the same. Sadly, the spread becomes much larger.

For the lipped profile, the worst-case scenario was not reached because of the a-symmetric distortional mode which is now proven to increase the critical load of the profile. The symmetric distortional profile shows more affinity to a worst-case situation.

05.1.3. Summarized

This research project has been and will be a continuous progress of learning. After this stage, the following statements can be made.

- Pinching effects are harmless to systems where the Local- and A-Symmetric buckling mechanisms are normative;
- Pinching effects can significantly reduce load capacity of systems initially prone to Symmetric Distortional buckling;
- Worst Case Scenario: Loss of capacity with 17% of initial strength, at 6 mm pinch. This is 3kN (2%) below the values ascribed by the standards (NEN 1993);
- Preferred test setup to find the effect would be a frame test setup;
- Numerical Simulations can estimate if a potential situation can be considered as worst-case with regard to mainly the triggered mode of failure;
- Numerical Finite Element simulation can be employed to estimate the failure load but experiments are always required to determine actual load capacity.

05.2. Recommendations

Results so far show that the developed frame test setup can be a valuable application for assessing effects of pinch. However, the used frame setup still requires a list of minor changes which are summarized hereafter:

- Obtain simulation results using Finite Element Method and the Finite Strip Method at a range of upright lengths. Attention should be drawn to potential normative modes and their expected behaviour towards pinch results.
- The normative mode should be a Symmetric distortional shape. This might not coincide with the minimum on the Load Factor curve generated by CU-FSM;
- Positions of Supports against flexural buckling and twisting or torsional effects of the complete frame is preferred to be 4 support at respectively the lowest point on the upright, at the height of the 1^{st} diagonal junction, the 3^{rd} diagonal junction and at the top most point at the upright;
- Improvement of the Finite Element model can be realized by using more flexible supports;
- Future tests are required at the actual worst case point.

In case of test results that do not reach capacity ascribed by the standards, one or a combination of the following measurements should be considered:

- Decrease acceptable production tolerances. In practice this will mean that the people who adjust the roller components of the upright production line have to carry out their regular maintenance work more frequently;
- Apply a reduction factor in the used value of A_{eff} in the database of the profiles. The consequences would be that designs of existing storage might become ‘inadequate’ in terms of meeting the standards;
- Additional rings between the diagonal and the upright profile might ensure the space is reduced.
- Add an additional check in the design phase: exclude certain diagonal- & where possible beam- centre-to-centre distances. This could be different for every profile and will also reduce flexibility in design.

References

(n.d.). Retrieved from http://www.colorado.edu/engineering/CAS/courses.d/AFEM.d/AFEM.Ch10.d/AFEM.Ch10.pdf

Anderson, J. J. (2011). *Fundamentals of Aerodynamics* (5th Edition in SI Units ed.). New York, United States of America: McGraw-Hill. Retrieved May 5, 2015

Assink, M., & Horácek, M. (2014). *Prediction of the normative upright distortional buckling test length Nedcon procedure.* Research Project Report, Nedcon, Design Principles, Doetinchem. doi:Ncon 11-291 (Internal)

Carlos Felippa. (2013). CH10: The Quadratic Tetrahedron. In U. o. Boulder, *Advanced Finite Element Methods.* Boulder: University of Colorado at Boulder. Retrieved June 12, 2015, from http://www.colorado.edu/engineering/CAS/courses.d/AFEM.d/AFEM.Ch10.d/AFEM.Ch10.pdf

Casafont, Pastor, Roure, Bonada, & Pekoz. (2011). *ECCS - TWG 7.5 meeting, October 2011.* Cornell University in Ithaca (United States): Cornell University. Retrieved April 22, 2015, from http://lerma.upc.edu/news-1/tc7-meeting?set_language=en

Cheung. (1976). *Finite Strip Method.* Retrieved February 4, 2015

Cheung, Y. (1976). *Finite Strip Method in Structural Analysis* (1st ed.). Adelaide. Retrieved February 9, 2015, from https://books.google.nl/books?hl=en&lr=&id=zIZGBQAAQBAJ&oi=fnd&pg=PP1&dq=finite+strip+method&ots=BcDXJUtG9e&sig=Du5JvGCBxSW-3dQb7gKmGzJx60o#v=onepage&q=finite%20strip%20method&f=false

Cook, R. D., Malkus, D. S., Plesha, M. E., & Witt, R. J. (n.d.). *Concepts and Applications of Finite Element Analysis* (4th ed.). Madison, United States of America: John Wiley & Sons, Inc. . Retrieved February 10, 2015

Eastman, C., Teichholz, P., Sacks, R., & Liston, K. (2008). BIM Tools and Parametric Modeling. In C. Eastman, P. Teichholz, R. Sacks, & K. Liston, *BIM Handbook* (1st Edition ed., pp. 25-64). New Jersey, United States of America: John Wiley & Sons, Inc. . Retrieved May 15, 2015, from www.wiley.com/go/permissions

Erkmen, R., & Mohareb, M. (2008, February 12). Buckling analysis of thin-walled open members—A finite element formulation. *Thin Walled Structures, 46*(6), pp. 1-2. doi:doi:10.1016/j.tws.2007.12.002

European Committee for Standardization. (2009, March). Steel static storage systems - Adjustable pallet racking systems - Principles for structural design. *EN 15512:2009: E(Compressive Tests on Uprights)*, 84-98. Brussels, Europe: European Committee for Standardization. doi:ICS 53.080

Gerard, G., & Becker, H. (1957). *Handbook of Structural Stability.* New York, Washington, Uniterd States of America: New York University. Retrieved June 11, 2015, from naca.central.cranfield.ac.uk/reports/1957/naca-tn-3781.pdf

IDRE. (2015, January). *Statistical analyses using Stata*. Retrieved March 20, 2015, from One sample t-test: http://www.ats.ucla.edu/stat/stata/whatstat/whatstat.htm

Lanzo, A. D., & Garcea, G. (1996). Koiter's Analysis of Thin-Walled Structures by a Finite Element Approach.

Li, Z. (2009). *BUCKLING ANALYSIS OF THE FINITE STRIP METHOD AND THEORETICAL EXTENSION OF THE CONSTRAINED FINITE STRIP METHOD FOR GENERAL BOUNDARY CONDITIONS.* Johns hopkins University. Retrieved February 4, 2015

Li, Z., & Schafer, B. (2010). Buckling analysis of cold-formed steel members with general boundary conditions using CUFSM: conventional and constrained finite strip methods. *Twentieth International Specialty Conference on Cold-Formed Steel Structures*, (pp. 1-15). Saint Louis, Missouri, USA. Retrieved April 22, 2015, from http://www.ce.jhu.edu/bschafer/cufsm/cufsm403/zli_schafer_new_CUFSM_v5_revised.pdf

Megson, T. (2014). *Introduction to Aircraft Structural Analysis* (2nd ed.). Oxford, United Kingdom. Retrieved February 24, 2015

NEDCON. (2015, January 1). *About Us*. Retrieved April 16, 2015, from NEDCON: http://www.nedcon.com/en/about-us/

Peterson, S. (2014, July 15). *Computing Constrained Delaunay Triangulations.* Retrieved May 22, 2015, from GeoM: http://www.geom.uiuc.edu/~samuelp/del_project.html

Podolskii, G. S. (1979). *Thin-Walled Structures*, 3rd Edition. Retrieved May 4, 2015, from The Free Dictionary - Encyclopedia: encyclopedia2.thefreedictionary.com/Thin-Walled+Structures

Schafer, B. (1998). Elastic Buckling Solution Methods for Cold-Formed Steel Elements and Members. In B. W. Schafer, *Cold-Formed Steel Behavior and Design: Analytical and Numerical Modeling of Elements and Members with Longitudinal Stiffeners* (pp. 1-18 (908 pages)). Ithaca, United States of America: Cornell University. Retrieved May 17, 2015, from https://books.google.nl/books/about/Cold_formed_steel_behavior_and_design.html?id=7S9UAAAAYAAJ&hl=en

Slivker, V. (2006). *Mechanics of Structural Elements: Theory and Applications (Google eBook).* Petersburg, Russia: Springer-Verlag. Retrieved March 5, 2015, from https://books.google.nl/books?id=Iac87raqE6AC&printsec=frontcover&source=gbs_ge_summary_r&cad=0#v=onepage&q&f=false

van Benthem, A. (2015). *Connectoren Systeemvloeren.* University of Twente, Department of Mechanical Engineering, Enschede. Retrieved April 10, 2015

Yiu, F. (2005). *A Geometrically Exact Thin-Walled Beam Theory Considering In-Plane Cross-Section Distortion.* Partial Fulfillment of the Requirements for the Degree of Doctor of Philosophy, Cornell University, Ithaca, New York. Retrieved March 25, 2015, from https://dspace.library.cornell.edu/bitstream/1813/2131/2/FinalThesis080505.pdf

Zaras, J., Kowal-Michalska, K., & Rhodes, J. (2001). *Thin-Walled Structures - Advances and Developments.* Google eBook. Retrieved March 3, 2015

Appendices

List of Appendices:

A. List of Abbreviations and definitions

Abbreviation:	**Meaning / Explanation:**
'100-68-20' or '68' or 'Non-lipped'	Short for Upright Profile PRF 100-68-2.0-4050 PR (S355); one of the used profiles. See Appendix D.4. for explanation of profile codes.
'100-72-25' or '72' or 'Lipped'	Short for Upright Profile PRF 100-72-2.5-4050 PR (S355); one of the used profiles. See Appendix D.4. for explanation of profile codes.
'120-78' or '78' or 'Non-lipped'	Short for Upright Profile PRF 120-78-2.5-5070 PR (S355); one of the used profiles. See Appendix D.4. for explanation of profile codes.
'120-83' or '83' or 'Lipped'	Short for Upright Profile PRF 120-83-2.5-5070 PR (S355); one of the used profiles. See Appendix D.4. for explanation of profile codes.
BIM	Building Information Modelling
BSc.	Bachelor of Science
CAD/CAM/CAE	Computer Aided Design / Computer Aided Modelling / Computer Aided Engineering
cFSM	Constrained Finite Strip Method; Method in which a number of strips are used to access the buckling modes and load factor of thin walled cross sections. See also section '03.2 ; Constrained Finite Strip Method'.
CiT	Civil Engineering
CU-FSM	Application Cornell University Finite Strip Method solver using cFSM, see above.
DOF (also nDOF)	Degrees of Freedom, used to indicate number of degrees of freedom in discretized Finite Elements
DTB	Distortional Buckling testing (As described in Annex A of EN 15512:2009). The DTB-test setup with spacer, as used in this research, is described in Figure 6 on page 17.
FBy	Flexural Buckling over Major (y-)Axis (See section 02.1)
FBz	Flexural Buckling over Major (z-)Axis (See section 02.1)
FE	Finite Elements
FEA	Finite Elements Analysis
FEM	Finite Elements Method; Not to be confused with its homonyme abbreviation for: Federation Europeenne De La Manutention, the committee for Eurocodes involving storage racks and similar structures.
FSM	Finite Strip Method
ISO	Isometric View
OTW	Open Thin Walled; (~Profiles or ~Sections) Structural components are classified as 'Thin Walled' when one of the dimensions is small compared to the other two. (Podolskii, 1979) Profiles are considered 'Open'-sections when no closed paths are present in it cross-section. A closed path will deliver additional torsional resistance.
UTS	Ultimate Tensile Strength

B. Initial single STUB- and DTB setup tests: Method of Evaluation

The first series of experiments are quite similar to ones done many times at NEDCON.

<u>Test Setup: Effect of Tolerances</u> Upright opening on Buckling Capacity

From the tested specimen, the useful samples need to be selected on the basis of their failure modes and therefor corresponding loads. Failure modes that are clearly not normative should be marked as 'not usable'. The expectation is that the STUB-tests will fail under local buckling circumstances while the DTB (Distortional Compressional Buckling Test) fail due to deformation within the plane. For shape of the failure modes, see also the figure below.

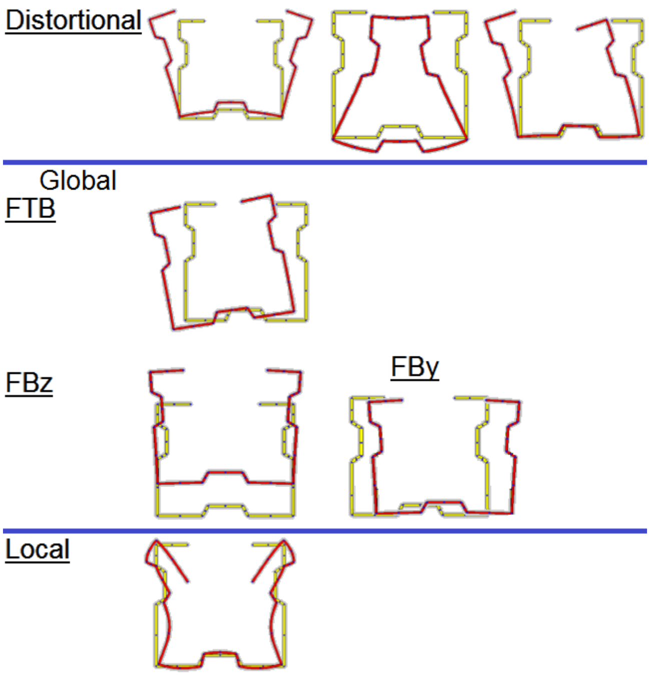

Figure 49. Possible Failure Modes. In fact, there will be many more (theoretically infinetely) modes, the 'pure' ones observed are displayed here. In the results, mostly combinations of these modes will occur.

Most of the specimen seemed useful according to their shape of failure except for the DTB testing of the '120-83' profiles. All of the DTB-'120-83'-tests but one seemed to fail under flexural (Global) conditions and not distortional. Although it seemed that the set-up configuration of the DTB for the '120-83' profiles did not really developed at planned, the results will be taken into account.

For the selected specimen, corrections need to be taken into account for the actual yield-strength and the thickness compared to the design values of the steel. The corrections should be calculated according to the following formulas:

$$F_{ni} = F_{ti}\left(\frac{f_y}{f_t}\right)^{\alpha}\left(\frac{t}{t_t}\right)^{\beta}$$

Where:

F_{ni} = The corrected failure load for test number (i);

F_{ti} = The observed failure load for test number (i);

f_y = The nominal yield stress;

f_t = The observed yield stress for the specimen;

t = The design thickness;

t_t = The observed thickness for the specimen;

α = 0 when $f_y \geq f_t$;

1.0 when $f_y < f_t$;

For $t \geq t_t$: $\beta = 0$

For $t < t_t$: $$\beta = \frac{\frac{b_p}{t}}{k * sqrt\left(\frac{E}{f_t}\right)} - 1$$ but $1 \leq \beta \leq 2$

where:

k = 0.64 for stiffened elements

0.21 for unstiffened elements

and where b_p is the notional plane width, see Annex D for profile details.

The observed yield strength and thickness is measured by tensile testing. The results of these tests are displayed in Annex B within Appendix D.

After applying the correction factors, a 2nd order polynomial can be fitted using the least squares technique. The polynomial is displayed in the figure below.

Figure 50. Polynomial trend fitting, along with the real test data and their corrected values.

To obtain the final characteristic loads of the configuration, a statistical evaluation requires to be carried. This needs to be done according to the following formulas.

The average of the normalized values is calculated using the following formula: $$\frac{F_{ni}}{F_{t\ m}} = \frac{1}{n} * \Sigma_{\mathrm{i=1}}^{\mathrm{n}} \left(\frac{F_{ni}}{F_t}\right)$$

The standard deviation of the normalised values is calculated by: $$s = \sqrt{\frac{1}{n-1} * \sum_{i=1}^{n} \left(\frac{F_{ni}}{F_t} - \frac{F_{ni}}{F_{t\ m}}\right)^2}$$

Final results which give an insight in the pinching effect can be found in the conclusion, see section 02.1.1 in the main report.

C. Detailed Evaluation of Earlier Test Results

The detailed calculations according to NEN EN 1993-1-8:2005 and EN 15512:2009 are written out here.

Evaluation

Graphical representation of the test results is included in Annex A. Tensile test results can be found in Annex B. Photographic evidence of the test series is provided in Annex C.

Overview of test results

Measured critical loads (Failure loads) of the specimen. Only the tests with equal e (= estimated ditance to CG) are displayed.

	Diagonal space, $E_{D,M}$ [mm]	12078255070 PR S355		12083255070 PR S355	
		STUB	DTB	STUB	DTB
		F_{ti} [kN]	F_{ti} [kN]	F_{ti} [kN]	F_{ti} [kN]
Test 1	0.0	288.596		346.68	
Test 2	0.0		198.355		205.88
Test 3	0.0				186.23
Test 4	0.0	288.908	203.305		196.355
Test 5	-3.0	287.348	176.13	341.376	185.48
Test 6	-3.0	285.736	168.18	334.928	195.905
Test 7	-6.0	281.004	149.005	330.612	192.255
Test 8	-6.0	279.704	153.93	331.548	220.055
Common e		28	29	35	34

Observed failure modes

Based on observation of tested samples, the failure modes can be described. Corresponding colors indicate the most common failure modes.
Failure modes, according to nomenclature: DTB, FTB, FB_y, FB_z and Local shapes, displayed below.

		Test 1	Test 2	Test 3	Test 4	Test 5	Test 6	Test 7	Test 8
	$E_{D,m}$ [mm]	0.0	0.0	0.0	0.0	-3.0	-3.0	-6.0	-6.0
12078255070 PR S355	STUB	Local	0	0	Local	Local	Local	Local	Local
	DTB	0	DTB	0	FBz	DTB	DTB	DTB	DTB
12083255070 PR S355	STUB	Local	0	0	0	Local	Local	Local	Local
	DTB	0	FBz	FBz	FBz	FBz	FBz	DTB	FBz

Distortional

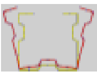

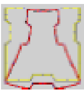

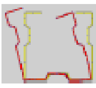

Legend Colors

DTB
FTB
Fby
FBz
Local

FTB

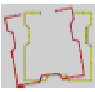

FBz

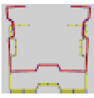

Local

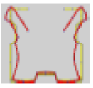

Note: Along with the photographs of the failed samples a quick description of the failure modes is given in Appendic C.

Check samples on relevant behaviour.

A selection of samples is made to exclude tested specimen that failed in non-normative modes with substantial higher corresponding critical loads.

	Diagonal space, ED,M [mm]	12078255070 PR S355		12083255070 PR S355	
		STUB	DTB	STUB	DTB
		Fti [kN]	Fti [kN]	Fti [kN]	Fti [kN]
Test 1	0	OK.	OK.	OK.	OK.
Test 2	0		OK.		OK.
Test 3	0				OK.
Test 4	0	OK.	OK.		OK.
Test 5	-3	OK.	OK.	OK.	OK.
Test 6	-3	OK.	OK.	OK.	OK.
Test 7	-6	OK.	OK.	OK.	OK.
Test 8	-6	OK.	OK.	OK.	NotNormative

Instructions:
For all executed test this checkbox can determine if a result is used for calculation and evaluation. To involve a test sample into calculation, type "OK. " or "ok." into the corresponding cells. If you would like to prevent a test sample to be taken into account, type anything else. The colors of the cells indicate the current status of a sample. When "de-activating" a sample, a copy will still remain save for propable later usage. WARNING: For all types of tests (columns) at least 1 sample is required in the ranges "Test 1" - "Test 4" (Rows), the samples "Test 5" & "Test 6" are IN ALL CASES REQUIRED. For the rows "Test 7" & "Test 8", again at least 1 sample value needs to be used.

Overview of left over (usefull) samples

	Diagonal space, $E_{D,M}$ [mm]	12078255070 PR S355 STUB F_{ti} [kN]	12078255070 PR S355 DTB F_{ti} [kN]	12083255070 PR S355 STUB F_{ti} [kN]	12083255070 PR S355 DTB F_{ti} [kN]
Test 1	0.0	288.596		346.68	
Test 2	0.0	0	198.355	0	205.88
Test 3	0.0	0	0	0	186.23
Test 4	0.0	288.908	203.305	0	196.355
Test 5	-3.0	287.348	176.13	341.376	185.48
Test 6	-3.0	285.736	168.18	334.928	195.905
Test 7	-6.0	281.004	149.005	330.612	192.255
Test 8	-6.0	279.704	153.93	331.548	0

Corrections to test results

The following formula should be used to apply a correction to the failure loads due to variations in the yield stress of the material and the thickness of the test specimen.

$$F_{ni} = F_{ti}\left(\frac{f_y}{f_t}\right)^{\alpha}\left(\frac{t}{t_t}\right)^{\beta}$$

Where:

F_{ni} = The corrected failure load for test number (i);

F_{ti} = The observed failure load for test number (i);

f_y = The nominal yield stress;

f_t = The observed yield stress for the specimen;

t = The design thickness;

t_t = The observed thickness for the specimen;

α = 0 when $f_y \geq f_t$;
1.0 when $f_y < f_t$;

For $t \geq t_t$: $\beta = 0$

For $t < t_t$: $\beta = \dfrac{\frac{b_p}{t}}{k * sqrt\left(\frac{E}{f_t}\right)} - 1$ but $1 \leq \beta \leq 2$

where:

k = 0.64 for stiffened elements
0.21 for unstiffened elements

and where b_p is the notional plane width, see Annex D for profile details.

Correction in yield stress

All the profiles of the same type originate from the same steel profiles order and are assumed to posses the same yield strenght. To acces this yield strength, 2 tensile tests have been executed for both profiles. The outcomes and conlusion of the Tensile Tests can be found in Annex B.

	Type Upright Profiles	Nominal f_y [N/mm²]	Observed f_t [N/mm²]	α [-]	Correction Factor
1	12078255070 PR S355	355	422	1.0	0.841232227
2	12083255070 PR S355	355	420	1.0	0.845238095

Correction in specimen thickness

	Type Upright Profiles	Design t [mm]	Observed t_t [mm]	k [-]	β [-]	Correction Factor
1	12078255070 PR S355	2.5	2.51	0.21	1	0.996015936
2	12083255070 PR S355	2.5	2.6	0.64	1	0.961538462

Corrected test results

	Diagonal space, $E_{D,M}$ [mm]	12078255070 PR S355 STUB F_{ni} [kN]	12078255070 PR S355 DTB F_{ni} [kN]	12083255070 PR S355 STUB F_{ni} [kN]	12083255070 PR S355 DTB F_{ni} [kN]
Correction Factor C_1 [-]		0.837881		0.812729	
Test 1	0.0	241.809		281.757	
Test 2	0.0		166.198		167.325
Test 3	0.0				151.355
Test 4	0.0	242.070	170.345		159.583
Test 5	-3.0	240.763	147.576	277.446	150.745
Test 6	-3.0	239.413	140.915	272.206	159.218
Test 7	-6.0	235.448	124.848	268.698	156.251
Test 8	-6.0	234.359	128.975	269.459	

Statistical evaluation of the results

Profile 12078255070 PR S355

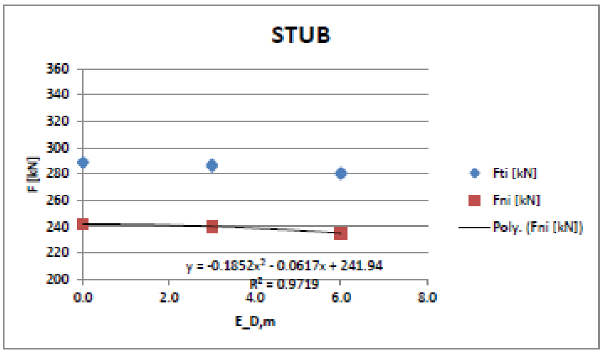

Profile 12083255070 PR S355

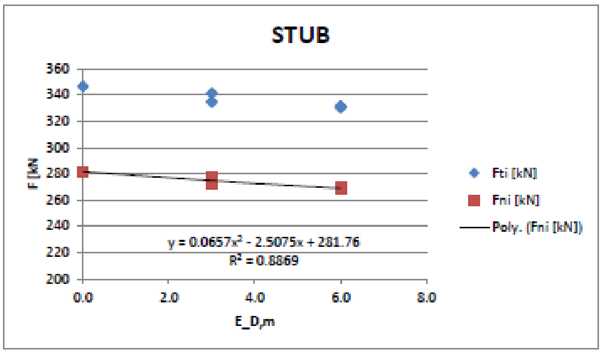

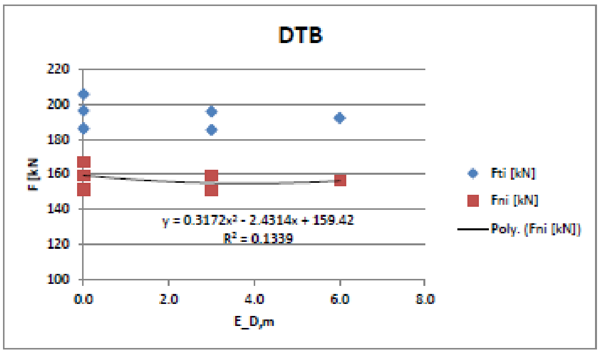

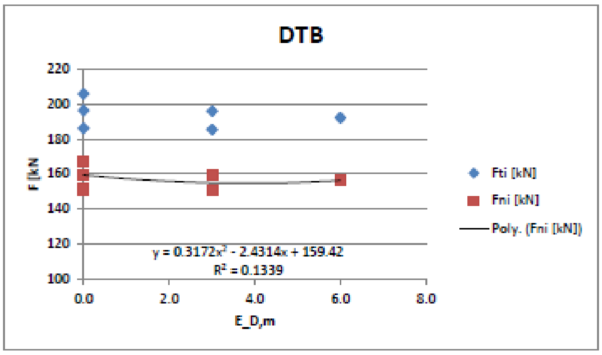

The average of the normalized values is calculated using the following formula:

$$\frac{F_{ni}}{F_{t\ m}} = \frac{1}{n} * \Sigma_{i=1}^{n} \left(\frac{F_{ni}}{F_t}\right)$$

The standard deviation of the normalised values is calculated by:

$$s = \sqrt{\frac{1}{n-1} * \sum_{i=1}^{n} \left(\frac{F_{ni}}{F_t} - \frac{F_{ni}}{F_{t\ m}}\right)^2}$$

Normalised Loads, mean and standard deviations.

Relative differences normalised loads and polynome results.

Diagonal space, $E_{D,M}$ [mm]	12078255070 PR S355 STUB F_{ni} / F_t	12078255070 PR S355 DTB F_{ni} / F_t	12083255070 PR S355 STUB F_{ni} / F_t	12083255070 PR S355 DTB F_{ni} / F_t
0.0	0.999460		1.000000	
0.0		0.987676		1.049578
0.0				0.949402
0.0	1.000540	1.012324		1.001020
3.0	1.002813	1.023090	1.009534	0.972665
3.0	0.997187	0.976910	0.990466	1.027335
6.0	1.002318	0.983742	0.998586	1.000000
6.0	0.997682	1.016258	1.001414	
Usefull tests n =	6	6	5	6
Average relative differences $(F_{ni} / F_t)_m$	1.000000	1.000000	1.000000	1.000000
Standard deviation s_n	0.002330617	0.019486608	0.006815373	0.036092996

Characteristic Loads

The characteristic value of the buckling force shall be calculated as follows: $F_k = F_t * (1 - k_s * s_n)$

where k_s can be taken from the table EN 15512:2009

n	3	4	5	6	7	8	9	10	15	20	30	40	50	100	∞
ks	3.37	2.63	2.33	2.18	2.08	2.00	1.95	1.92	1.82	1.76	1.73	1.71	1.69	1.68	1.64

Statistical confidence of the results are based on the 95% fractile at confidence 75%.

	2[nd] order polynome for estimating F_t: (with x is the diagonal space $E_{D,M}$)	Polynome estimate Diagonal space, ED,M [mm] 0	3	6		Characteristic Load Diagonal space, ED,M [mm] 0	3	6
Profile type / test type		F_t [kN]	F_t [kN]	F_t [kN]	ks	F_k [kN]	F_k [kN]	F_k [kN]
12078255070 PR S355								
STUB	-0.1852 *x2 + -0.0617 *x + 241.9397 =	241.940	240.088	234.903	2.18	240.710	238.868	233.710
DTB	0.3718 *x2 + -9.1242 *x + 168.2716 =	168.272	144.245	126.912	2.18	161.123	138.118	121.520
12083255070 PR S355								
STUB	0.0657 *x2 + -2.5075 *x + 281.7569 =	281.757	274.826	269.078	2.33	277.283	270.462	264.805
DTB	0.3172 *x2 + -2.4314 *x + 159.4208 =	159.421	154.981	156.251	2.18	157.052	152.679	143.957

Conclusion

The effect pinching the endsheets of the profile, relative to his original strength can be captured in the following graph:

Profile 12078255070 PR S355
STUB

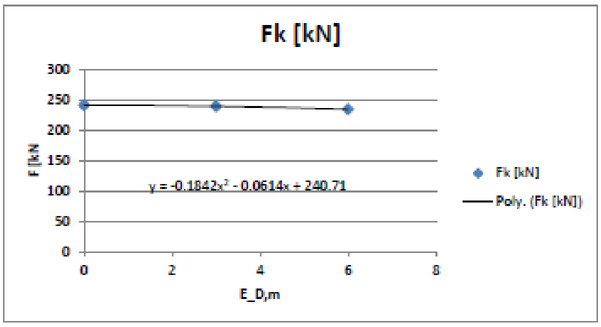

Profile 12083255070 PR S355
STUB

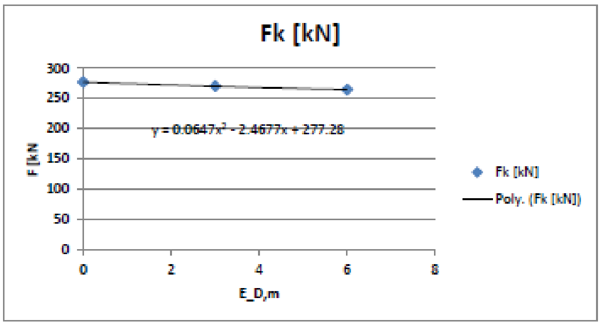

DTB

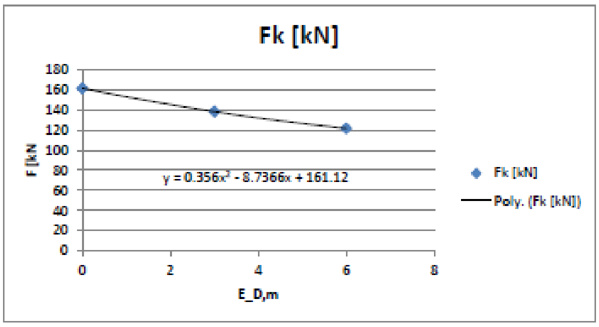

DTB

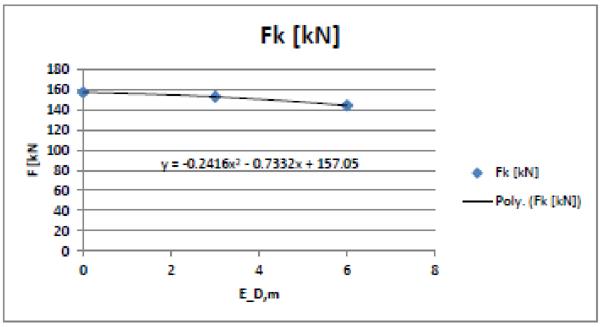

Increase in initial strength due to diagonal-spacer.

The tests with a diagonal spacer "bus"-component and a initial pinching of ED,m = 0 mm can be compared with the "plain" tests with same profiles and test setup, but without diagonal spacer "bus"-component. It is believed that the diagonal bus will stabilize the structure resulting in an increase in characteristic buckling load. The "plain" test results have been investigated earlier at NEDCON Research.

Pinching Effect

Characteristic Loads, Including diagonal spacer; Results valid for lenghts:

Profile	Test type	$F_{k,spacer}$ [kN] ($E_{D,m}$ = 0)	$F_{k,spacer}$ [kN] ($E_{D,m}$ = 3)	$F_{k,spacer}$ [kN] ($E_{D,m}$ = 6)	CTC [mm]
12078255070 PR S355	STUB	240.71	238.87	233.71	560
	DTB	161.12	138.12	121.52	2160
12083255070 PR S355	STUB	277.28	270.46	264.81	560
	DTB	157.05	152.68	143.96	2760

Characteristic loads, relative to no-pinchinig situation, but including diagonal-spacer.

$F_{k,ED,m=3}$ / $F_{k,ED,m=0}$ [-]	$F_{k,ED,m=6}$ / $F_{k,ED,m=0}$ [-]
0.992	0.971
0.857	0.754
0.975	0.955
0.972	0.917

Effect of diagonal-spacer

"Plain" tests, no diagonal spacer. Source: Earlier tests at NEDCON and corresponding valid for lenghts:

Profile	Test type	$F_{k,spacer}$ [kN] ($E_{D,m}$ = 0)	$F_{k,plain}$ [kN]	CTC [mm]
12078255070 PR S355	STUB	240.71	223.29	560
	DTB	161.12	194.29	1160
12083255070 PR S355	STUB	277.28	276.77	560
	DTB	157.05	255.39	1460

Relative bearing capacity with spacer over plain testing (WARNING! Different buckling-lengths for DTB!)

$F_{k,spacer}$ / $F_{k,plain}$ [-]
1.078000892
0.829308951
1.001857994
0.61495691

Effect of spacer compared with NEN EN 1993

Critical load, according to NEN EN 1993. Only for compared situation of DTB-testing. The lengths correspond to the tests with spacers.

Profile	Test type	$F_{k,NEN1993}$ [kN]	CTC [mm]
12078255070 PR S355	DTB	112.8	2160
12083255070 PR S355	DTB	111.9	2760

Test with spacer, without pinching, relative to NEN EN 1993 without spacer.

$F_{k,spacer}$ / $F_{k,NEN1993}$ [-]
1.428397781
1.40350534

D. Frame Test Evaluation

Experiments of the executed frame test setup.

D.1. 100-68-20-4050

Evaluation of Test Results

Overview of Rough test data

Upright:	10068204050
Steel:	355
Perforation:	PR

Test #	Pinch	F_FrameF	R_ti,SingleUpright	Failure mode	Valid Resu	Comment
[#]	[mm]	[kN]	[kN]	FBy / FBz / FTB / DTB	[Y/N]	
1	0.0	311.9	156.0	FTB / DTB	N	0
2	0.0	296.7	148.4	FTB / DTB	Y	0
3	3.0	270.6	135.3	FTB	Y	0
4	3.0	256.3	128.1	FTB	Y	Bij eerste maal Diagonalen niet
5	6.0	267.2	133.6	FTB	Y	0 aangedraaid!!
6	6.0	299.7	149.9	FTB	N	Knooppunten aangedraaid iov JWF
7	0.0	0.0	0.0	0	Y	0
8	0.0	0.0	0.0	0	Y	0
9	0.0	0.0	0.0	0	Y	0
10	0.0	0.0	0.0	0	Y	0
11	0.0	0.0	0.0	0	Y	0
12	0.0	0.0	0.0	0	Y	0

Number of Valid Results: n = 4

Corrections for actual yield point and thickness

Design Yield	f_y =	355	MPA
Actual Yield	f_t =	445	MPA
Design Thickness	t =	2	mm
Actual Thickness =	t_t =	2	mm

R_ni = R_ti * (f_y/f_t)^alpha * (t/t_t)^beta

b_p,stiffened =	40	mm	Notional Plane width		
b_p,unstiffened =	18	mm			
k_stiffened =	0.64	-			
k_unstiffened =	0.21	-			
alpha =	1	-			
beta_stiffened =	1	-	beta_t<tt,stiff =	0.438535	-
beta_unstiffened =	1	-	beta_t<tt,unstiff =	0.972848	-
beta =	1	-			

Correction on Yield:	C_Yield =	0.797753	-
Correction on Sheet thickness:	C_thick =	1	-

Corrected Test Values

Test #	Pinch [mm]	R_ti [kN]	R_ni [kN]
1	0.0	148.4	118.4
2	3.0	135.3	107.9
3	3.0	128.1	102.2
4	6.0	133.6	106.6
5	0.0	0.0	0.0
6	0.0	0.0	0.0
7	0.0	0.0	0.0
8	0.0	0.0	0.0
9	0.0	0.0	0.0
10	0.0	0.0	0.0
11	0.0	0.0	0.0
12	0.0	0.0	0.0

Polynome Fit for pinch-effect

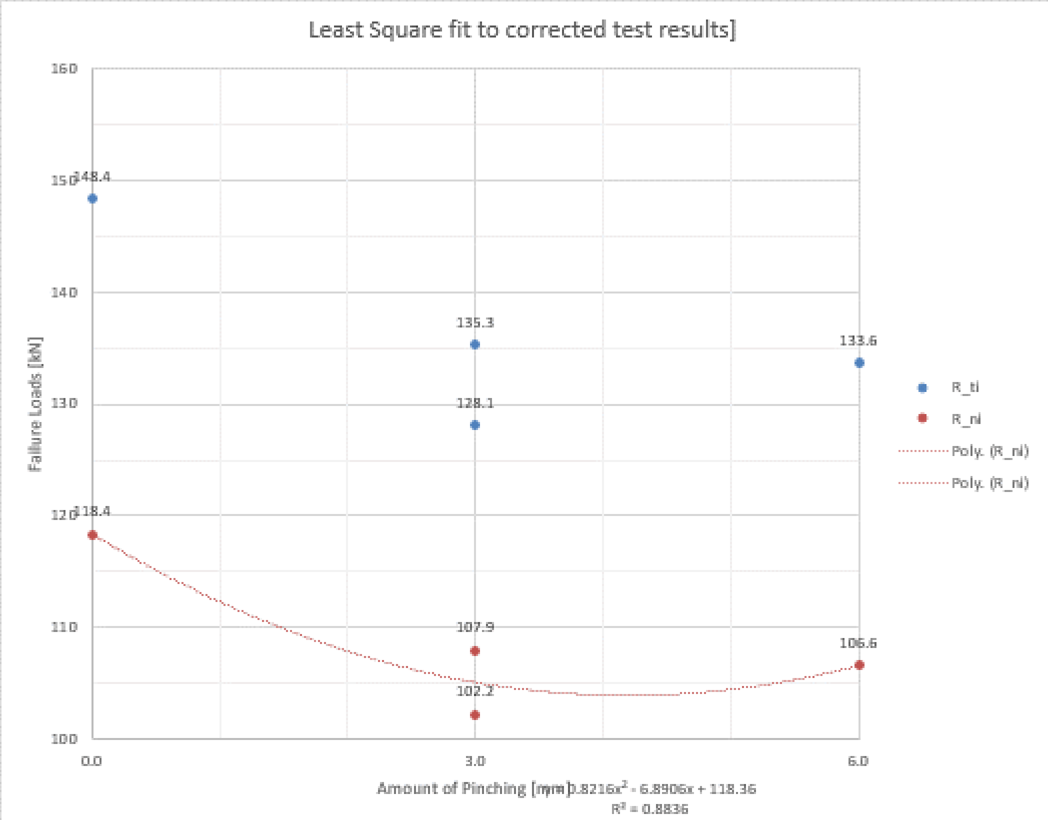

Single Upright Failure Load vs Amount of Pinching Effect

Coefficient for Polynome: c1*x^2 + c2*x + c3

c1 =	0.822	x^2
c2 =	-6.891	x
c3 =	118.359	

Derivation of Characteristic Values

Characteristic

Test	Pinch	Correcte	PolynomeValue	Normalized values
		F_ni	F_t (pinch) = 0.822 * pinch^2 + -6.891 * x + 118.359	F_ni / F_t
[#]	[mm]	[kN]	[kN]	[-]
1	0	118.4	118.4	1
2	3	107.9	105.1	1.0272
3	3	102.2	105.1	0.9728
4	6	106.6	106.6	1
5	0	0.0	118.4	0
6	0	0.0	118.4	0
7	0	0.0	118.4	0
8	0	0.0	118.4	0
9	0	0.0	118.4	0
10	0	0.0	118.4	0
11	0	0.0	118.4	0
12	0	0.0	118.4	0

n =	4	-	Average:	1.00000000
k_s =	2.63	[-]	Standard Deviation	0.022198987

n	3	4	5	6	7	8	9	10	15	20	30	40	50	100	∞
ks	3.37	2.63	2.33	2.18	2.08	2.00	1.95	1.92	1.82	1.76	1.73	1.71	1.69	1.68	1.64

Pinch	F_t	F_k = F_t * (1-k_s*s_n)
[mm]	[kN]	[kN]
0.0	118.4	111.4
3.0	105.1	98.9
6.0	106.6	100.4
NEN-1993		92.471

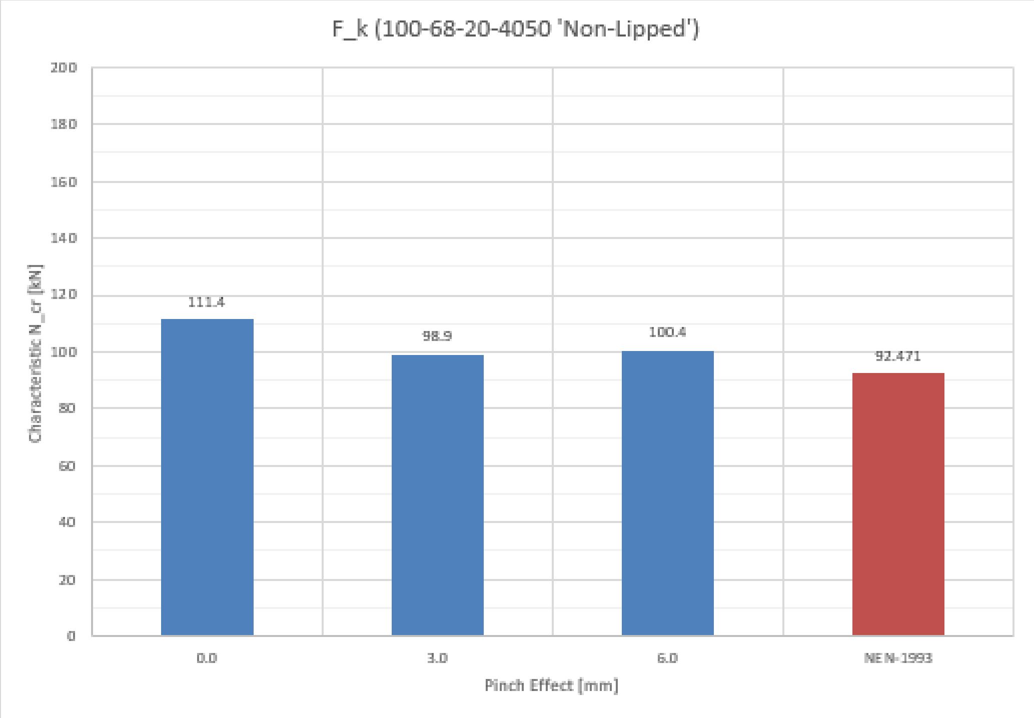

Conclusion

Current State of checks: Up-to-date

Pinch	A_eff	Reduction factor (0.0pinch = index100)
[mm]	[mm2]	
0	388.1	1.000
3	334.5	0.862
6	340.4	0.877

Reference (No-Spacer 'clean' DTB)

A_eff = 472.03238 mm2

Note: Without allowed eccentricity.

Initial Reduction due to different test Setup:

0.8222119 -

D.2. 100-72-25-4050

Evaluation of Test Results

Overview of Rough test data

Upright:	10072254050
Steel:	355
Perforation:	PR

Test #	Pinch	F_Frame	R_ti,SingleUpright	Failure mode	Valid Res	Comment
[#]	[mm]	[kN]	[kN]	FBy / FBz / FTB / D1	[Y/N]	
1	0.0	374.7	187.3	FTB / DTB	N	Diagonalen waren niet goed aan gedraaid!! Diagonals were not fastened tight enough.
2	0.0	404.8	202.4	FTB / DTB	Y	0
3	3.0	436.2	218.1	FTB	Y	0
4	3.0	425.2	212.6	FTB	Y	0
5	6.0	373.3	186.7	FTB	Y	0
6	6.0	434.6	217.3	FTB	Y	0
7	0.0	0.0	0.0	0	Y	0
8	0.0	0.0	0.0	0	Y	0
9	0.0	0.0	0.0	0	Y	0
10	0.0	0.0	0.0	0	Y	0
11	0.0	0.0	0.0	0	Y	0
12	0.0	0.0	0.0	0	Y	0

Number of Valid Results: n = 5

Corrections for actual yield point and thickness

Design Yield	f_y =	355	MPA
Actual Yield	f_t =	373.91	MPA
Design Thickness	t =	2.5	mm
Actual Thickness =	t_t =	2.52	mm

R_ni = R_ti * (f_y/f_t)^alpha * (t/t_t)^beta

b_p,stiffened =	40	mm	Notional Plane width		
b_p,unstiffened =	18	mm			
k_stiffened =	0.64	-			
k_unstiffened =	0.21	-			
alpha =	1	-			
beta_stiffened =	1	-	beta_t<tt,stiff =	0.0465	-
beta_unstiffened =	1	-	beta_t<tt,unstiff =	0.4352	-
beta =	1	-			

Correction on Yield:	C_Yield =	0.949	-
Correction on Sheet thickness:	C_thick =	0.992	-

Corrected Test Values

Test #	Pinch	R_ti	R_ni
	[mm]	[kN]	[kN]
1	0.0	202.4	190.6
2	3.0	218.1	205.4
3	3.0	212.6	200.3
4	6.0	186.7	175.8
5	6.0	217.3	204.7
6	0.0	0.0	0.0
7	0.0	0.0	0.0
8	0.0	0.0	0.0
9	0.0	0.0	0.0
10	0.0	0.0	0.0
11	0.0	0.0	0.0
12	0.0	0.0	0.0

Polynome Fit for pinch-effect

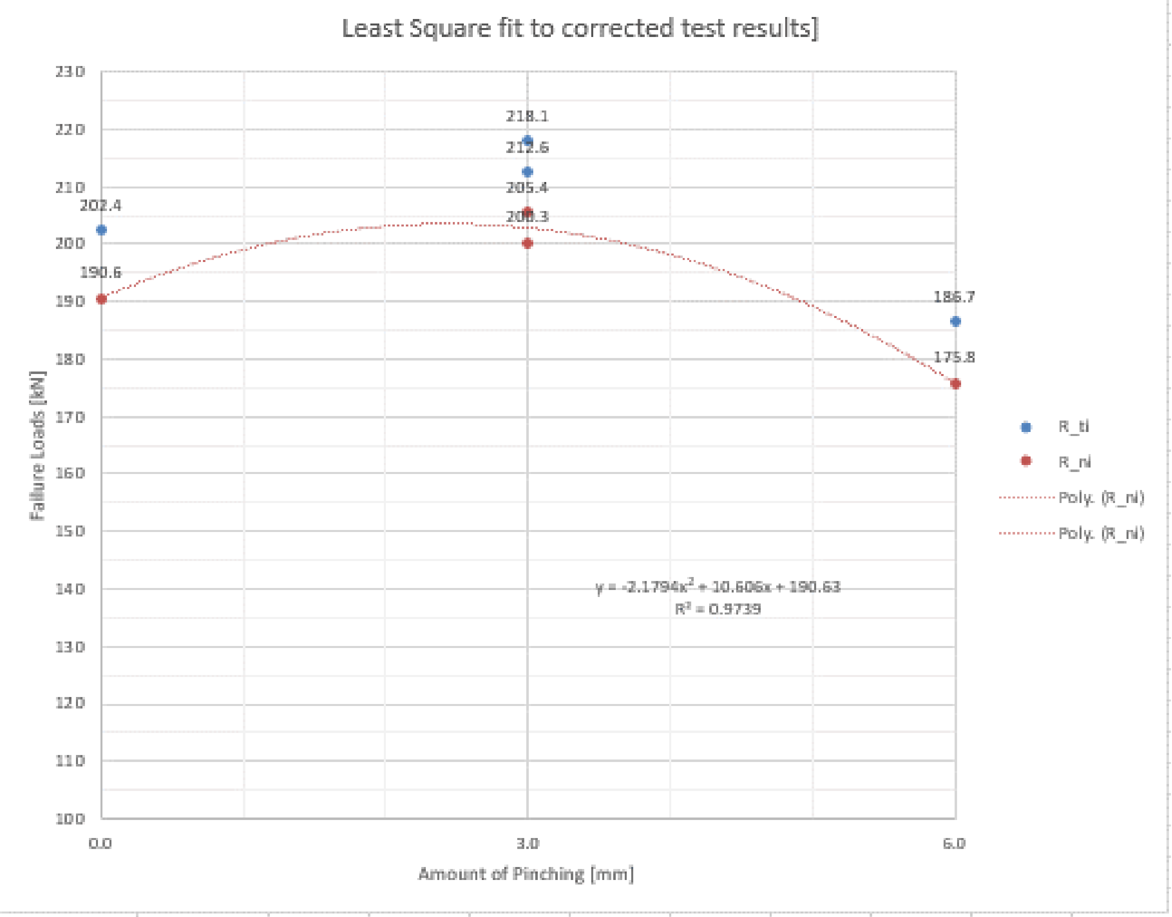

Single Upright Failure Load vs Amount of Pinching Effect

	Coefficient for Polynome: c1*x^2 + c2*x + c3		
	c1 =	-1.378	x^2
	c2 =	8.202	x
	c3 =	190.629	

Derivation of Characteristic Values

Characteristic Test	Pinch	Corrected F_ni	PolynomeValue F_t (pinch) = -1.378 * pinch^2 + 8.202 * x + 190.629	Normalized values F_ni / F_t
[#]	[mm]	[kN]	[kN]	[-]
1	0	190.6	190.6	1
2	3	205.4	202.8	1.0127
3	3	200.3	202.8	0.9873
4	6	175.8	190.2	0.9242
5	6	204.7	190.2	1.0758
6	0	0.0	190.6	0
7	0	0.0	190.6	0
8	0	0.0	190.6	0
9	0	0.0	190.6	0
10	0	0.0	190.6	0
11	0	0.0	190.6	0
12	0	0.0	190.6	0

n = 5 - Average: 1.00000000

k_s = 2.33 [-] Standard Deviation 0.054356082

n	3	4	5	6	7	8	9	10	15	20	30	40	50	100	∞
ks	3.37	2.63	2.33	2.18	2.08	2.00	1.95	1.92	1.82	1.76	1.73	1.71	1.69	1.68	1.64

Pinch	F_t	F_k = F_t * (1-k_s*s_n)
[mm]	[kN]	[kN]
0.0	190.6	166.5
3.0	202.8	177.1
6.0	190.2	166.1
NEN-1993		92.471

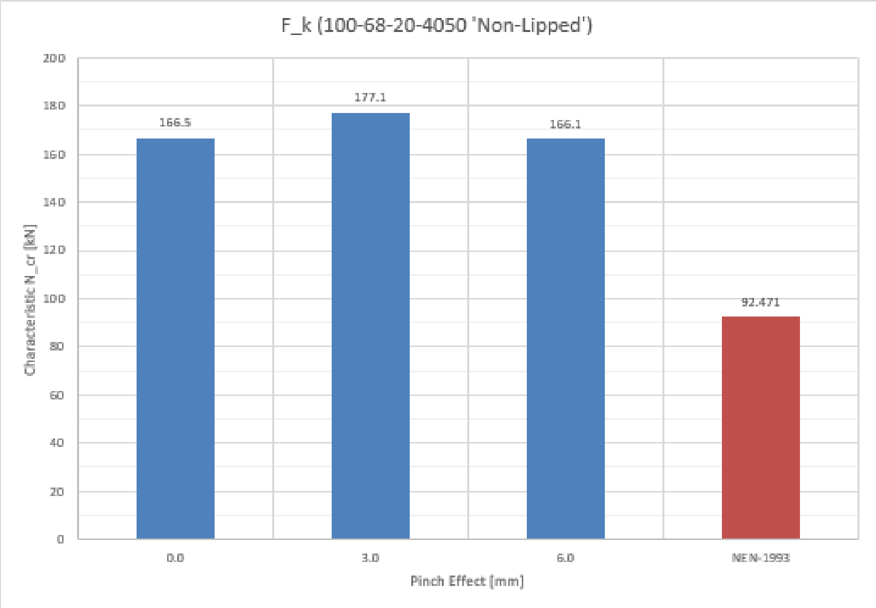

Conclusion

Current State of checks: Up-to-date

Pinch	A_eff	Reduction factor (0.0pinch = index100)
[mm]	[mm2]	
0	541.1	1.000
3	582.0	1.076
6	539.7	0.998

Reference (No-Spacer 'clean' DTB)

A_eff = 707.6056 mm2

Note: Without allowed eccentricity.

Initial Reduction due to different test Setup:

0.7646431 -

D.3. Determination of Effective Area

Procedure of required input		
	Effective Buckling Lengths	
	Design or tensile test yield steel strengths?	
	Corrected test results or characteristic loads?	
	Effective Buckling Lengths [mm]	
	10068204050PR355	
	Frame Setup	
$L_{cr,y}$	1100	
$L_{cr,z}$	1100	
$L_{cr,FTB}$	550	

Constants			
	E =	#####	MPa
	G =	81,000	MPa
	γ_{M1} =	1.0	-
Design	f_y =	355	MPa
TensileTest	f_y =	445	MPa
Used f_y, "D" is design and "T" is test:		D	[D/T]
	f_y =	355	MPa
Use corrected test results? Or characteristic?		fk	[ni/fk]

Criterea for imperfection factor torsional		
12078255070 PR S355		
	h/b =	1.5484
	if ((h / b) <= 2.0 ; curve a	
	if ((h / b) > 2.0 ; curve b	
Selected Buckling Curve		
	a	
12083255070 PR S355		
	h/b =	1.4201
	if ((h / b) <= 2.0 ; curve a	
	if ((h / b) > 2.0 ; curve 2	
	if ((h / b) > 2.0 ; curve b	
Selected Buckling Curve		
	a	

<INSERT PICTURE OF EFFECTIVE BUCKLING LENGTHS!>

Profile Properties		
	10068204050PR355	
$I_{yy,net}$ =	641,450	mm^4
$I_{zz,net}$ =	187,900	mm^4
$I_{\omega,net}$ =	719,325,000	mm^4
$I_{T,net}$ =	585	mm^4
y_M =	51	mm^4

Imperfection Factor α per curve:	
0a0	0.13
a	0.21
b	0.34
c	0.49
d	0.76

Used imperfection factors	12078	12083
Flexural	b	b
	0.34	0.34
Torsional	a	a
	0.21	0.21

10068204050PR355

Frame Setup

		Test 1	Test 2	Test 3	Test 4	Test 5	Test 6	Test 7	Test 8	Test 9
Pinch [mm]		0	3	3	6	0	0			
F_{NI} [kN]		118.36	107.94	102.22	106.59	0	0			
F_k [kN]		111.45	111.45	98.946	98.946	100.37	100.37			
Used failure force [kN]		111.45	111.45	98.946	98.946	100.37	100.37			
Observed Failure mode (during test)		DTB	DTB	DTB	DTB	DTB	DTB			
Effective Buckling Lengths [mm]										
	$L_{cr,y}$	1100	1100	1100	1100	1100	1100			
	$L_{cr,z}$	1100	1100	1100	1100	1100	1100			
	$L_{cr,FTB}$	550	550	550	550	550	550			
Current Ratio F_test/Nb,Rd [-]		1	1	1	1	1	1			
A_{eff} [mm²]	Goal Seek A_eff (x86_v423)	388.1	388.1	334.5	334.5	340.4	340.4			
N_Rk = A_eff * f_y		137779	137779	118734	118734	120835	120835			
$N_{b,Rd}$ [kN] (Calculated)		111.45	111.45	98.946	98.946	100.37	100.37			
Failrue mode (Calculation)		FBz	FBz	FBz	FBz	FBz	FBz			
Flexural Buckling, y-axis; FB_y	$N_{b,Rk,y}$ [N] $(\chi_y A_{eff} f_y)/\gamma_{M1}$ =	130050	130050	113210	113210	115082	115082			
Flexural Buckling, z-axis; FB_z	$N_{b,Rk,z}$ [N] $(\chi_z A_{eff} f_y)/\gamma_{M1}$ =	111448	111448	98946	98946	100368	100368			
Flexural Torsional Buckling; FTB	$N_{b,Rk,FT}$ [N] $(\chi_{FT} A_{eff} f_y)/\gamma_{M1}$ =	128488	128488	111719	111719	113585	113585			
Critical Torsional (Non-Normative) FB_T (!)	$N_{b,Rk,T}$ [N] $(\chi_T A_{eff} f_y)/\gamma_{M1}$ =	132610	132610	114692	114692	116674	116674			
Reduction Factors										
χ_y =	$1/(\Phi_y + sqrt(\Phi_y^2 - \lambda_y^2))$ but χ_y <= 1.0	0.9439	0.9439	0.9535	0.9535	0.9524	0.9524			
χ_z =	$1/(\Phi_z + sqrt(\Phi_z^2 - \lambda_z^2))$ but χ_z <= 1.0	0.8089	0.8089	0.8333	0.8333	0.8306	0.8306			
χ_{FT} =	$1/(\Phi_{FT} + sqrt(\Phi_{FT}^2 - \lambda_{FT}^2))$ but χ_{FT} <= 1.0	0.9326	0.9326	0.9409	0.9409	0.94	0.94			
χ_T =	$1/(\Phi_T + sqrt(\Phi_T^2 - \lambda_T^2))$ but χ_T <= 1.0	0.9625	0.9625	0.966	0.966	0.9656	0.9656			
Φ_y =	$0.5 * (1 + \alpha_{FLEX} * (\bar{\lambda}_y - 0.2) + \bar{\lambda}_y^2)$	0.5889	0.5889	0.5759	0.5759	0.5774	0.5774			
Φ_z =	$0.5 * (1 + \alpha_{FLEX} * (\bar{\lambda}_z - 0.2) + \bar{\lambda}_z^2)$	0.7913	0.7913	0.7537	0.7537	0.7579	0.7579			
Φ_{FT} =	$0.5 * (1 + \alpha_{TORS} * (\bar{\lambda}_{FT} - 0.2) + \bar{\lambda}_{FT}^2)$	0.6403	0.6403	0.624	0.624	0.6258	0.6258			
Φ_T =	$0.5 * (1 + \alpha_{TORS} * (\bar{\lambda}_T - 0.2) + \bar{\lambda}_T^2)$	0.5826	0.5826	0.5762	0.5762	0.5769	0.5769			
λ_y =	$sqrt((A_{eff} * f_y) / N_{cr,y})$	0.3541	0.3541	0.3287	0.3287	0.3316	0.3316			
λ_z =	$sqrt((A_{eff} * f_y) / N_{cr,z})$	0.6543	0.6543	0.6074	0.6074	0.6127	0.6127			
λ_{FT} =	$sqrt((A_{eff} * f_y) / N_{cr,FT})$	0.4726	0.4726	0.4436	0.4436	0.4469	0.4469			
λ_T =	$sqrt((A_{eff} * f_y) / N_{cr,T})$	0.3622	0.3622	0.3482	0.3482	0.3498	0.3498			
$N_{cr,y}$ =	$(\pi^2 EI_{yy}) / L_{cr,y}^2$	1E+06	1E+06	1E+06	1E+06	1E+06	1E+06			
$N_{cr,z}$ =	$(\pi^2 EI_{zz}) / L_{cr,z}^2$	321855	321855	321855	321855	321855	321855			
$N_{cr,FT}$ =	$(N_{cr,y} / (2*\beta)) * (1 + N_{cr,T}/N_{cr,y} - sqrt((1-N_{cr,T}/N_{cr,y})^2 + 4(y_o/i_o)^2 N_{cr,T}/N_{cr,y}))$	616827	616827	603301	603301	605004	605004			
$N_{cr,T}$ =	$(1/i_o^2) * (G*I_T + (\pi^2 E I_W)/L^2_{eT})$	1E+06	1E+06	979392	979392	987776	987776			
*Formula 30, 31 and 32; p62 of EN 15512:2009 (E)										
β =	$1 - (y_o / i_o)^2$ (With $y_o = y_M$; distance from CG to shear centre.)	0.451	0.451	0.4881	0.4881	0.4837	0.4837			
i_o =	$sqrt((I_{yy}+I_{zz}) / A_{eff} + y_M^2)$	68.832	68.832	71.279	71.279	70.976	70.976			

E. Test Evaluation Appendices

The sub-annexes for the test setup refer to here.

E.1. Graphical Representation of Test Data

Annex A Graphical representation of test data

STUB			Top	Midden	Voet	
12078255070 PR	e		mm	mm	mm	Ftest
test 1	0.0 mm	28	70.9	70.9	70.9	288.596
test 2	0.0 mm	30	70.9	70.8	70.9	278.716
test 3	0.0 mm	29	70.7	70.8	70.6	286.984
test 4	0.0 mm	28	70.8	70.8	70.8	288.908
test 5	-3.0 mm	28	70.9	67.9	70.8	287.348
test 6	-3.0 mm	28	70.8	67.9	70.8	285.736
test 7	-6.0 mm	28	71	64.8	70.8	281.004
test 8	-6.0 mm	28	70.9	64.9	70.8	279.704

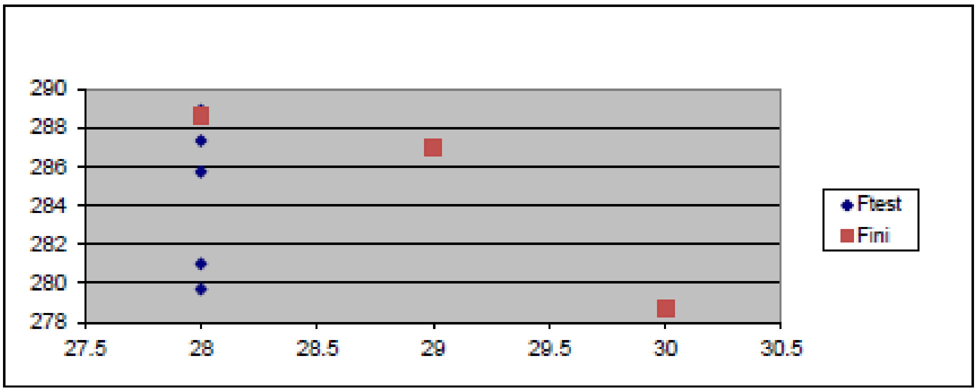

DTB			Top	Midden	Voet	
12078255070 PR	e		mm	mm	mm	Ftest
test 1	0.0 mm	28	70.8	71.2	70.8	155.005
test 2	0.0 mm	29	70.9	71.3	70.8	198.355
test 3	0.0 mm	30	70.9	71.1	71	155.43
test 4	0.0 mm	29	70.9	71.1	70.8	203.305
test 5	-3.0 mm	29	70.7	70	70.7	176.13
test 6	-3.0 mm	29	70.9	70	70.7	168.18
test 7	-6.0 mm	29	71.2	69.2	70.9	149.005
test 8	-6.0 mm	29	71	69	70.8	153.93

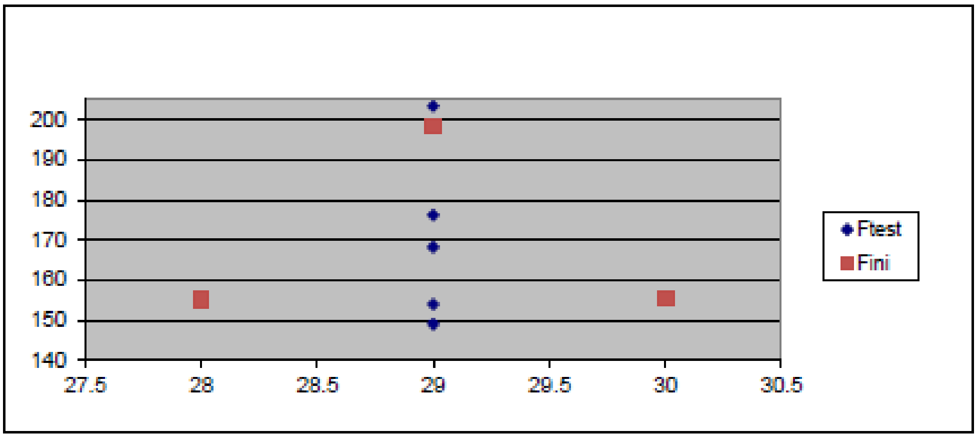

Annex A

STUB			Top	Midden	Voet	
12083255070 PR		e	mm	mm	mm	Ftest
test 1	0.0 mm	35	71	71	70.9	346.68
test 2	0.0 mm	37	72.4	71	71	330.3
test 3	0.0 mm	36	72.2	71	71	349.54
test 4	0.0 mm	36	72.3	71.1	71	344.496
test 5	-3.0 mm	35	70.7	68.1	70.7	341.376
test 6	-3.0 mm	35	70.9	68	70.8	334.928
test 7	-6.0 mm	35	70.7	65.1	70.8	330.612
test 8	-6.0 mm	35	70.6	65.2	70.7	331.548

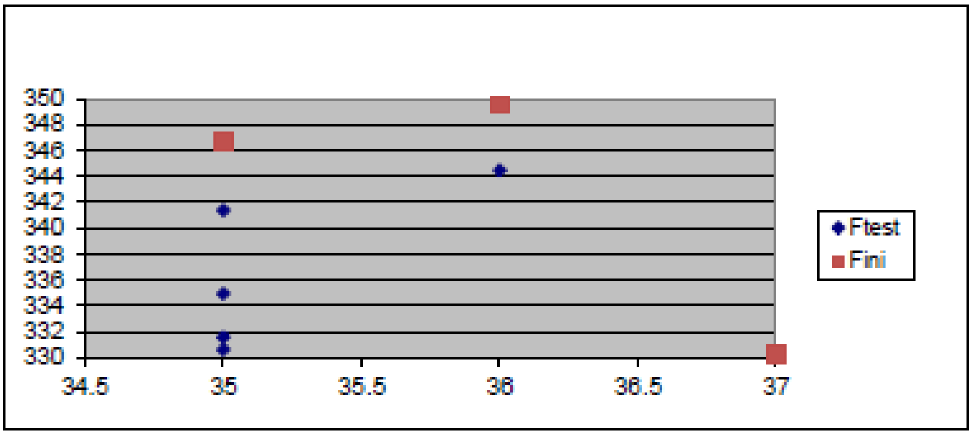

DTB			Top	Midden	Voet	
12083255070 PR		e	mm	mm	mm	Ftest
test 1	0.0 mm	35	71.7	71.2	70.5	155.28
test 2	0.0 mm	34	71	71.1	70.4	205.88
test 3	0.0 mm	34	70.9	71.6	70.8	186.23
test 4	0.0 mm	34	71.4	71.5	70.7	196.355
test 5	-3.0 mm	34	70.9	70.1	70.4	185.48
test 6	-3.0 mm	34	71	69.9	70.5	195.905
test 7	-6.0 mm	34	71	68.6	70.5	192.255
test 8	-6.0 mm	34	71.2	68.7	70.8	220.055

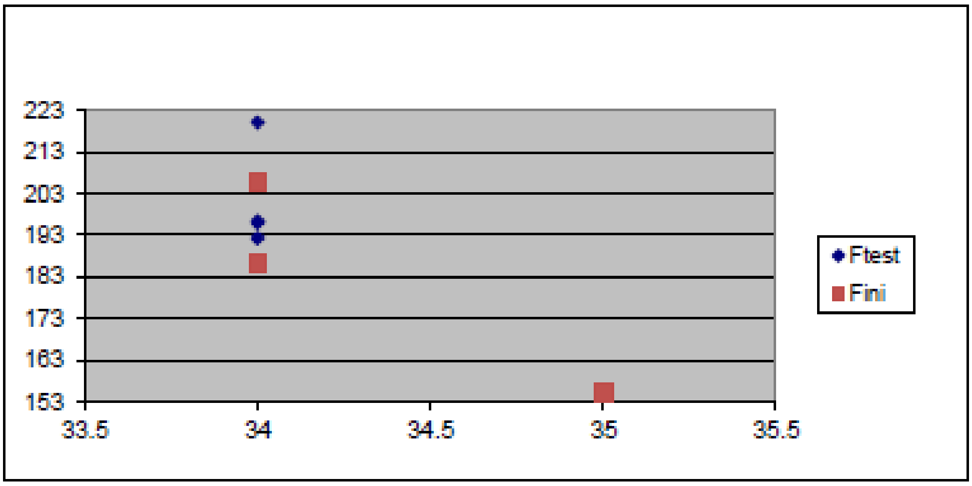

E.2. Tensile test data

Annex B Tensile Test Results

Profile: 12078255070 PR
Standard tensile test

D.D. 08-04-2015

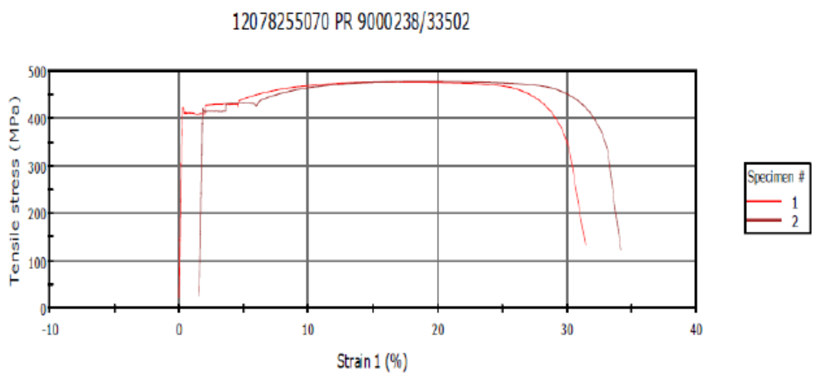

	ReH (MPa)	prf 0,2 % (MPa)	UTS (MPa)	elong (%)	gauge (mm)	Width (mm)
1	423	411	477	30	2,52	11,05
2	421	415	478	31	2,50	11,05
Maximum	423	415	478	31	2,52	11,05
Mean	422	413	477	31	2,51	11,05
Minimum	421	411	477	30	2,50	11,05

Profile: 12083255070 PR
Standard tensile test

D.D. 08-04-2015

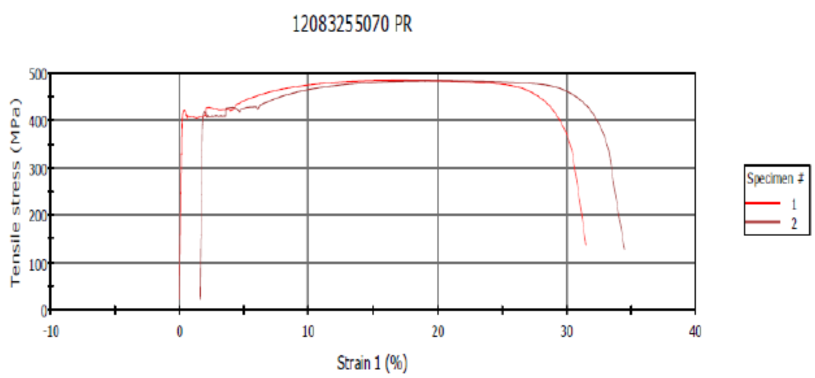

	ReH (MPa)	prf 0,2 % (MPa)	UTS (MPa)	elong (%)	gauge (mm)	Width (mm)
1	421	420	484	30	2,60	11,05
2	419	418	483	32	2,60	11,05
Maximum	421	420	484	32	2,60	11,05
Mean	420	419	484	31	2,60	11,05
Minimum	419	418	483	30	2,60	11,05

Conclusion

The normative yield strengths an thickness of the specimen are:

Profiles	Yield Strength f_y [N/mm^2 or MPa]	Thickness t_t [mm]
12078255070 PR	422 (ReH_m)	2.51
12083255070 PR	420 (ReH_m)	2.60

E.3. Photographic Evidence of Test Results

Annex C1 Photographic Evidence of Test Setup

12078255070 PR

STUB

Not displayed:	e	Top mm	Midden mm	Voet mm	Ftest
test 2 0.0 mm	30	70.9	70.8	70.9	278.716
test 3 0.0 mm	29	70.7	70.8	70.6	286.984

Displayed Results

Test 1	Test 5	Test 7
Test 4	Test 6	Test 8

12078255070 PR

STUB

	e	Top mm	Midden mm	Voet mm	Ftest
test 1 0.0 mm	28	70.9	70.9	70.9	288.596

Failure Mode:

Local

	e	Top mm	Midden mm	Voet mm	Ftest
test 2 0.0 mm	30	70.9	70.8	70.9	278.716

<Not used, differentent e-distance>

Failure Mode:

Local

	e	Top mm	Midden mm	Voet mm	Ftest
test 3 0.0 mm	29	70.7	70.8	70.6	286.984

<Not used, differentent e-distance>

Failure Mode:

Local

	e	Top mm	Midden mm	Voet mm	Ftest
test 4 0.0 mm	28	70.8	70.8	70.8	288.908

Failure Mode:

Local

		e	Top mm	Midden mm	Voet mm	Ftest
test 5	-3.0 mm	28	70.9	67.9	70.8	287.348

Failure Mode:
Local

		e	Top mm	Midden mm	Voet mm	Ftest
test 6	-3.0 mm	28	70.8	67.9	70.8	285.736

Failure Mode:
Local

		e	Top mm	Midden mm	Voet mm	Ftest
test 7	-6.0 mm	28	71	64.8	70.8	281.004

Failure Mode:
Local

		e	Top mm	Midden mm	Voet mm	Ftest
test 8	-6.0 mm	28	70.9	64.9	70.8	279.704

Failure Mode:
Local

Annex C2 Photographic Evidence of Test Setup

12078255070 PR

DTB

Not displayed:	e	Top mm	Midden mm	Voet mm	Ftest
test 1	0.0 mm	28	70.8	71.2	70.8	155.005
test 3	0.0 mm	30	70.9	71.1	71	155.43

Displayed Results

Test 2	Test 5	Test 7
Test 4	Test 6	Test 8

12078255070 PR

DTB

	e	Top mm	Midden mm	Voet mm	Ftest
test 1	0.0 mm	28	70.8	71.2	70.8	155.005

<Not used, differentent e-distance>

Failure Mode:

FBz

	e	Top mm	Midden mm	Voet mm	Ftest
test 2	0.0 mm	29	70.9	71.3	70.8	198.355

Failure Mode:

DTB

	e	Top mm	Midden mm	Voet mm	Ftest
test 3	0.0 mm	30	70.9	71.1	71	155.43

<Not used, differentent e-distance>

Failure Mode:

DTB

	e	Top mm	Midden mm	Voet mm	Ftest
test 4	0.0 mm	29	70.9	71.1	70.8	203.305

Failure Mode:

FBz

		e	Top mm	Midden mm	Voet mm	Ftest
test 5	-3.0 mm	29	70.7	70	70.7	176.13

Failure Mode:

DTB

		e	Top mm	Midden mm	Voet mm	Ftest
test 6	-3.0 mm	29	70.9	70	70.7	168.18

Failure Mode:

DTB

		e	Top mm	Midden mm	Voet mm	Ftest
test 7	-6.0 mm	29	71.2	69.2	70.9	149.005

Failure Mode:

DTB

		e	Top mm	Midden mm	Voet mm	Ftest
test 8	-6.0 mm	29	71	69	70.8	153.93

Failure Mode:

DTB

Annex C3 Photographic Evidence of Test Setup

12083255070 PR

STUB

12083255070 PR

STUB

Not displayed:							
	e		Top mm	Midden mm	Voet mm		Ftest
test 2	0.0 mm	37	72.4	71	71	330.3	
test 3	0.0 mm	36	72.2	71	71	349.54	
test 4	0.0 mm	36	72.3	71.1	71	344.496	

Displayed Results

Test 1	Test 5	Test 7
	Test 6	Test 8

	e		Top mm	Midden mm	Voet mm		Ftest
test 1	0.0 mm	35	71	71	70.9	346.68	

Failure Mode:

Mode: Local

Local

	e		Top mm	Midden mm	Voet mm		Ftest
test 2	0.0 mm	37	72.4	71	71	330.3	

<Not used, differentent e-distance>

Failure Mode:

Local

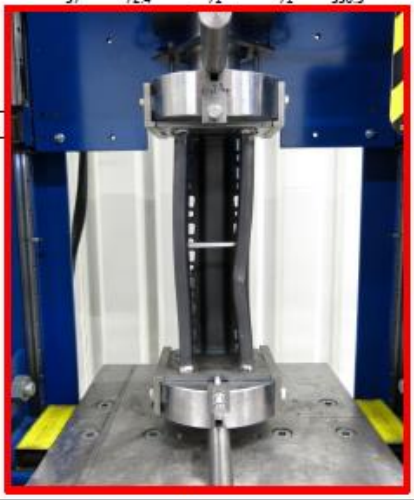

	e		Top mm	Midden mm	Voet mm		Ftest
test 3	0.0 mm	36	72.2	71	71	349.54	

<Not used, differentent e-distance>

Failure Mode:

Local

	e		Top mm	Midden mm	Voet mm		Ftest
test 4	0.0 mm	36	72.3	71.1	71	344.496	

<Not used, differentent e-distance>

Failure Mode:

Local

	e	Top mm	Midden mm	Voet mm	Ftest
test 5 -3.0 mm	35	70.7	68.1	70.7	341.376

Mode: Local

Failure Mode:

Local

	e	Top mm	Midden mm	Voet mm	Ftest
test 6 -3.0 mm	35	70.9	68	70.8	334.928

Mode: Local

Failure Mode:

Local

	e	Top mm	Midden mm	Voet mm	Ftest
test 7 -6.0 mm	35	70.7	65.1	70.8	330.612

Failure Mode:

Mode: Local

Local

	e	mm	mm	mm	Ftest
test 8 -6.0 mm	35	70.6	65.2	70.7	331.548

Failure Mode:

Mode: Local

Local

Annex C4 Photographic Evidence of Test Setup

12083255070 PR

DTB

12083255070 PR

DTB

Not displayed:

	e	Top mm	Midden mm	Voet mm	Ftest
test 1 0.0 mm	35	71.7	71.2	70.5	155.28

Displayed Results

Test 2	Test 5	Test 7
Test 3	Test 6	Test 8
Test 4		

	e	Top mm	Midden mm	Voet mm	Ftest
test 1 0.0 mm	35	71.7	71.2	70.5	155.28

<Not used, differenten e-distance>

Failure Mode:

FBz

	e	Top mm	Midden mm	Voet mm	Ftest
test 2 0.0 mm	34	71	71.1	70.4	205.88

Global buckling in direction of the opening.

Failure Mode:

FBz

	e	Top mm	Midden mm	Voet mm	Ftest
test 3 0.0 mm	34	70.9	71.6	70.8	186.23

Global buckling in direction of the opening.

Failure Mode:

FBz

	e	Top mm	Midden mm	Voet mm	Ftest
test 4 0.0 mm	34	71.4	71.5	70.7	196.355

Global buckling in direction of the opening.

Failure Mode:

FBz

	e	Top mm	Midden mm	Voet mm	Ftest
test 5 -3.0 mm	34	70.9	70.1	70.4	185.48

Global buckling in direction of the opening.

Failure Mode:

FBz

	e	Top mm	Midden mm	Voet mm	Ftest
test 6 -3.0 mm	34	71	69.9	70.5	195.905

Global buckling in direction of the opening.

Failure Mode:

FBz

	e	Top mm	Midden mm	Voet mm	Ftest
test 7 -6.0 mm	34	71	68.6	70.5	192.255

Local buckling of one endsheet, which collapses outwards.

Failure Mode:

DTB

	e	Top mm	Midden mm	Voet mm	Ftest
test 8 -6.0 mm	34	71.2	68.7	70.8	220.055

Global buckling in direction of the opening.

Failure Mode:

FBz

F. Definitions of Upright Profiles

F.1. General Nomenclature

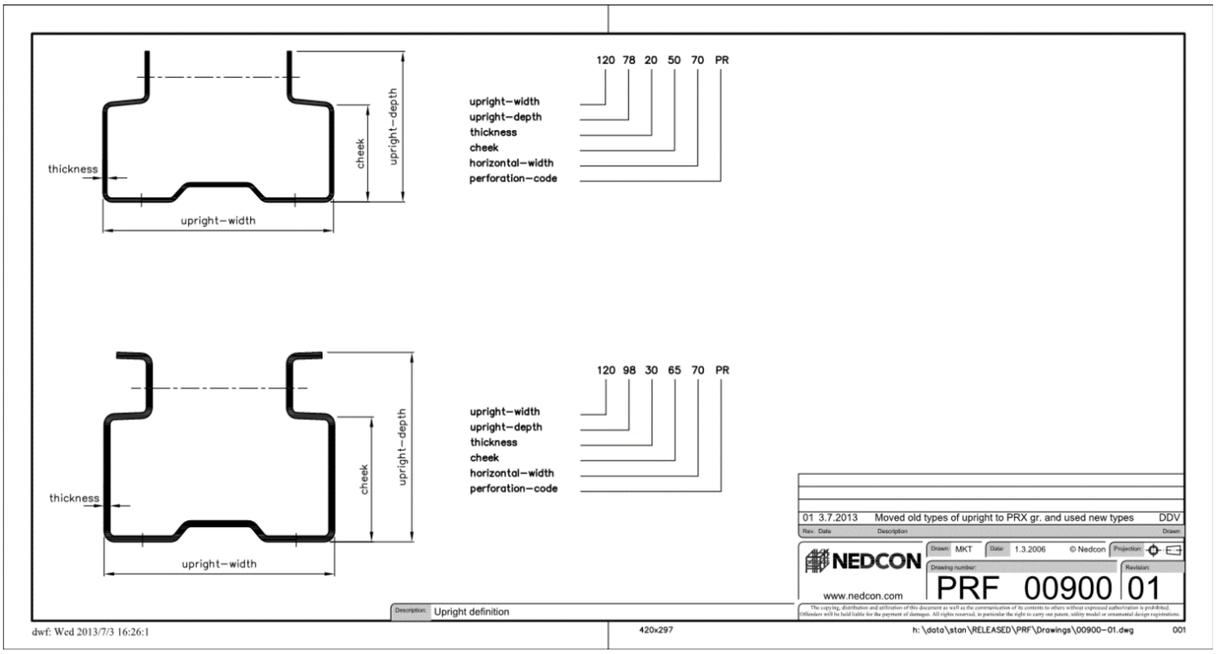

Figure 51. General nomenclature of NEDCON's Upright Profiles.

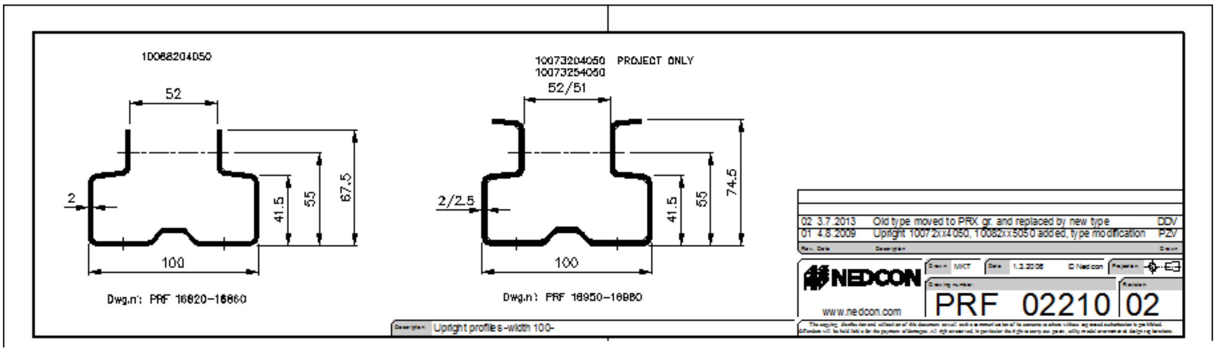

Figure 52. Dimensions of the 100-68 and 100-73 profile. The difference between the 72- and 73- profiles are some minor dimension changes that are assumed not to influence pinch-results.

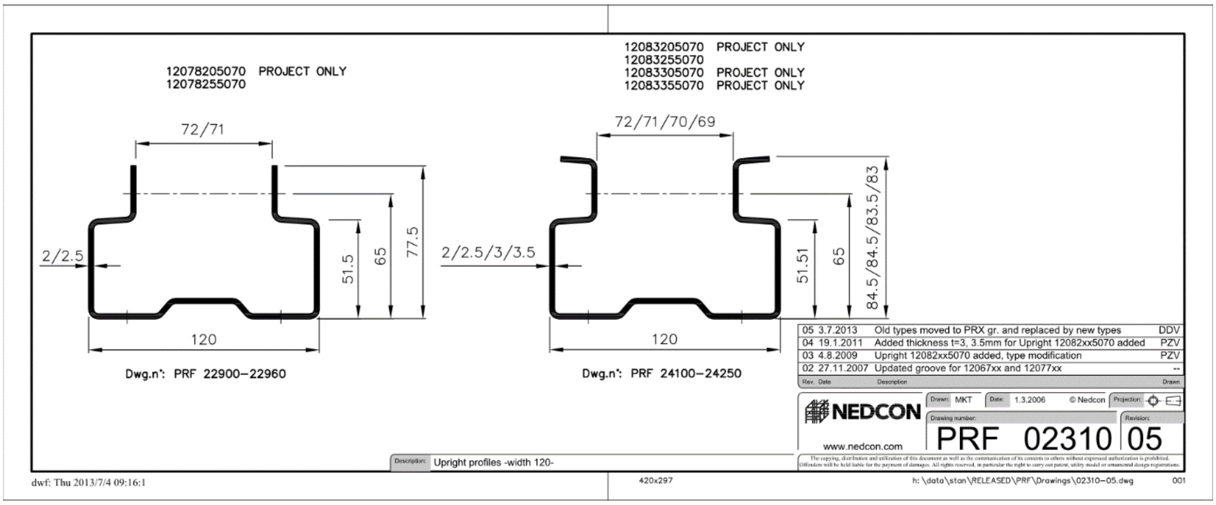

Figure 53. Dimensions of the 120-78 and 120-83 profile.

F.2. Definition of PR 120 78 25 5070

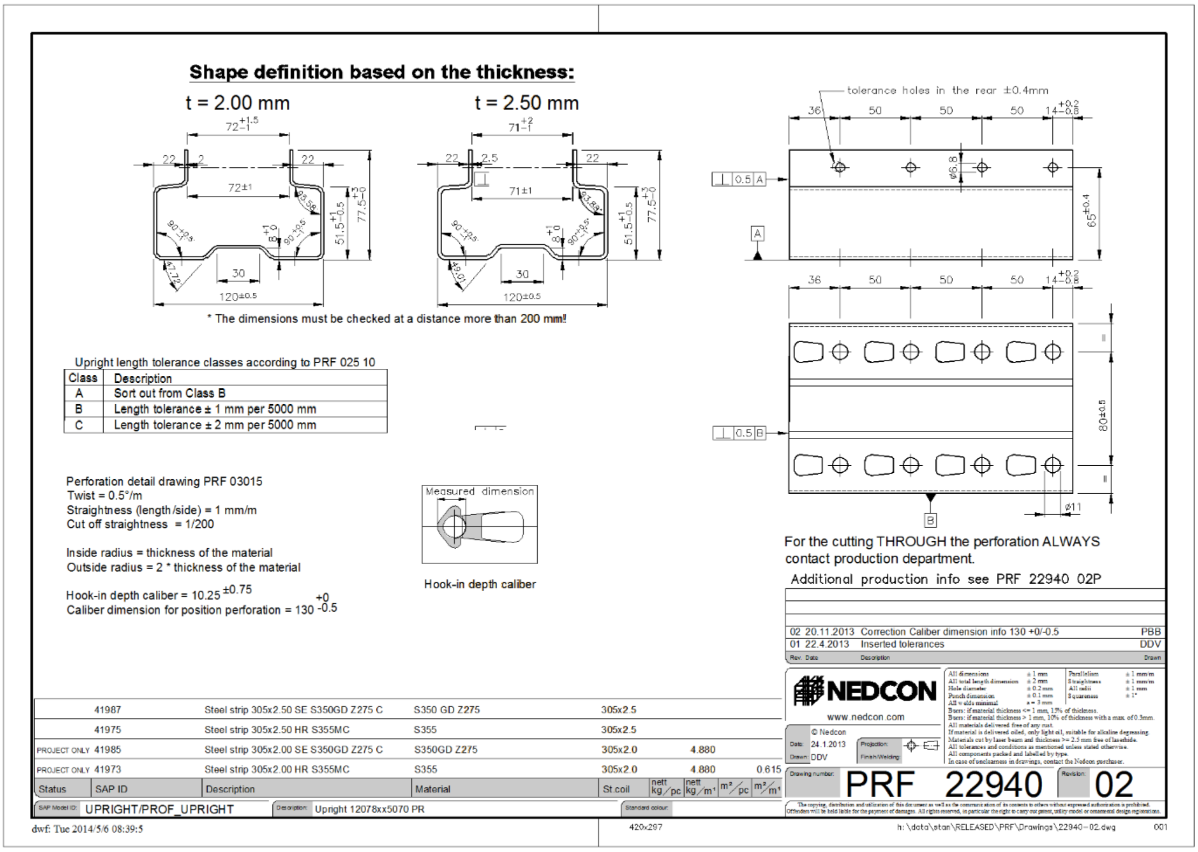

F.3. Definition of PR 120 83 25 5070

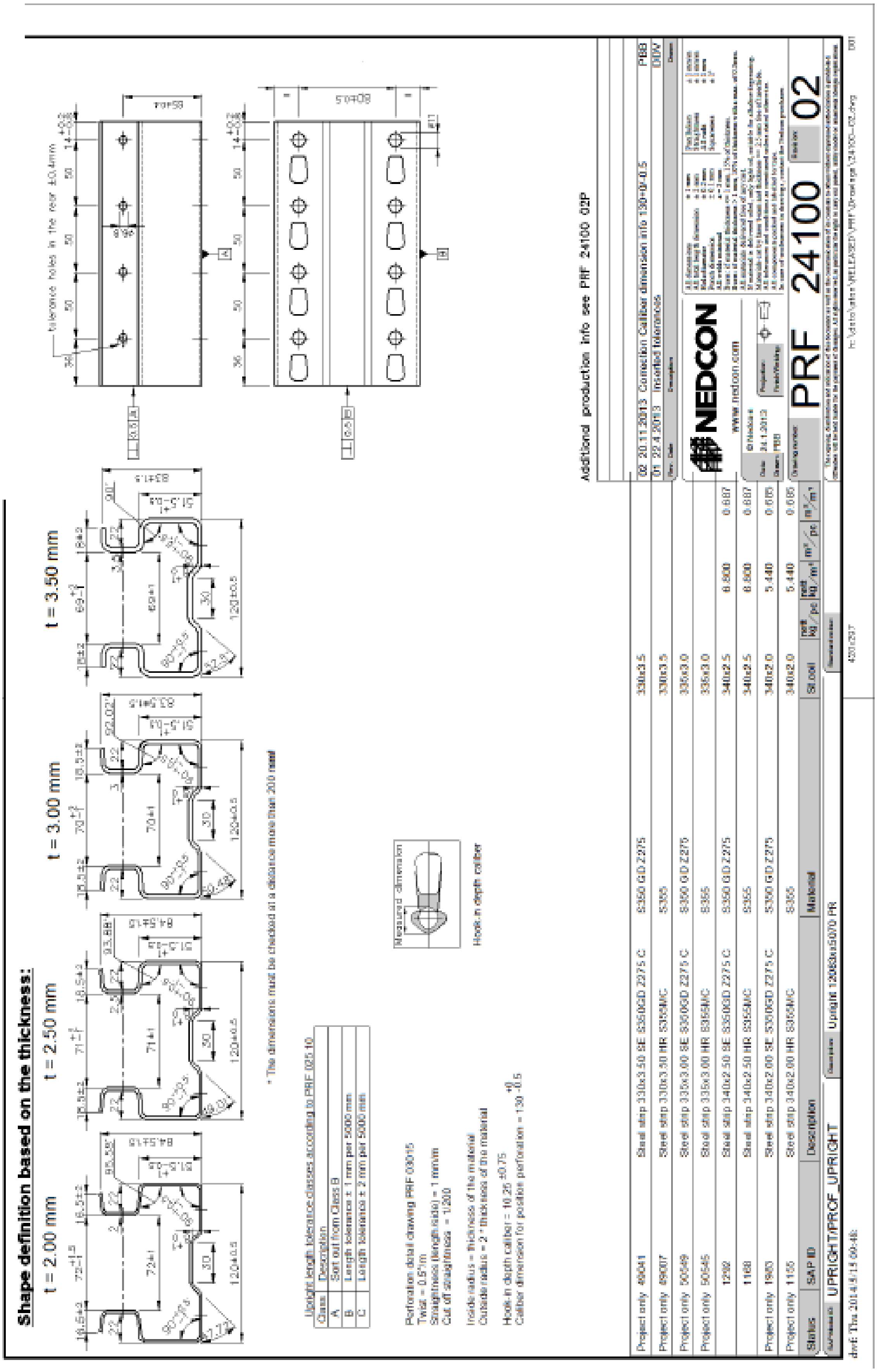
Shape definition based on the thickness:
t = 2.00 mm
t = 2.50 mm
t = 3.00 mm
t = 3.50 mm
Additional production info see PRF 24100 02P
NEDCON
www.nedcon.com
PRF 24100 02
UPRIGHT/PROF_UPRIGHT

F.4. Definition of PR 100 68 20 4050

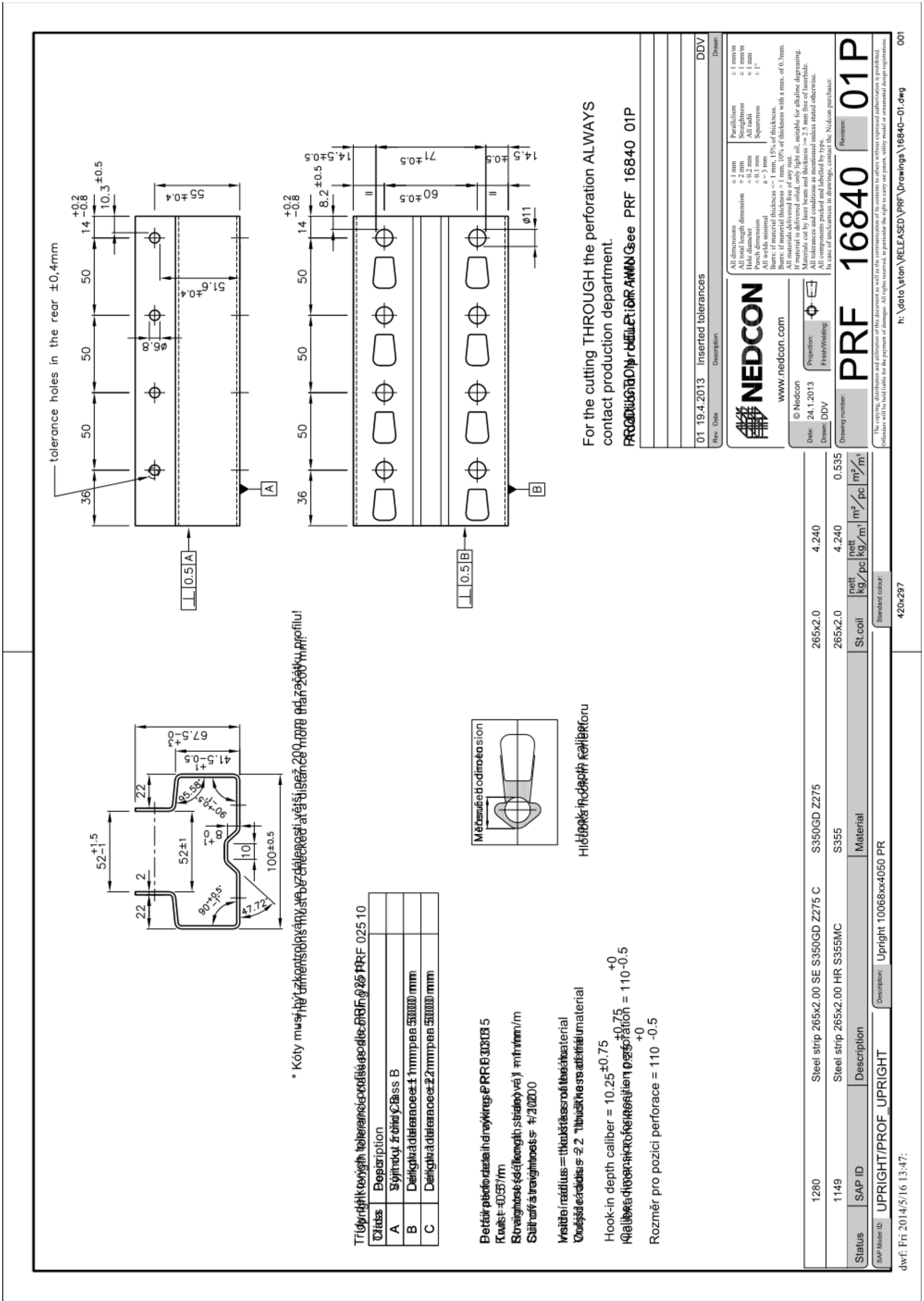

F.5. Definition of PR 100 72 25 4050

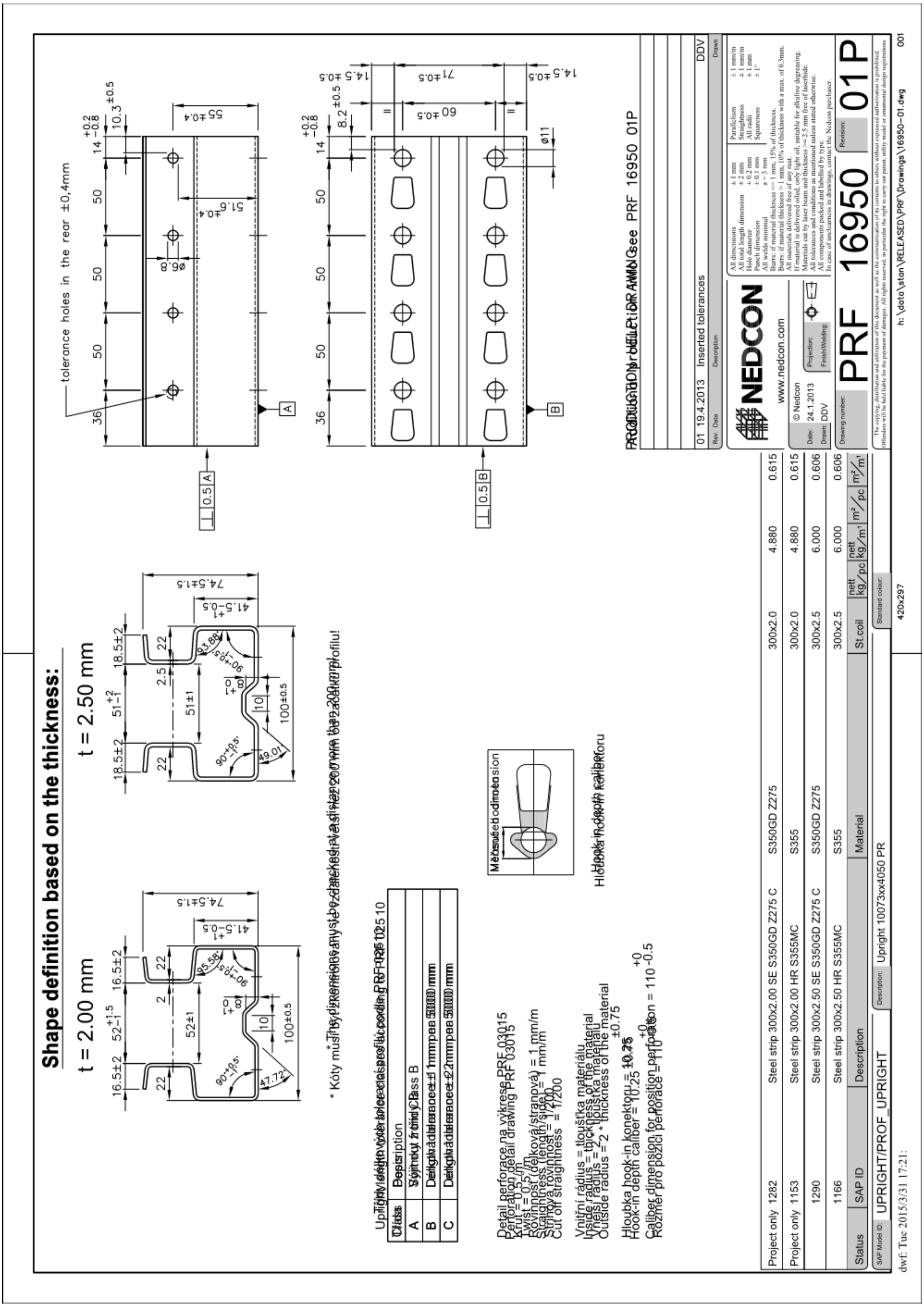

F.6. Perforation Pattern

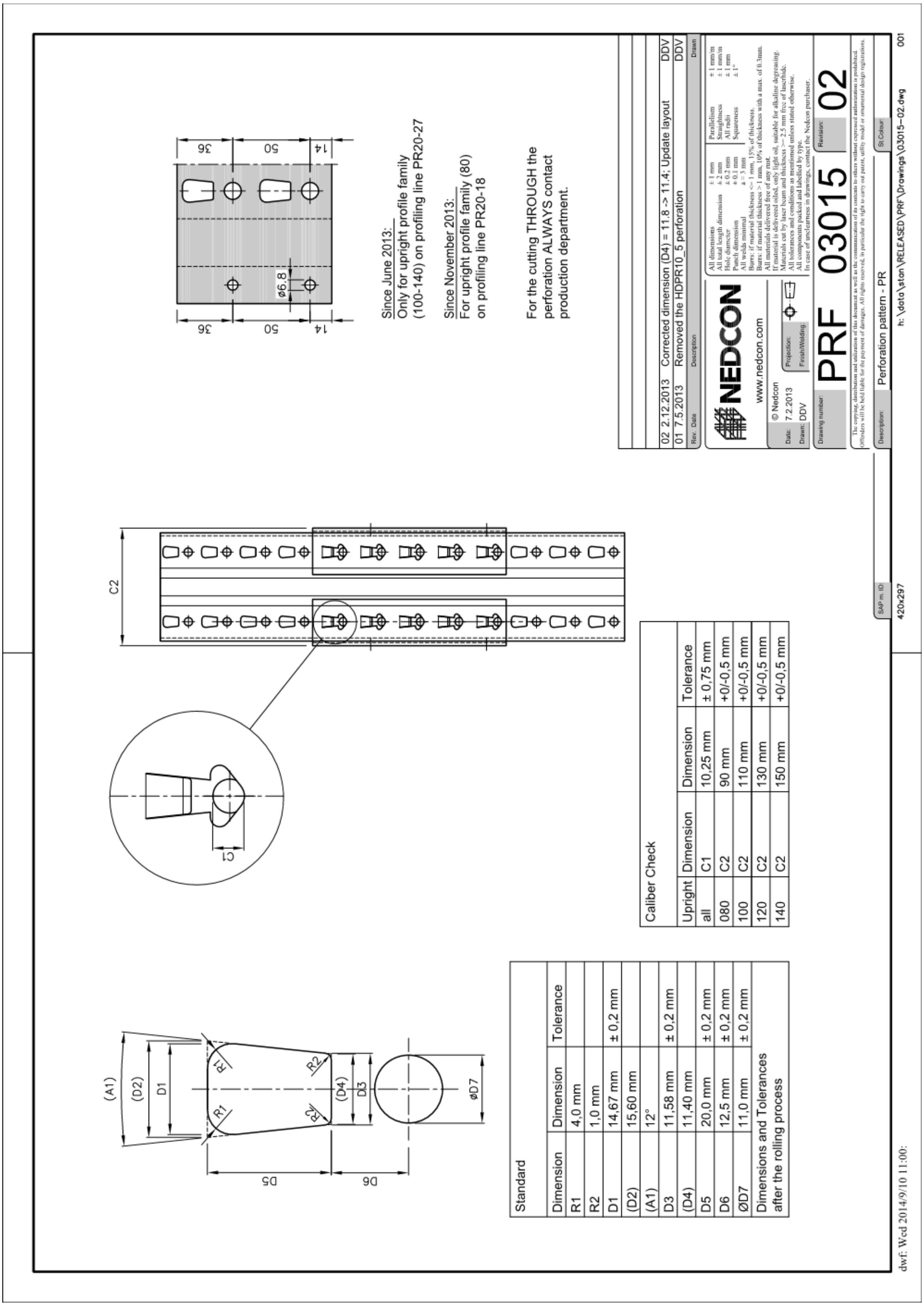

G. Reinforcements of Top Beam in Frame Setup

The top beam in the Frame Test setups requires strengthening with a few additional structural components. These are drawn out here.

Top Beam Stiffeners

A regular HEA-180 is prone to buckling within its mid-flange when large (local) pressure is applied. To prevent this, additional plates can be welded into the profile. A proposal would be to weld 8 plates of thickness at least 6 mm near the beginning and end of the cap plates of the bench press and at the centre of the uprights, at both sides in the HEA-profile. See also the pictures below.

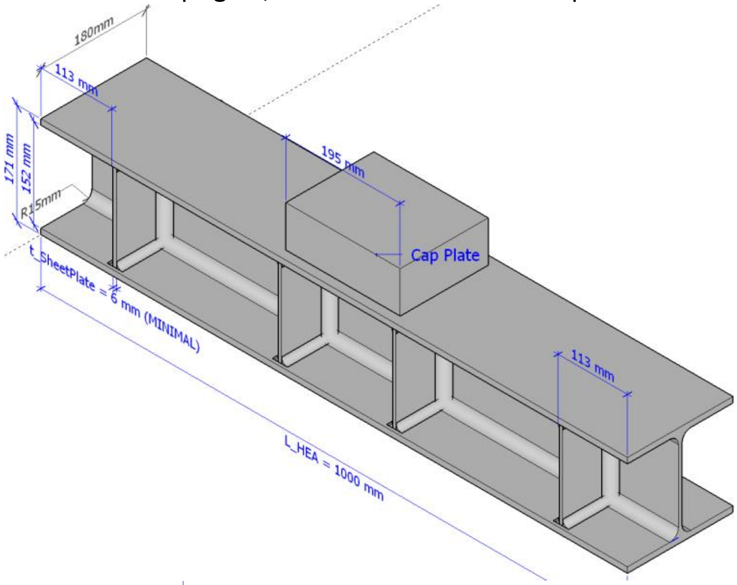

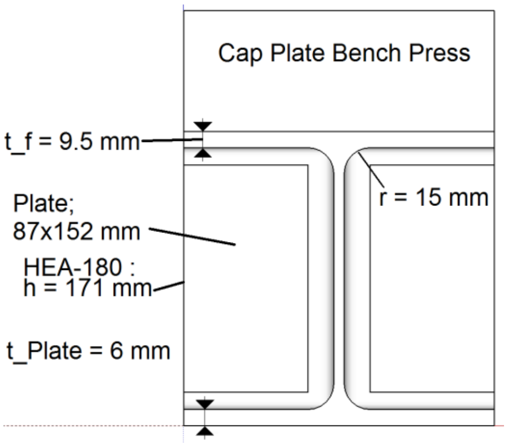

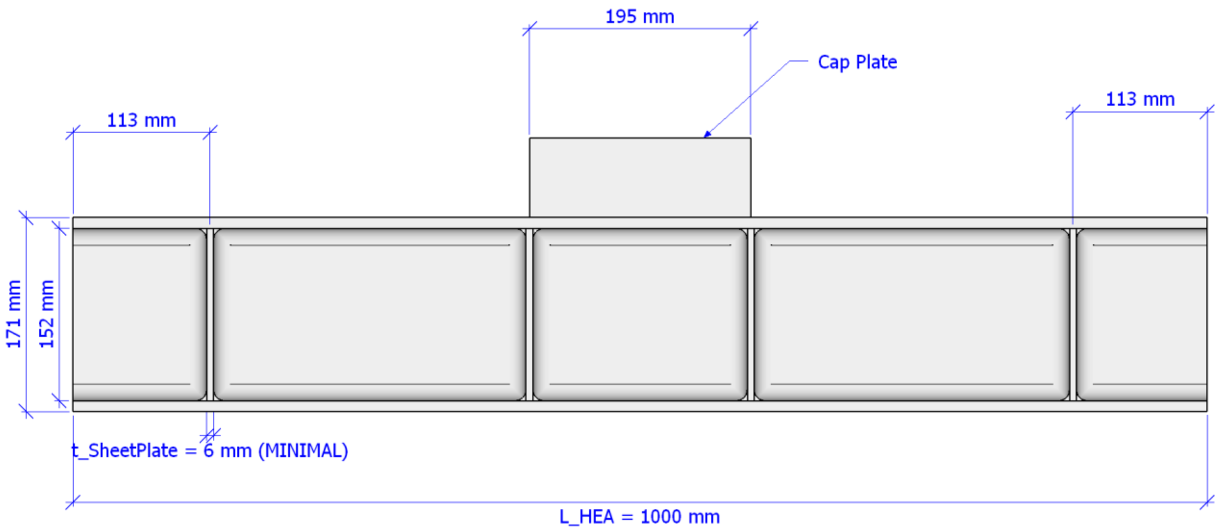

Figure 54. 3D and Cross Sectional Views of the welded plates in the HEA-Profile. For every HEA-profile 8 pieces of additional plate material are welded between the end-flanges. The dimensions of the additional plates are: 87 x 152 mm, thickness at least 6 mm. The distance between the middle 2 stiffeners is based on the cap-plate width while the position of the end-stiffeners is above the uprights.

Shear Force Diagonals

Simulation results have shown that shear force in the top-beam is still too large. This could be solved by welding additional diagonal plates into the HEA-profiles. For every HEA-profile, 4 additional plates are necessary to guarantee sufficient shear resistance in the beam. The required thickness of the plates is at least 8 mm. The length of the plates is 315.74 mm (corner-to-corner). The width of a plate can be 87 mm. Configuration can be as follows:

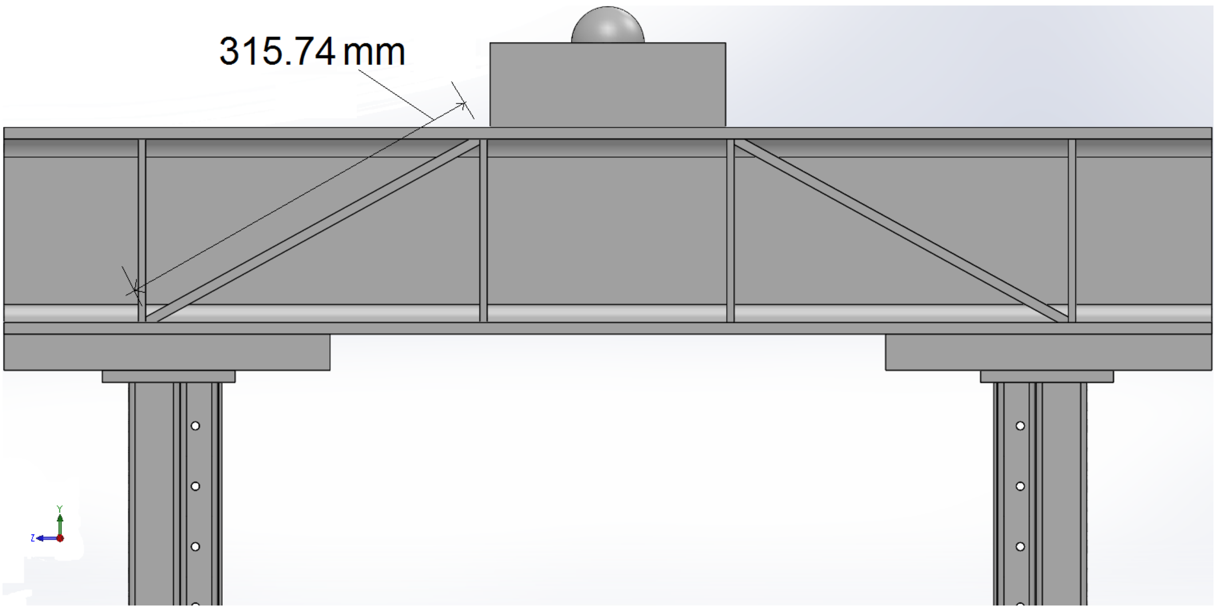

Figure 55. Shear Force Diagonals. Dimensions of the full (not-rounded) plate are: 315.74 x 87 x 8 mm. In the same picture also the consolidated Cap Pates can be seen. The uprights can be bolted onto these cap plates, on precondition of equal distribution of the load.

H. CU-FSM Analysis of the uprights applied in the Frame Test Setup

H.1. PRF 100-68-20-4050 S355

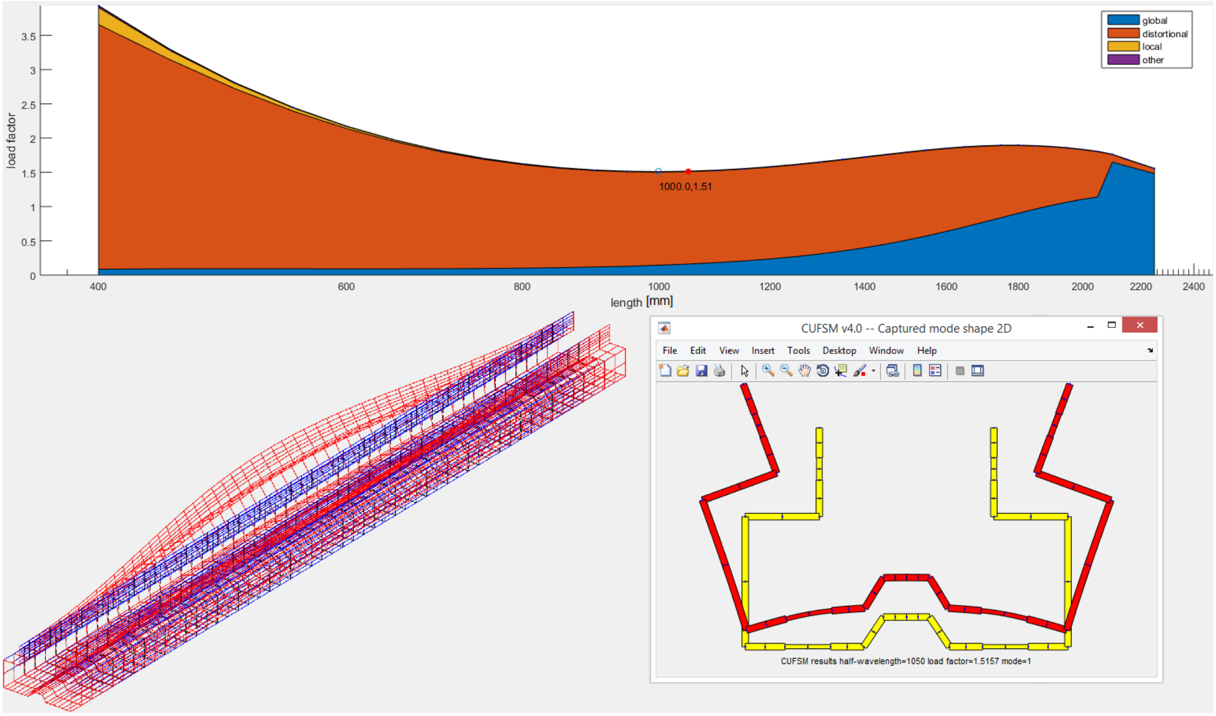

Figure 56. Load Factor Length Diagram of the Unlipped profile. The minimum in the curve shows a Symmetric Distortion mode. Both criteria for worst-case scenario in sense of pinch and 'no diagonal spacer' apply at the same point.

H.2. PRF 100-72-25-4050 S355

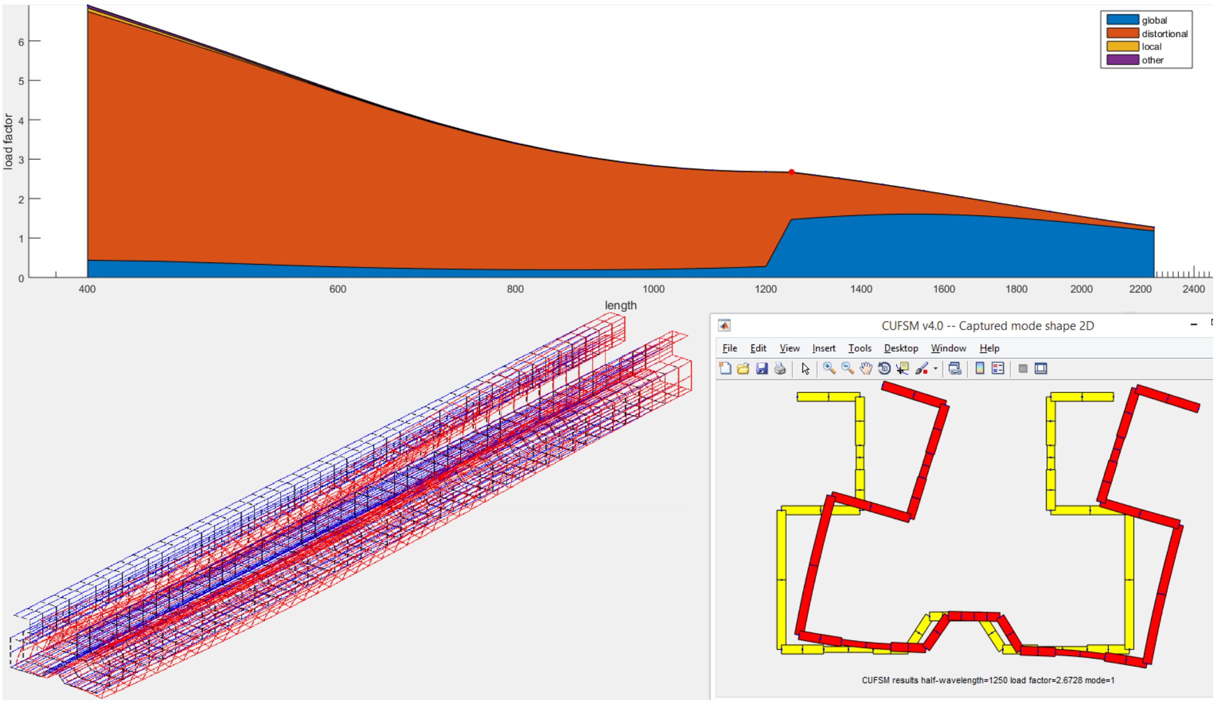

Figure 57. Load Factor Length Diagram of the Lipped profile. Notice the dominating Flexural Torsional Buckling (FTB).

H.3. Input 100-68-20-4050

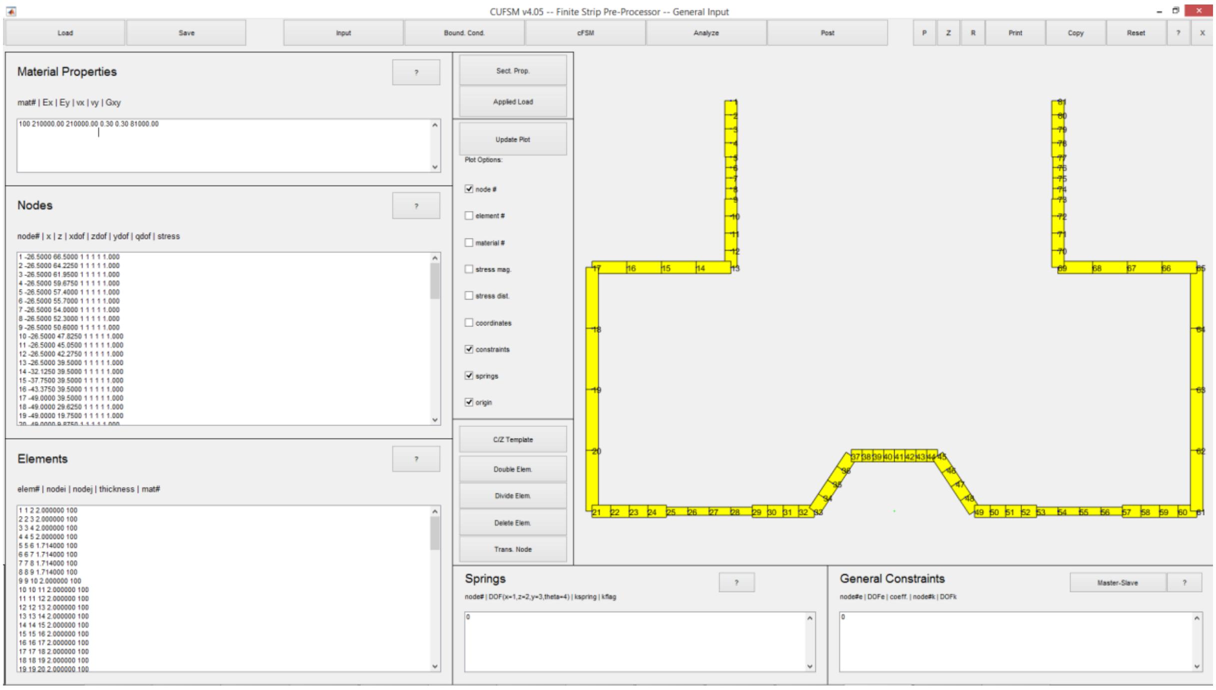

Figure 58. Input tab of CU-FSM

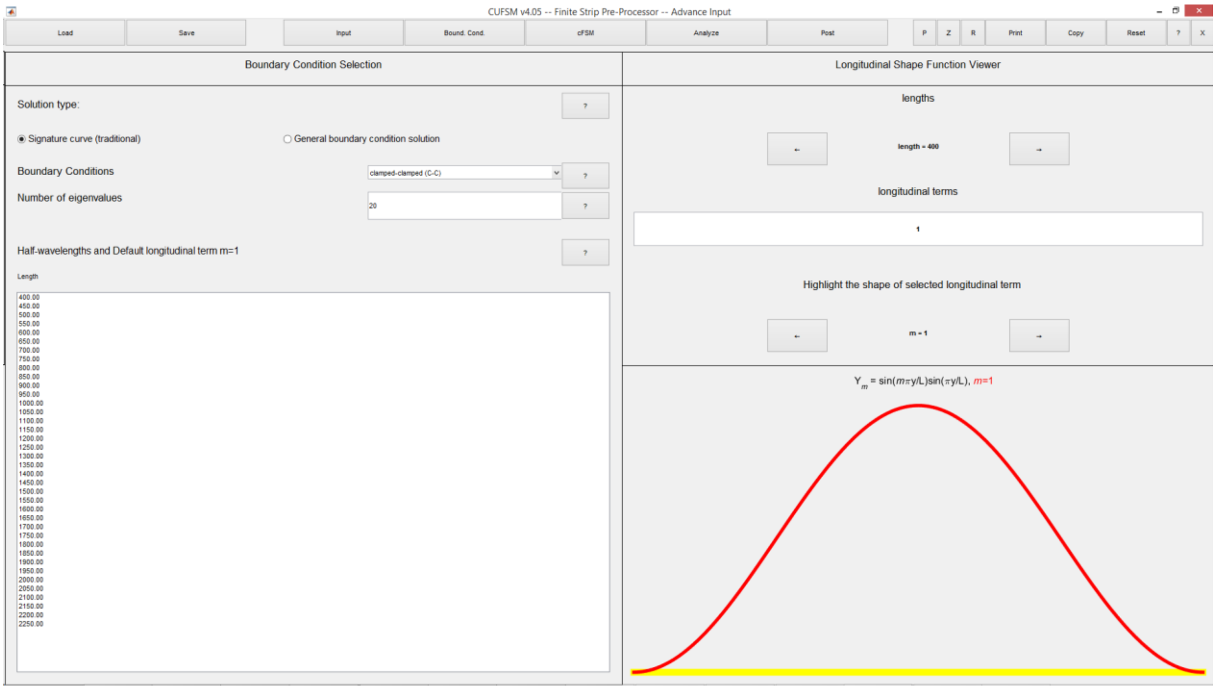

Figure 59. Boundary Conditions and devoured lengths.

H.4. Additional Analysis Close-to-Minimum Distortional Point

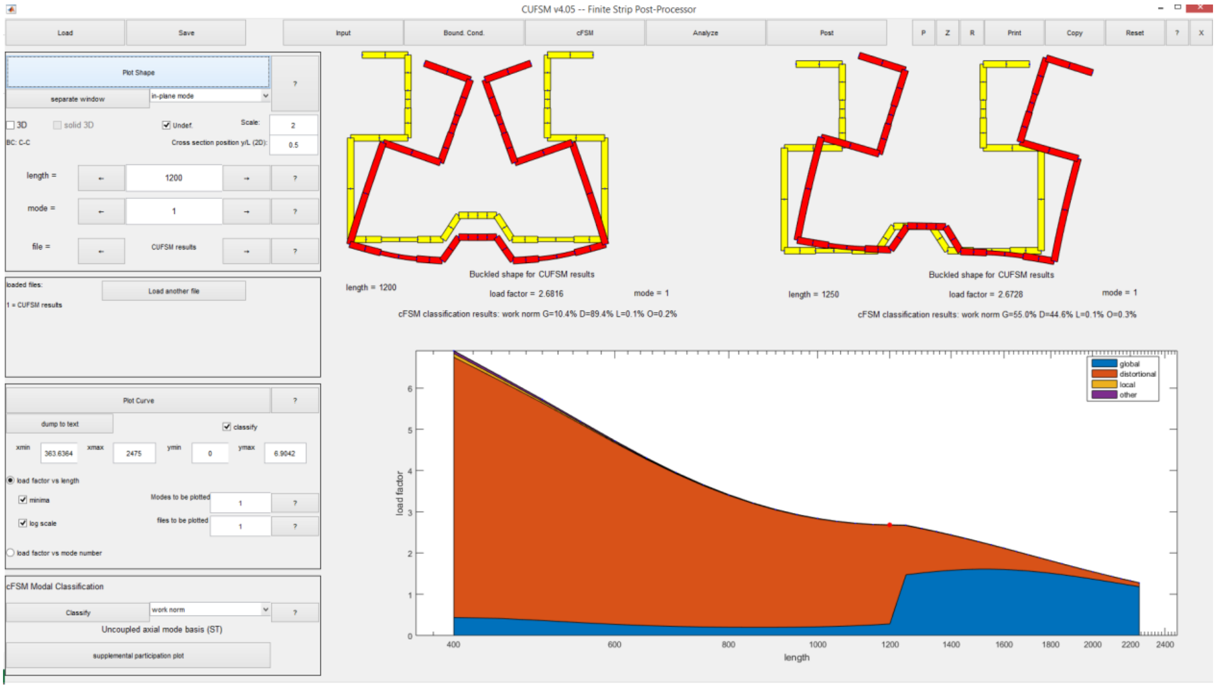

Figure 60. Modes at the turning-point according to CU-FSM.

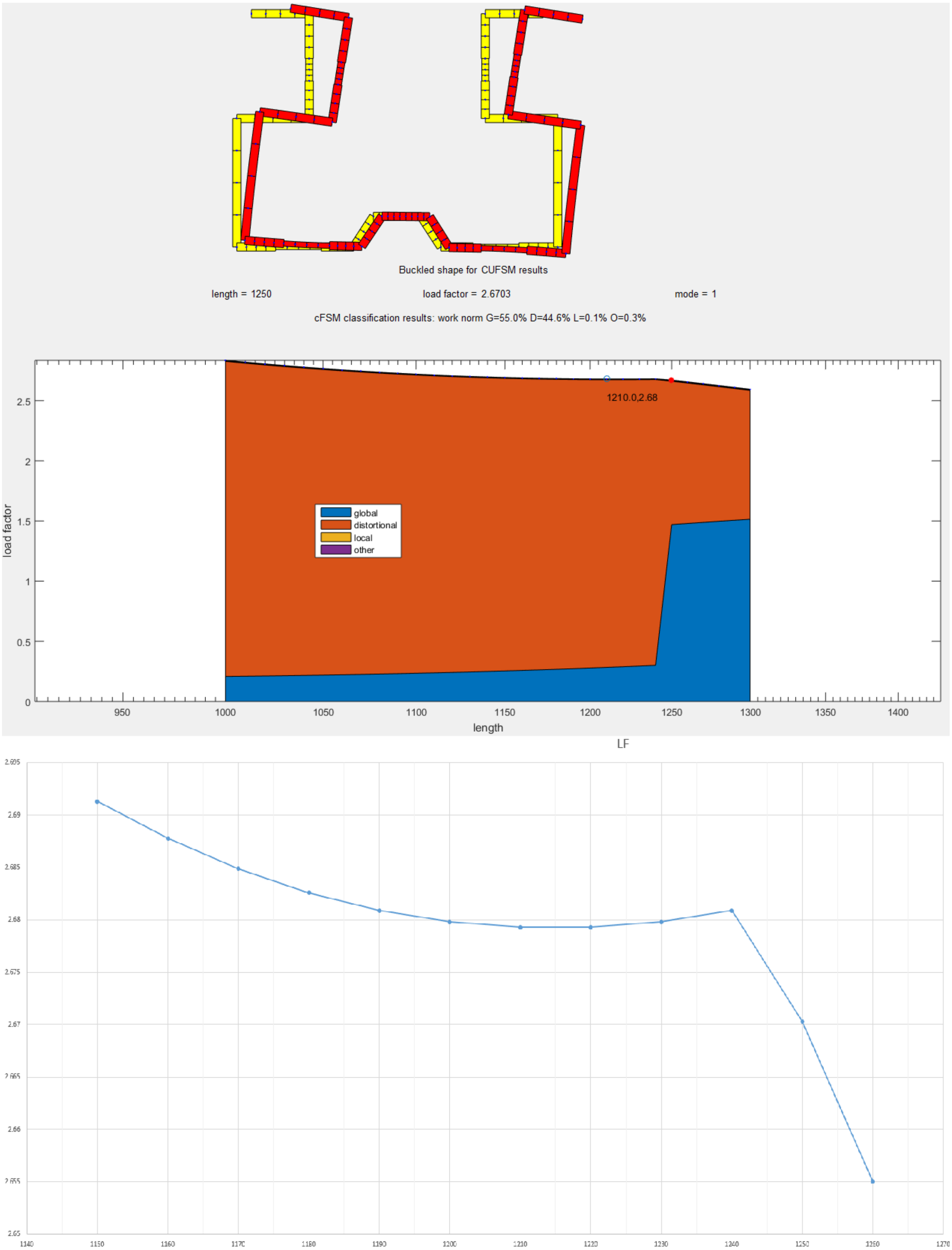

Figure 61. Analysis at high resolution between upright lengths of 1000 and 1300 mm. Notice a minimum still exists before the Flexural (Global) Buckling domain starts. A test setup always uses the perforation pitch (50 mm) which makes a minimum of 1215 mm a hard-to-get result.

I. Rough Bill of Materials for Frame Test Setup

A rough 'Bill of Materials' is given here to indicate the most important components of the setup.

Uprights

Table 17. Required Upright Profiles and lengths. Additional information: All uprights require cap plates at both ends.

Upright Profile	Lipped or Non-lipped	Length of Upright [mm]	# of parts of this length:	Required lengths from stock [m]
100 68 20 4050 PR S355	Non-lipped	2250	x12	4pieces x 9m (12pieces x 3m)
100 72 25 4050 PR S355	Lipped	2255	x12	6pieces x 6m

Top Beam

The 2 uprights can be connected with a HEA-180 S235 Profile. Its height is 171 mm. The beam will require bolt holes for the upright cap plates to be connected. Mass per length of an HEA-180 is: 35.52 kg/m. The top beam needs extra welded sheets to prevent the HEA from buckling within its mid-flange. In total at least 4 sheets need to be placed; at the beginning and end of the cap plates of the bench press and this at both sides of the flange of the HEA. See also the sketches in 'Shear Force Diagonals' in Appendix G.

Diagonals

All 12 frames contain 4 'standard' diagonals 503015 with CTC = 909.18 mm (4x12= 48 pieces), except: The outer diagonals of the 100 72 25 4050 frame have to be shortened to CTC = 791.6 mm, see also next section. The number of diagonals that require shortening is: 6frames x 2diagonals = 12pieces. Thickness of diagonals will be 1.5mm. Alternative solution for the diagonals are U40x40x4 or similar U-profiles with additional spacer rings.

Other

Diagonals need to be connected with spacers which are pinched in a press to the final diameters as given in Table 8.

J. CU-FSM analysis on lipped 120 upright

The input of the Cornell University Finite Strip Method application are given here.

Boundary Conditions

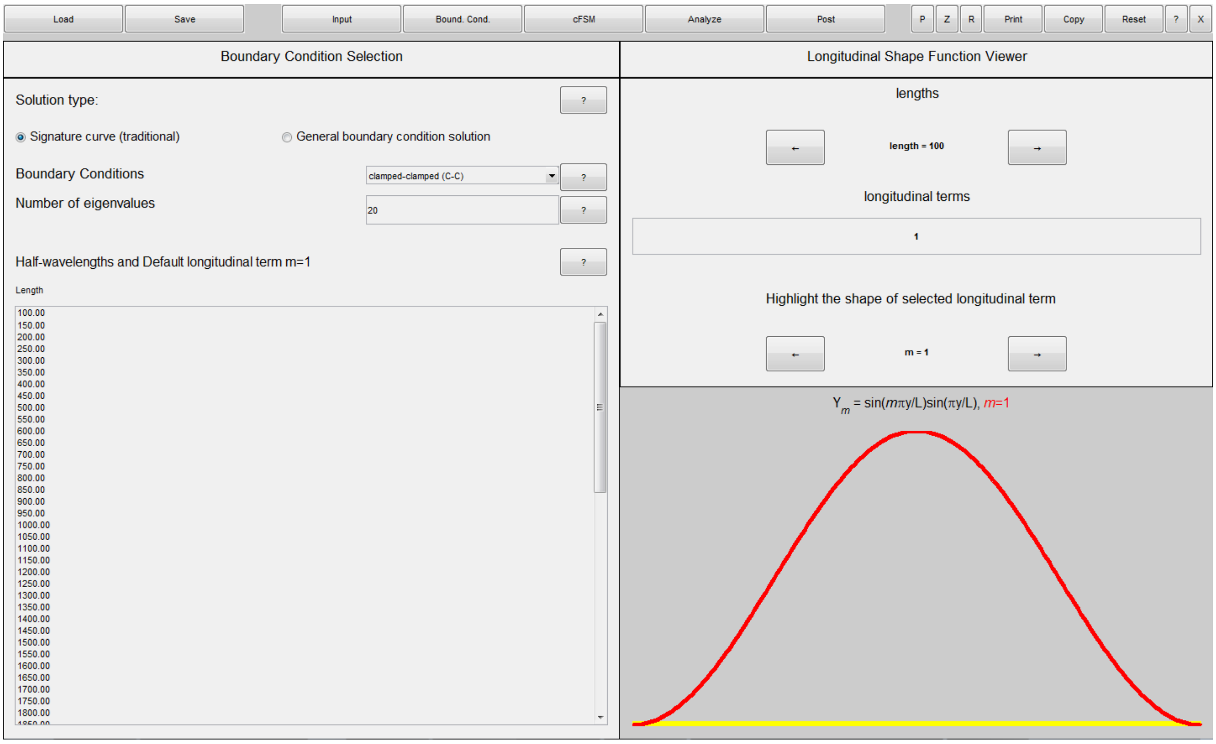

Figure 62. Boundary Conditions input.

120 83 25 5070, Input of Geometry

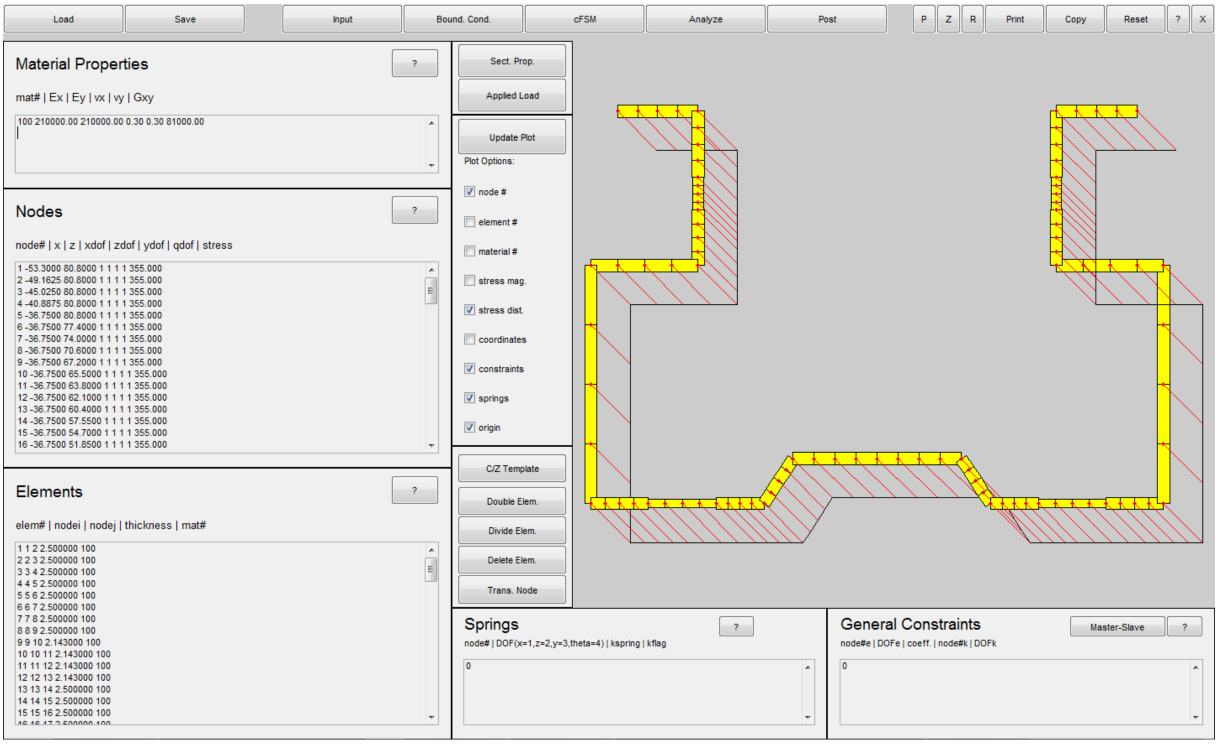

120 83 25 5070, Results in Load Factor Length Diagram

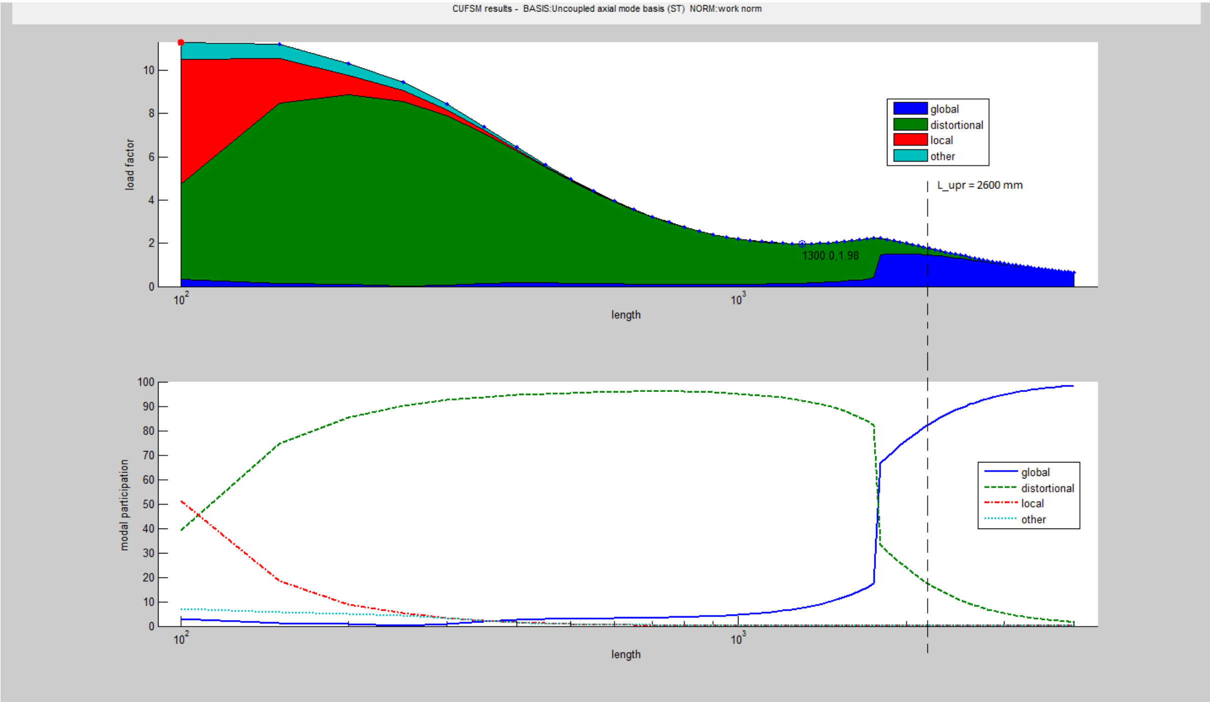

Figure 63. Load factor versus length diagram. Obviously, the executed DTB tests at 2600 mm are in the flexural buckling area.

Modes at various upright lengths

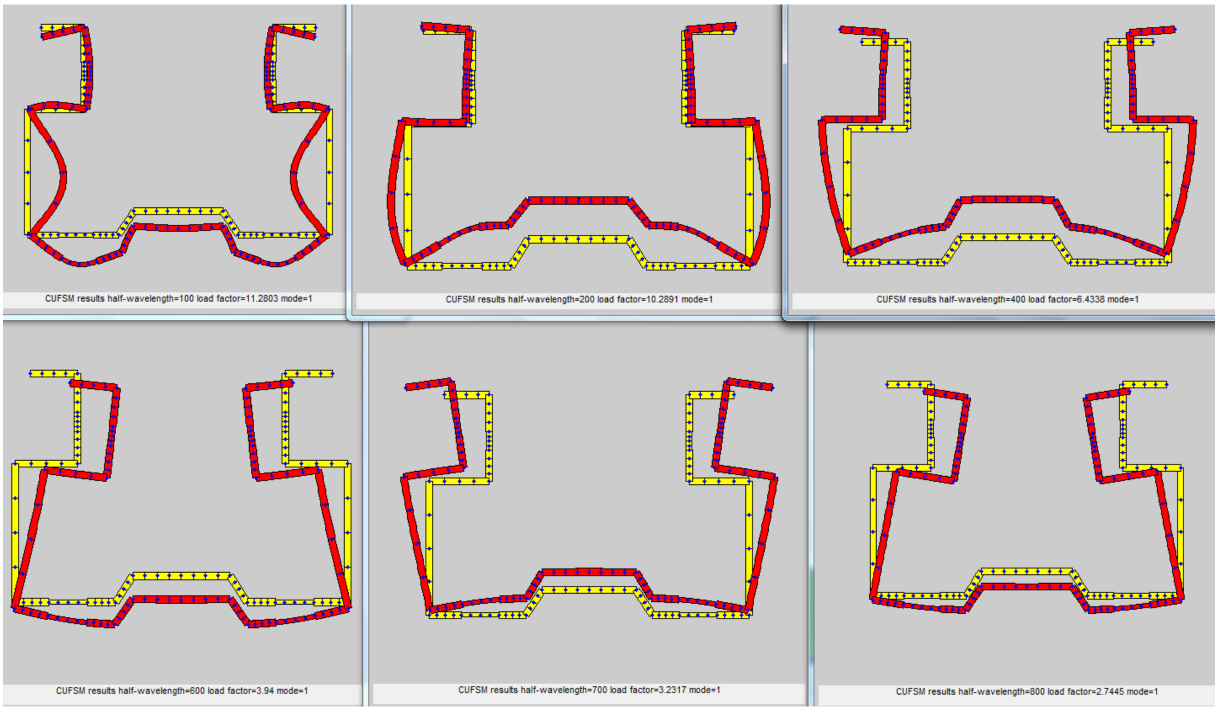

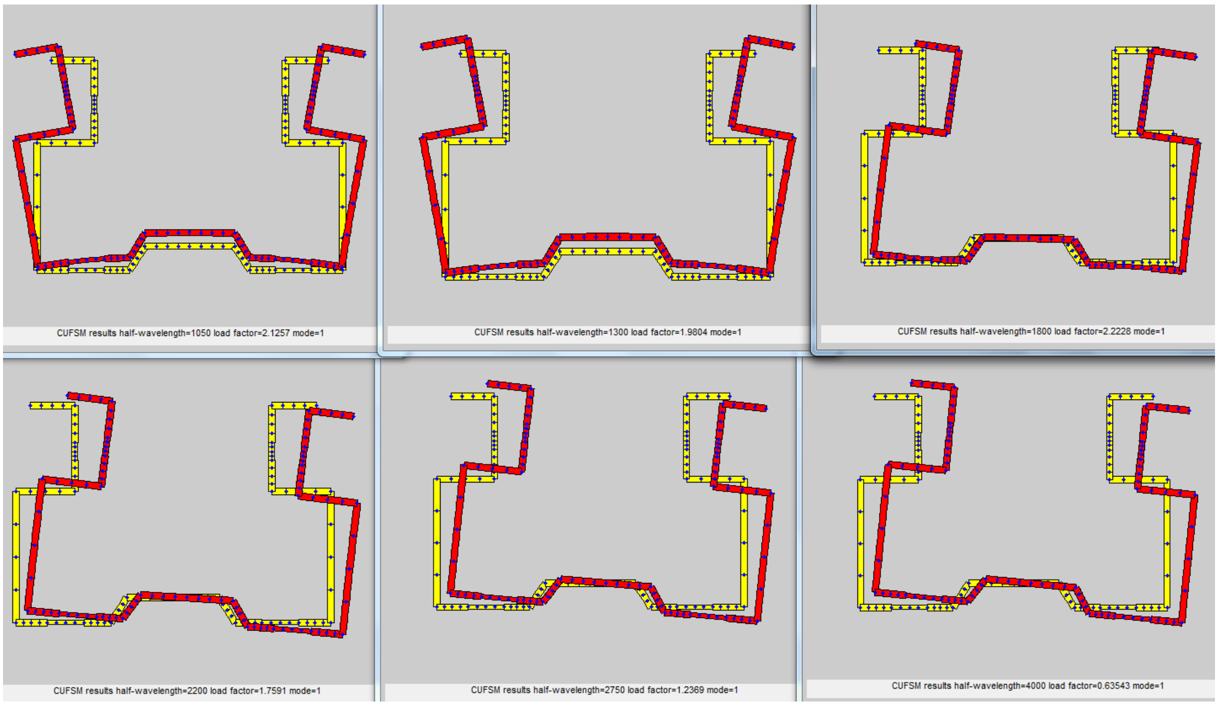
CUFSM results half-wavelength=1050 load factor=2.1257 mode=1
CUFSM results half-wavelength=1300 load factor=1.9804 mode=1
CUFSM results half-wavelength=1800 load factor=2.2228 mode=1
CUFSM results half-wavelength=2200 load factor=1.7591 mode=1
CUFSM results half-wavelength=2750 load factor=1.2369 mode=1
CUFSM results half-wavelength=4000 load factor=0.63543 mode=1

K. CU-FSM Modes at various upright lengths 120-78-25-5070

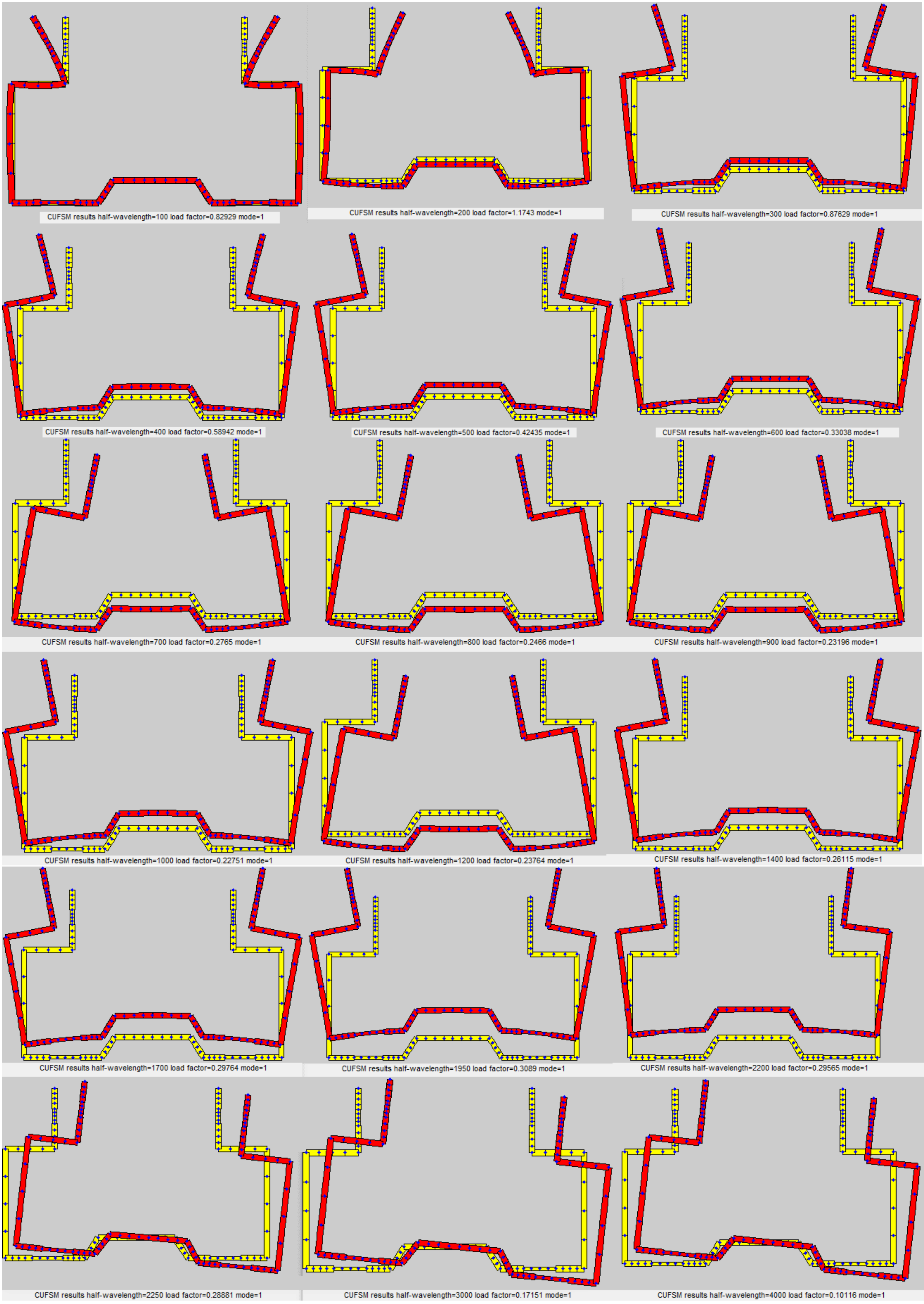

Figure 64. Modes at various uprights lengths.

L. SolidWorks Simulation Results

All SolidWorks Simulations, according to the scheme given in Table 16 on page 46.

<table>
<tr><td colspan="4">STUB 78 “unlipped”, “Free movement in y- and z”</td></tr>
<tr><td>No Spacer</td><td>$E_{D,m}$ = 0.0 mm</td><td>$E_{D,m}$ = -3.0 mm</td><td>$E_{D,m}$ = -6.0 mm</td></tr>
<tr><td>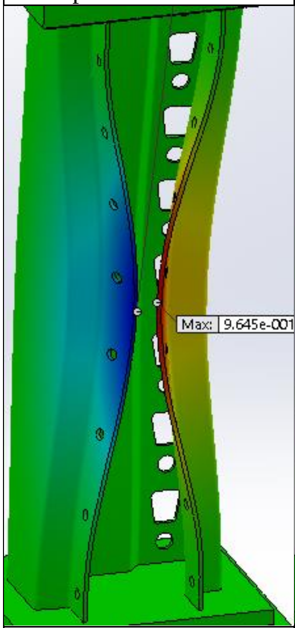
</td><td>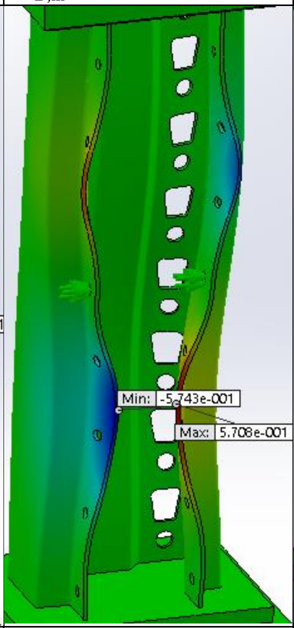
</td><td>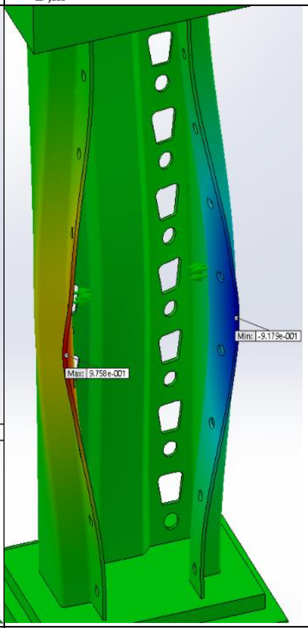</td><td>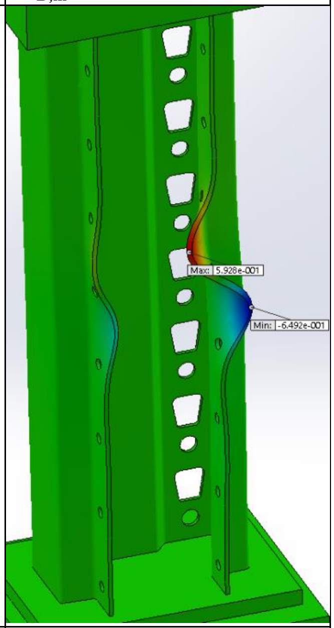</td></tr>
<tr><td>Distortional/Local</td><td>Local</td><td>Local, DTB</td><td>Local</td></tr>
<tr><td colspan="4">STUB 83 ‘Lipped’, “Free”</td></tr>
<tr><td>No Spacer</td><td>$E_{D,m}$ = 0.0 mm</td><td>$E_{D,m}$ = -3.0 mm</td><td>$E_{D,m}$ = -6.0 mm</td></tr>
<tr><td>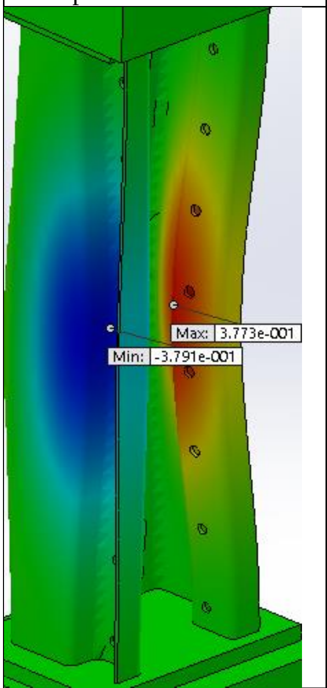
</td><td>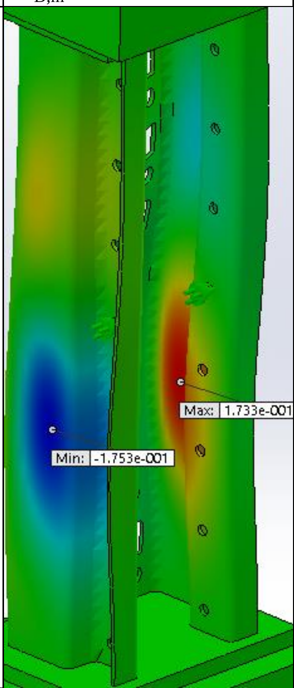
</td><td>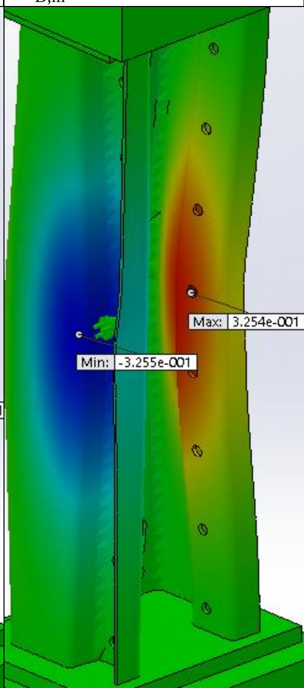
</td><td>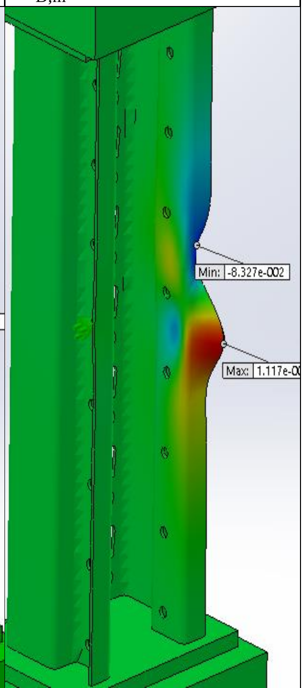
</td></tr>
<tr><td>Local, web</td><td>Local, web</td><td>Local, web</td><td>Local, end-flange (lip)</td></tr>
</table>

Figure 65. Results of numerical analysis of non-lipped and lipped STUB-test setup.

<table>
<tr><td colspan="4">DTB 78, “Free”</td></tr>
<tr><td>No Spacer</td><td>$E_{D,m}$ = 0.0 mm</td><td>$E_{D,m}$ = -3.0 mm</td><td>$E_{D,m}$ = -6.0 mm</td></tr>
<tr>
<td>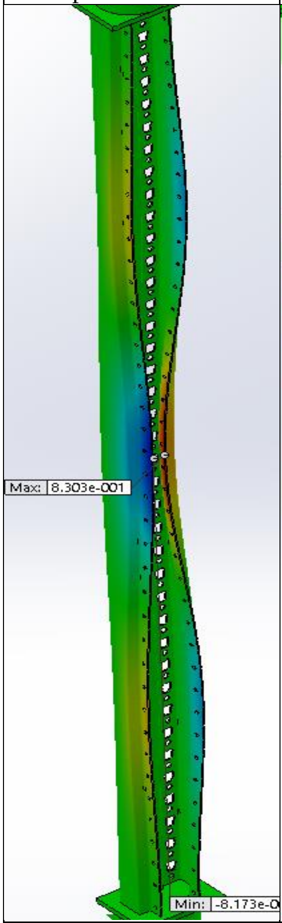</td>
<td>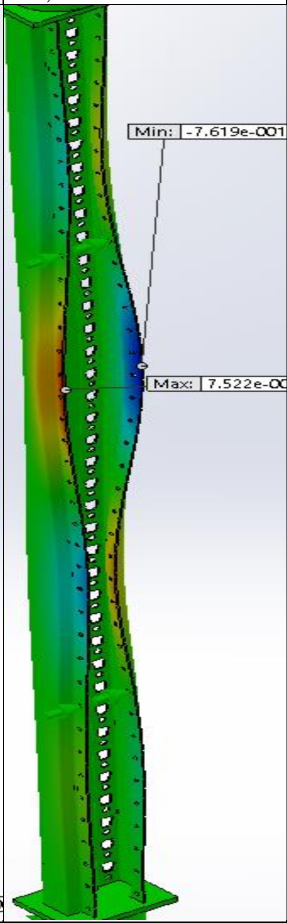</td>
<td>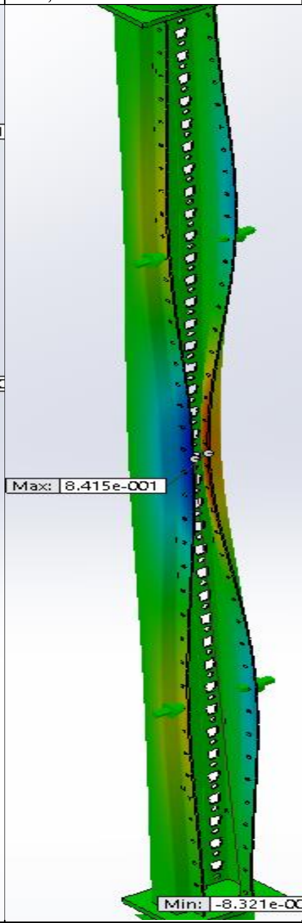</td>
<td>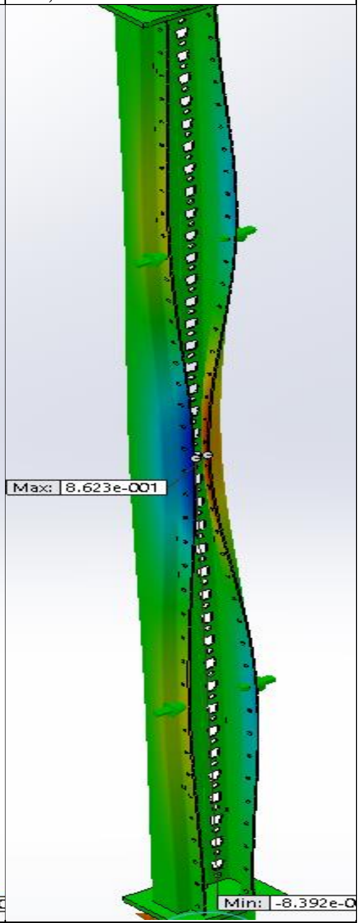</td>
</tr>
<tr><td>Distortional</td><td>Distortional</td><td>Distortional</td><td>Distortional</td></tr>
</table>

Figure 66. Results of numerical analysis of non-lipped and lipped DTB-test setup, while movement in in-depth-direction is allowed. Note the resulting flexural buckling behaviour in the lipped profiles. This was also encountered in the 'New DTB' setup from section 02.1.

DTB 83, "Free"			
No Spacer	$E_{D,m}$ = 0.0 mm	$E_{D,m}$ = -3.0 mm	$E_{D,m}$ = -6.0 mm
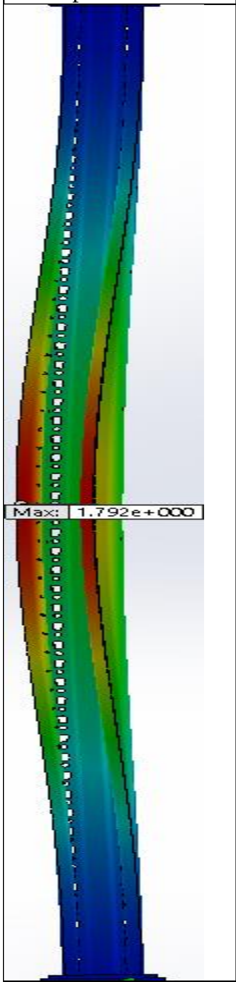	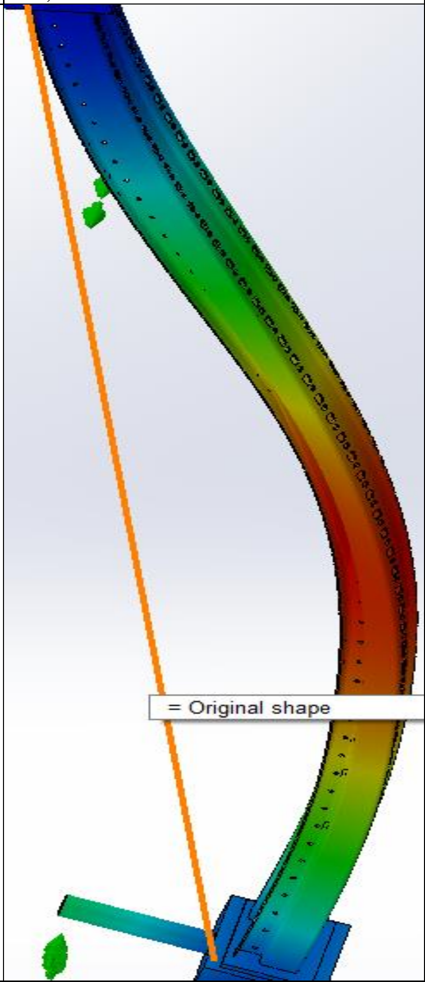	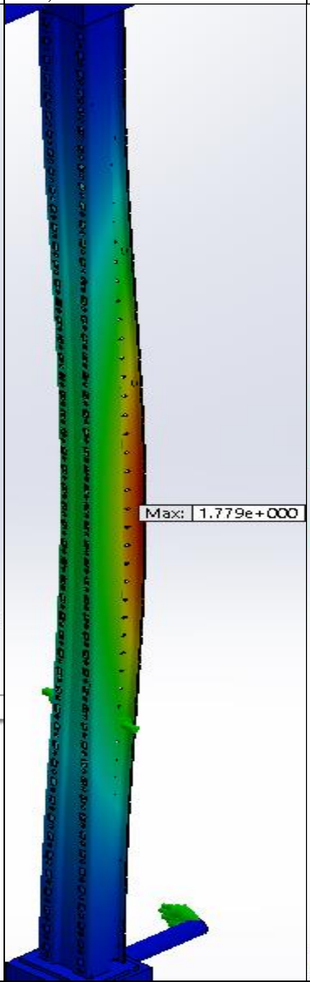	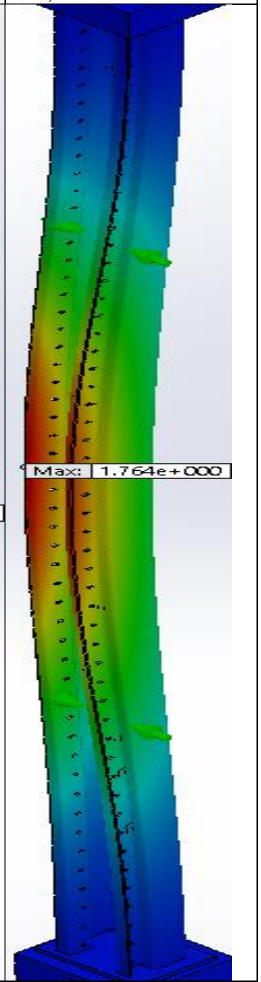
Flexural-Torsional	Flexural-Z (Weak axis) Closed direction	Flexural-Torsional	Flexural-Torsional

Figure 67. Lipped profile, free movement in in-depth-direction. This should simulate the 'New DTB' setup with extended lengths as close as possible.

The reduction in degrees of freedom as a result of actual diagonals in a frame can be modelled in innumerable alternatives. One way to model this into SolidWorks is simulating a single upright and adding constrains to disable movement in the horizontal plane (against flexural failure, any axis).

DTB 78, "yz Restrained"		
$E_{D,m}$ = 0.0 mm	$E_{D,m}$ = -3.0 mm	$E_{D,m}$ = -6.0 mm
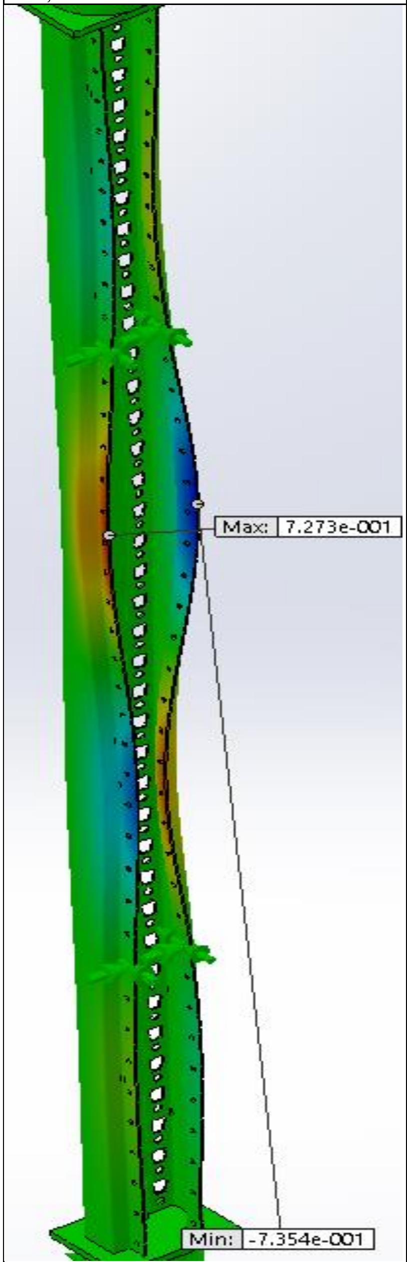	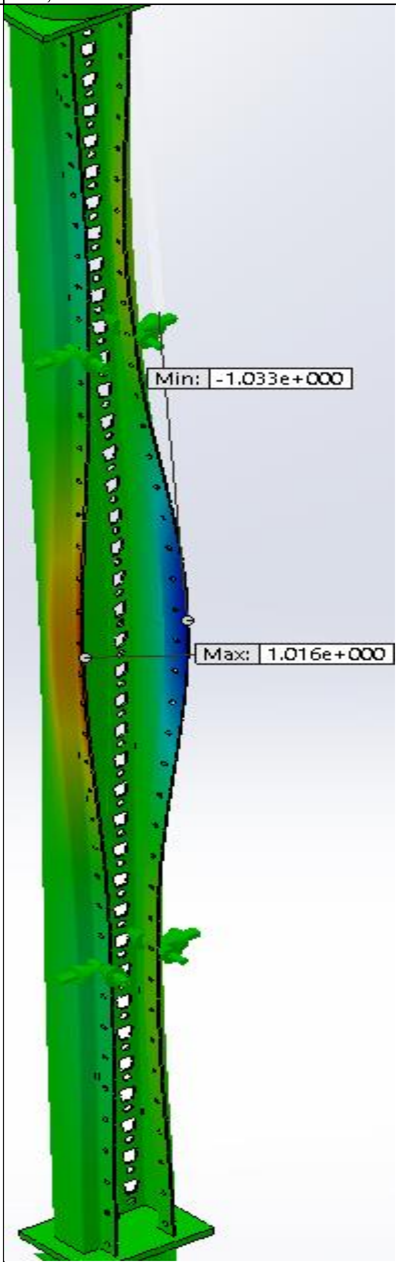	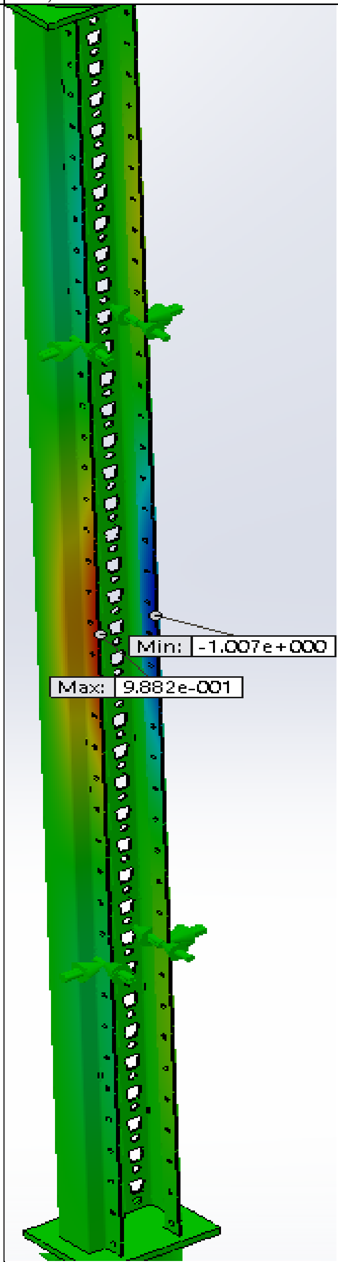
Distortional	Distortional	Distortional

Figure 68. Distortional buckling test of non-lipped profile, after restraining movement of the spacers in horizontal direction.

<table>
<tr><td colspan="3">DTB 83, “yz Restrained”</td></tr>
<tr><td>$E_{D,m}$ = 0.0 mm</td><td>$E_{D,m}$ = -3.0 mm</td><td>$E_{D,m}$ = -6.0 mm</td></tr>
<tr><td>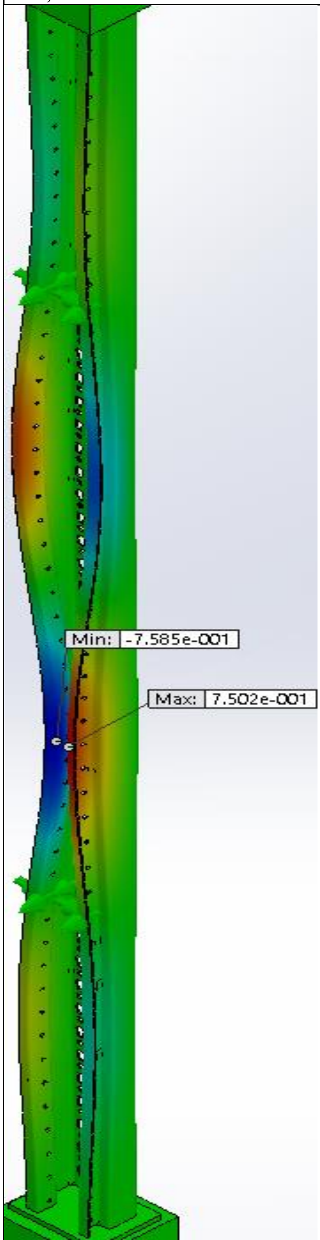</td><td>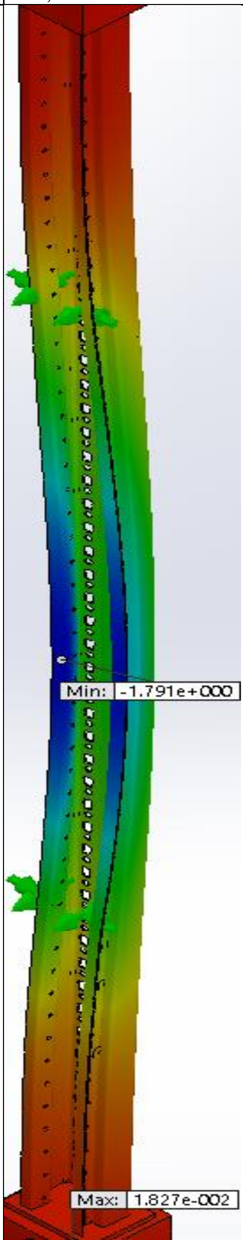</td><td>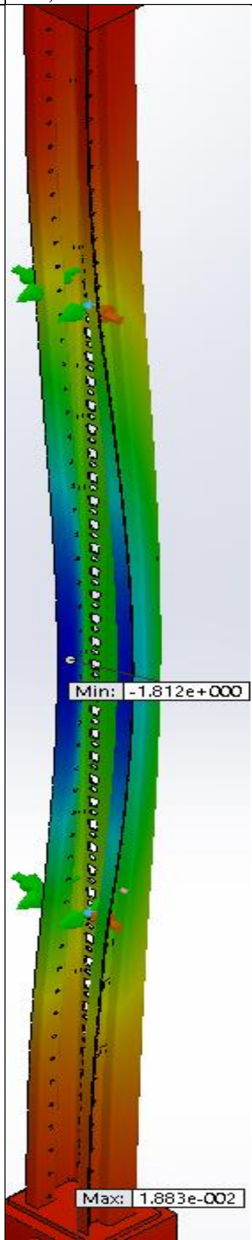</td></tr>
<tr><td>Distortional</td><td>Flexural-Torsional / Distortional</td><td>Flexural-Torsional / Distortional</td></tr>
</table>

Figure 69. Distortional buckling test of lipped profile, after restraining movement of the spacers in horizontal direction.

DTB 68, “yz Restrained” (Single potential length in Frame)			**DTB 68, “yz Restrained” (Double potential length in Frame)**		
$E_{D,m}$ = 0.0 mm	$E_{D,m}$ = -3.0 mm	$E_{D,m}$ = -6.0 mm	$E_{D,m}$ = 0.0 mm	$E_{D,m}$ = -3.0 mm	$E_{D,m}$ = -6.0 mm
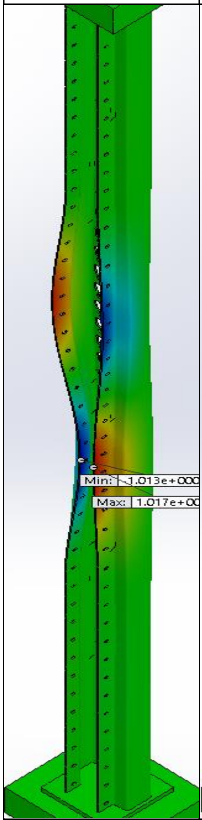	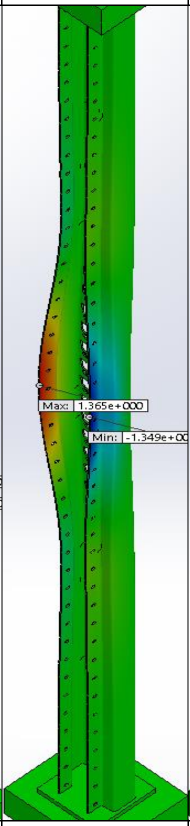	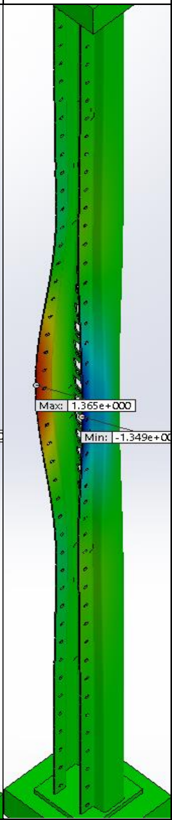	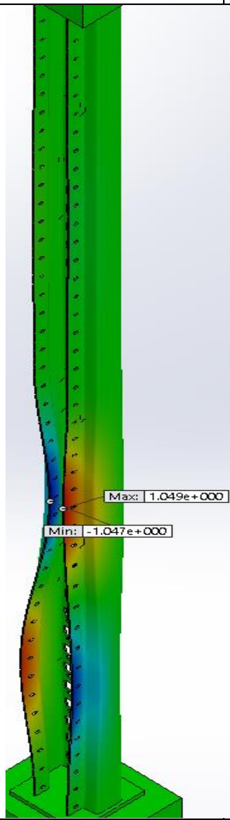	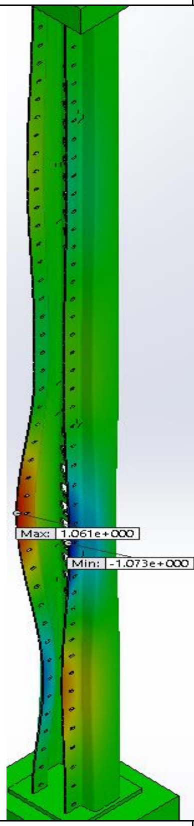	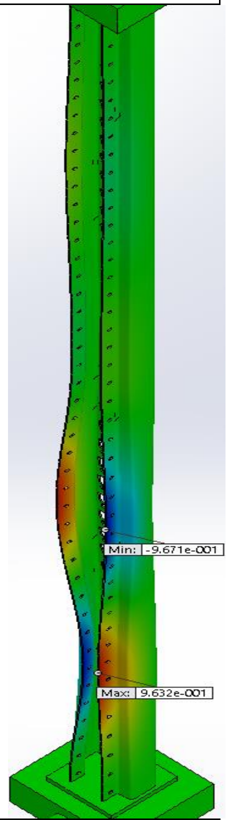
Distortional S	Distortional Outwards	Distortional Outwards	Distortional	Distortional, reverse direction	Distortional, reverse direction

Figure 70. Results of numerical analysis of 'cut-out' non-lipped single uprights used in the frame setup.

DTB 72, "yz Restrained" (Single potential length)			**DTB 72, "yz Restrained" (Double potential length)**		
$E_{D,m}$ = 0.0 mm	$E_{D,m}$ = -3.0 mm	$E_{D,m}$ = -6.0 mm	$E_{D,m}$ = 0.0 mm	$E_{D,m}$ = -3.0 mm	$E_{D,m}$ = -6.0 mm
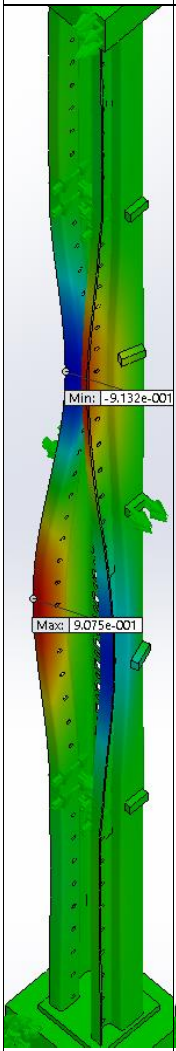	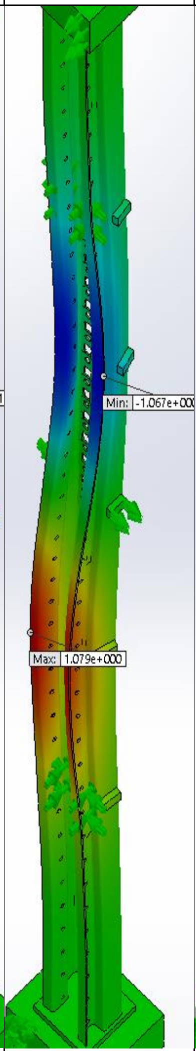	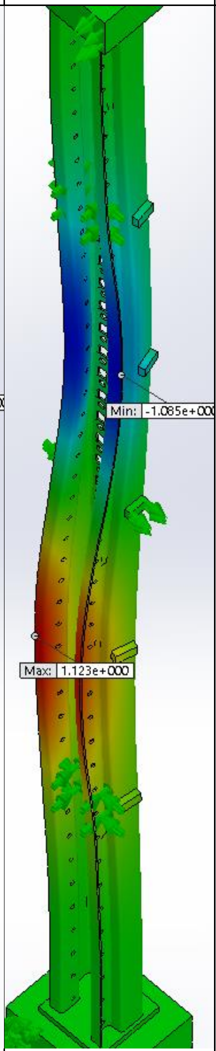	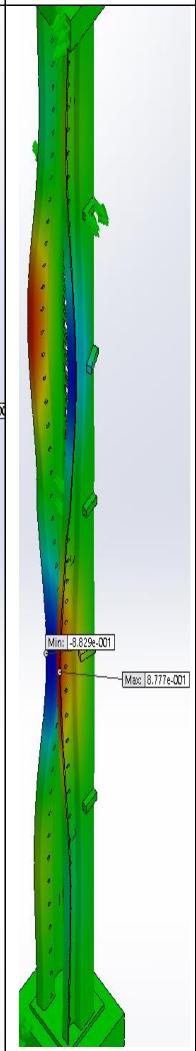	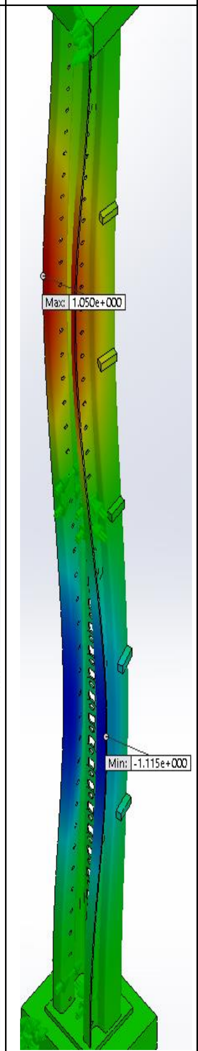	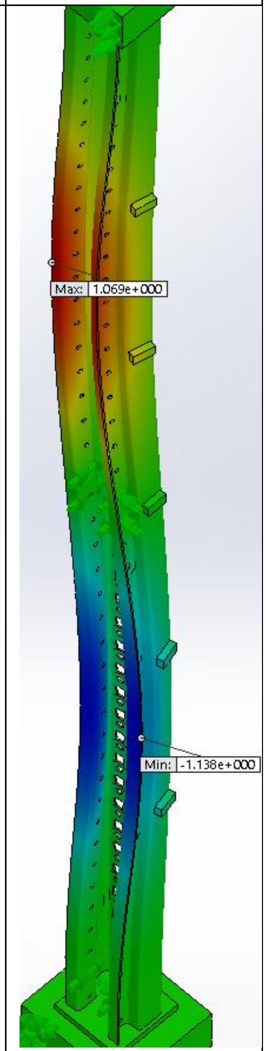
Distortional	Flexural Torsional	Flexural Torsional	Distortional	Flexural Torsional	Flexural Torsional

Figure 71. Results of numerical analysis of 'cut-out' lipped single uprights used in the frame setup.

Profile: 100-68-20-4050 PR S355

Selected Upright Profile in Frame:

"Left"

LF = Load Factor, compared with Situation A_tot * f_y

"Right"

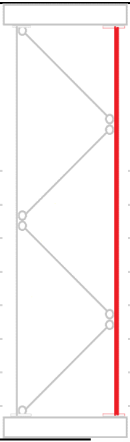

Pinch 0.0 mm	"Left"		"Right"	
	Distortional		Distortional	
LF =	0.829	-	0.881	-
	F_elastic = 2 x		F_elastic = 2 x	
	234.3	kN	249.0	kN

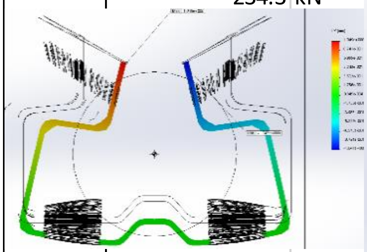

L = 843.75 mm

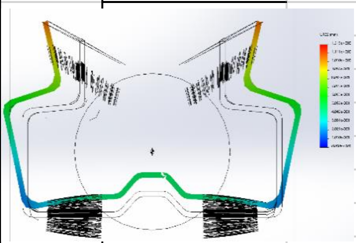

L = 331.25 mm

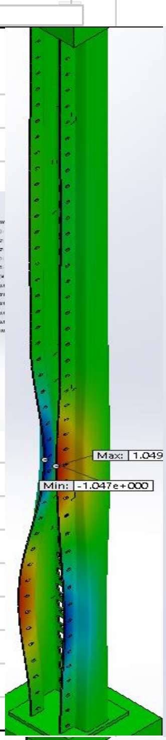

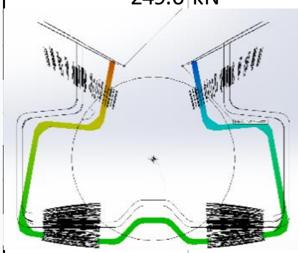

L = 843.75 mm

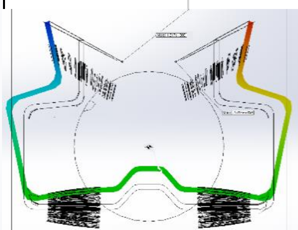

L = 1406.25 mm

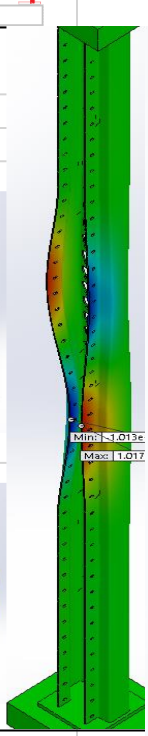

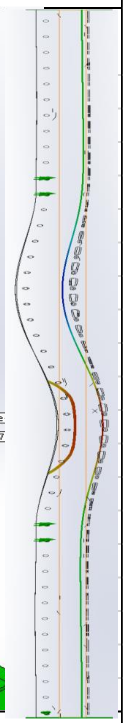

Pinch -3.0 mm	"Left"		"Right"	
	Distortional		Distortional	
LF =	0.814	-	0.809	-
	F_elastic = 2 x		F_elastic = 2 x	
	230.0	kN	228.6	kN

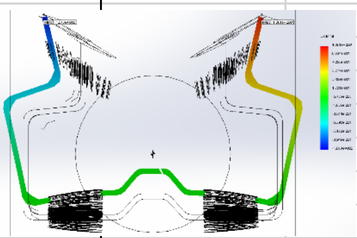

L = 843.75 mm

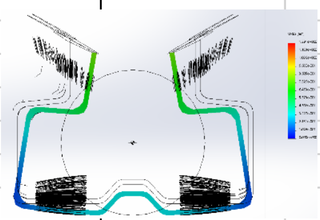

L = 281.25 mm

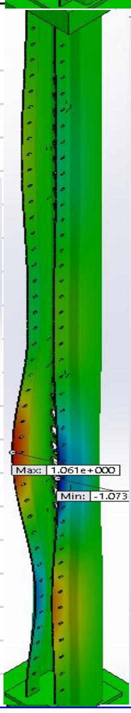

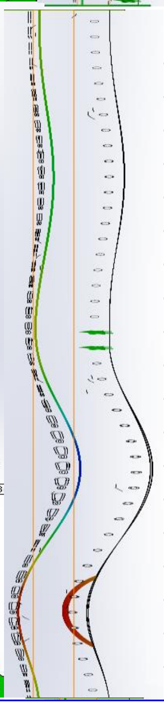

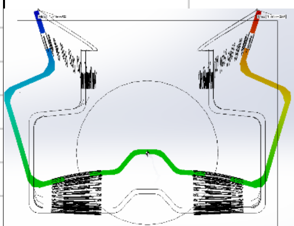

L = 1125 mm

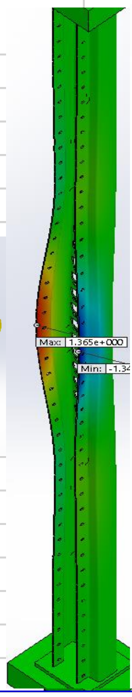

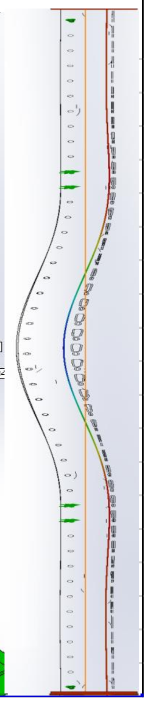

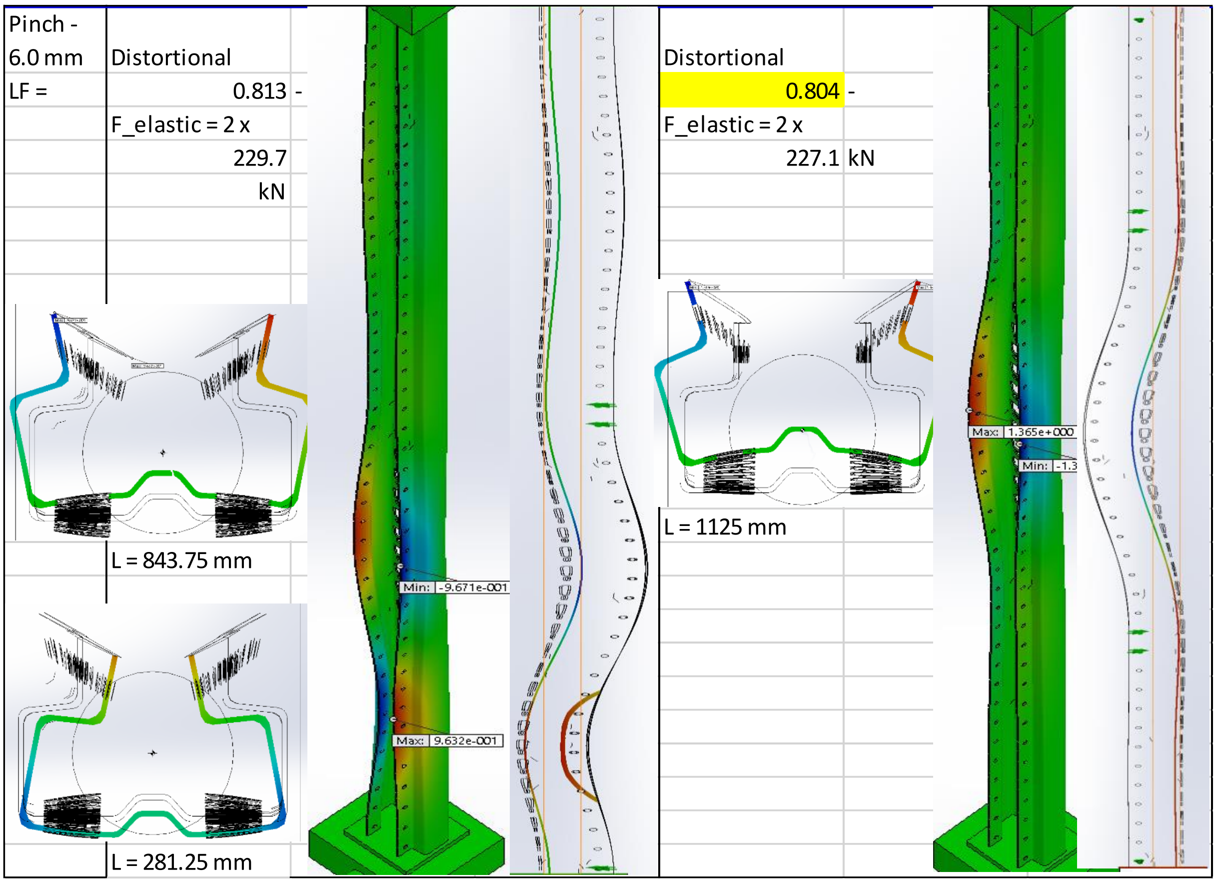

Figure 72. Detailed visualization of analysis of 'cut-out' non-lipped single uprights used in complete frame test.

Profile:	100-72-25-4050 PR S355			
Selected Upright Profile in Frame:	"Left", Double LF = Load Factor, compared with Situation A_tot * f_y		"Right", Single	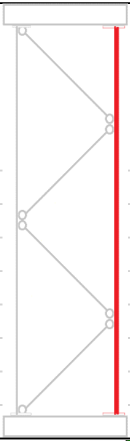
Pinch 0.0 mm	Distortional		Distortional	
LF =	2.710		2.525 -	
	F_elastic = 2 x		F_elastic = 2 x	
	871.3 kN		812.0 kN	

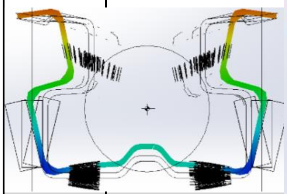

L = 1439 mm

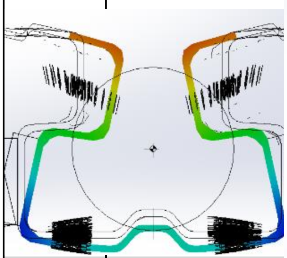

L = 878 mm

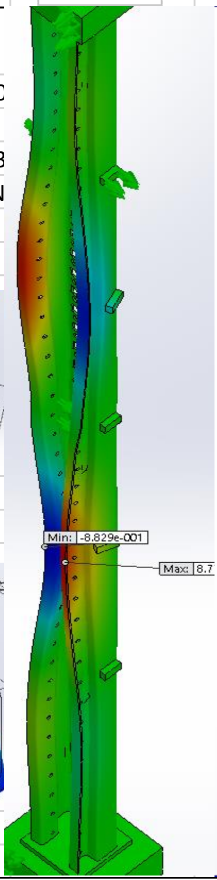

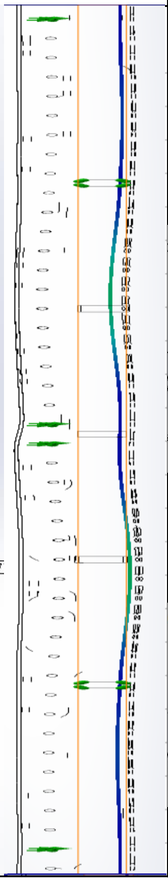

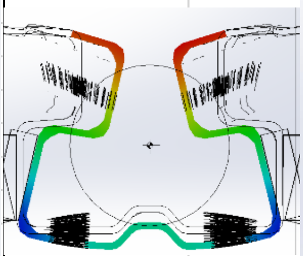

L = 1439 mm

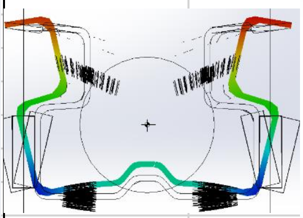

L = 878 mm

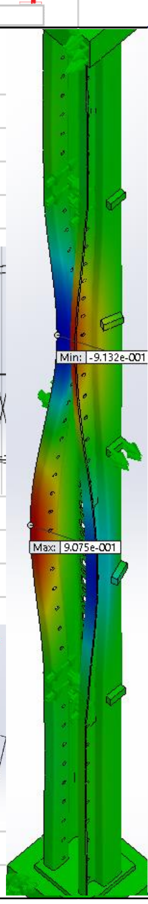

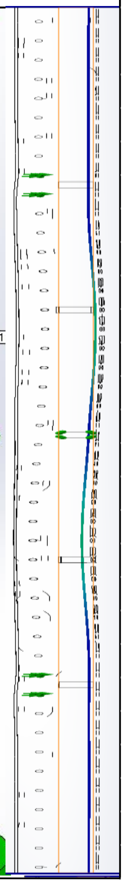

Figure 73. Detailed visualization of analysis of 'cut-out' lipped single uprights used in complete frame test.

Pinch - 3.0 mm

Distortional

LF = 2.34453605 -

F_elastic = 2 x 753.9 kN

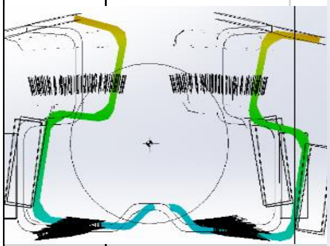

L = 1439 mm

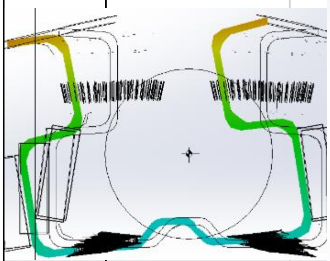

L = 878 mm

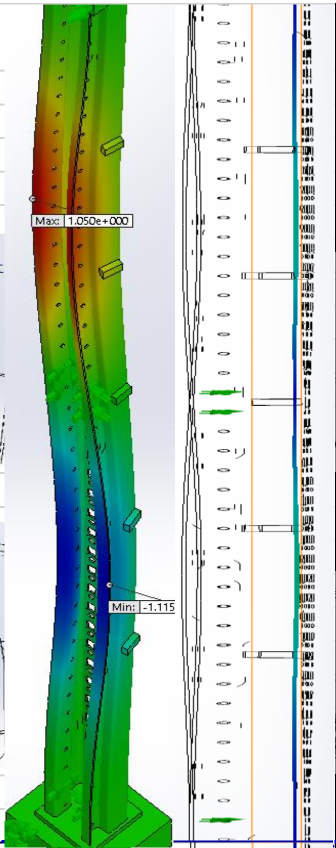

Distortional

2.149507935 -

F_elastic = 2 x 691.2 kN

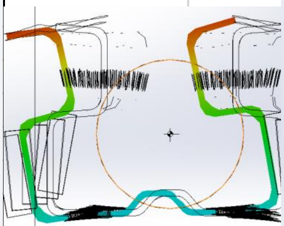

L = 1439 mm

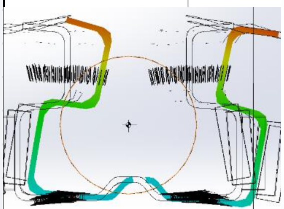

L = 878 mm

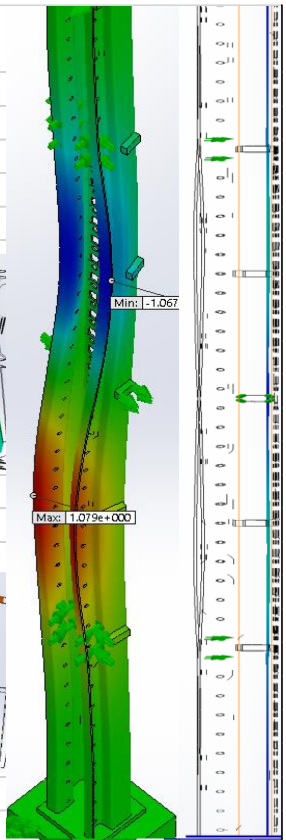

Pinch - 6.0 mm

Distortional

LF = 2.15951476 -

F_elastic = 2 x 694.4 kN

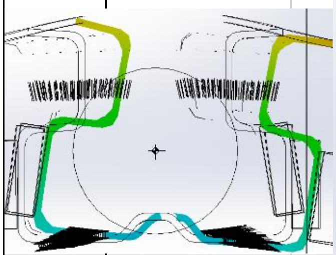

L = 1439 mm

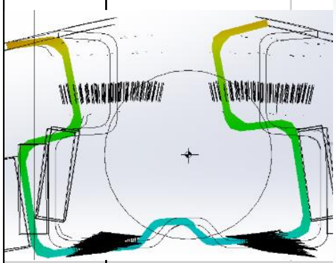

L = 878 mm

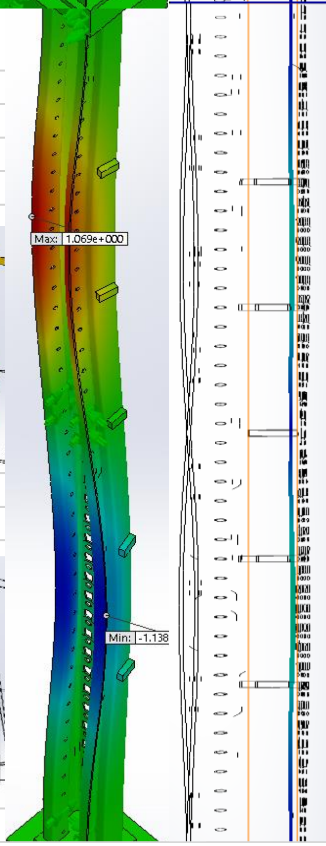

Distortional

2.091006498 -

F_elastic = 2 x 672.4 kN

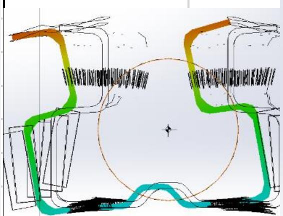

L = 1439 mm

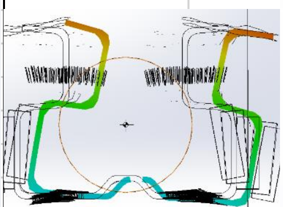

L = 878 mm

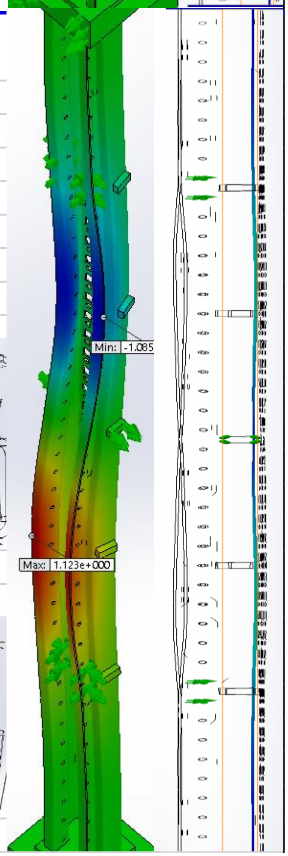

Complete Frames

To access the validity of modelling the full diagonals as simple constrains around the diagonal spacer perforations some simulations on full frames have been executed and results are visualized in Figure 44. When the results on the full frame simulation match the corresponding ‘single-upright-DTB’ setup, no further research is required.

<table>
<tr><th>Frame Setup 100-68-20-4050 (Non-Lipped)</th><th>Frame Setup 100-72-25-4050 (Lipped)</th></tr>
<tr><td>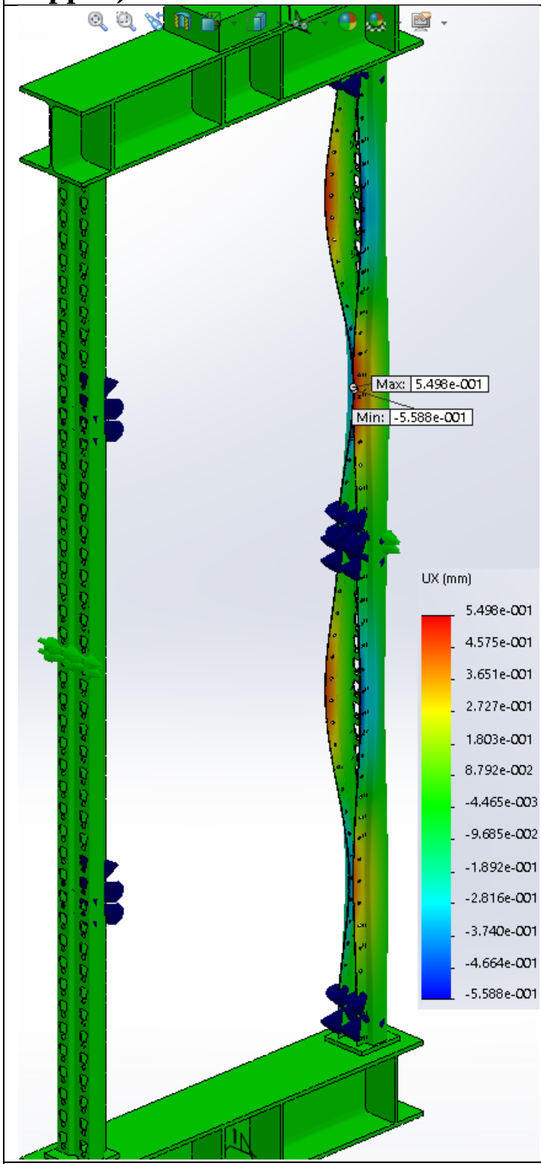
</td><td>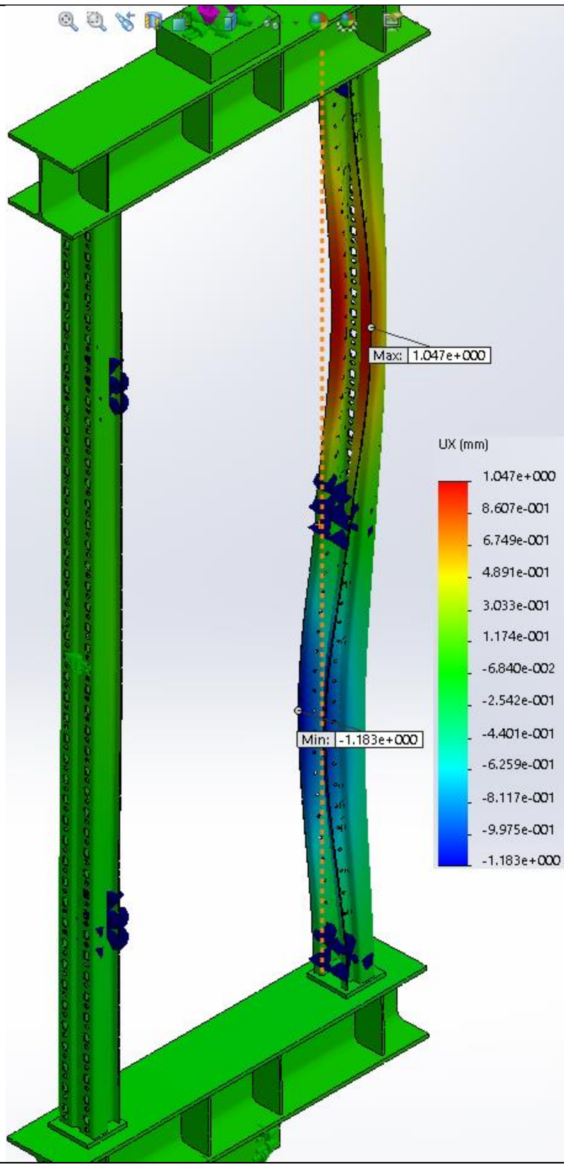
</td></tr>
<tr><td>Distortional</td><td>Flexural-Torsional / (Subordinate) Distortional</td></tr>
</table>

Figure 74. Results of numerical analysis of complete frames, using pin-pin diagonals. Notice similar behaviour as simulation of single uprights. Because the behaviour is similar, no additional simulations of complete frames are necessary.

. .